CHROMATIN DYNAMICS AT THE *Saccharomyces cerevisiae* *PHO5* PROMOTER

A Dissertation

by

WALTER JOSEPH JESSEN

Submitted to the Office of Graduate Studies of
Texas A&M University
in partial fulfillment of the requirements for the degree of

DOCTOR OF PHILOSOPHY

December 2004

Major Subject: Biochemistry

CHROMATIN DYNAMICS AT THE *Saccharomyces cerevisiae*

***PHO5* PROMOTER**

A Dissertation

by

WALTER JOSEPH JESSEN

Submitted to Texas A&M University
in partial fulfillment of the requirements
for the degree of

DOCTOR OF PHILOSOPHY

Approved as to style and content by:

Michael Kladde (Chair of Committee)	Michael Polymenis (Member)
James Hu (Member)	Terry Thomas (Member)
Gregory Reinhart (Head of Department)	

December 2004

Major Subject: Biochemistry

ABSTRACT

Chromatin Dynamics at the *Saccharomyces cerevisiae PHO5* Promoter.

(December 2004)

Walter Joseph Jessen, B.S., Purdue University

Chair of Advisory Committee: Dr. Michael Kladde

In eukaryotes, the organization of DNA into chromatin is a primary determinant of gene expression. Positioned nucleosomes in promoter regions are frequently found to regulate gene expression by obstructing the accessibility of cis-regulatory elements in DNA to trans-factors. This dissertation focuses on the chromatin structure and remodeling program at the *S. cerevisiae PHO5* promoter, extending the use of DNA methyltransferases as in vivo probes of chromatin structure. Our studies address the diversity of histone-DNA interactions in vivo by examining nucleosome conformational stabilities at the *PHO5* promoter. We present high-resolution chromatin structural mapping of the promoter, required to relate in vivo site accessibility to nucleosome stability and show that the *PHO5* promoter nucleosomes have different accessibilities. We show a correlation between DNA curvature and nucleosome positioning, which is consistent with the observed differences in accessibility/stability. Kinetic analyses of the chromatin remodeling program at *PHO5* show that nucleosomes proximal to the enhancer are disrupted preferentially and prior to those more distal, demonstrating bidirectional and finite propagation of chromatin remodeling from bound activators and providing a novel mechanism by which transactivation at a distance occurs.

DEDICATION

To my wife and closest friend Jenny Marie for her love, support, encouragement, and patience. You inspire the best in me. We've made our way together through many difficult times over the last six years. Together this is our success.

ACKNOWLEDGEMENTS

My scientific training began as an undergraduate at Purdue University Calumet. It was truly a unique experience that I will always remember as the best of times. The education that I received there was second-to-none – I am indebted to my undergraduate advisor Dr. Cliff Chancey, whose teaching, guidance, and support I will be forever thankful for.

I would like to thank my graduate advisor Dr. Mike Kladde for his training and guidance as well as the members of my advisory committee: Drs. Jim Hu, Michael Polymenis, and Terry Thomas. I would also like to thank Drs. Mary Bryk and John Mueller for their support.

I am grateful for the constant love, interest, and encouragement of my family over the past six years. To my parents, thank you for always believing in me and instilling in me the desire to always do the best that I can.

Finally, to special friends Marcos and Tori Trevino – your kindness and generosity will never be forgotten.

Satisfaction of one's curiosity is one of the greatest sources of happiness in life.

Linus Pauling

TABLE OF CONTENTS

LIST OF FIGURES

FIGURE Page

LIST OF TABLES

CHAPTER 1

INTRODUCTION

SCOPE

The primary scope of this dissertation is to characterize the chromatin organization at the *Saccharomyces cerevisiae PHO5* promoter and to discuss the changes that occur in nucleosome accessibility throughout the staging process of gene activation. Using the *S. cerevisiae PHO5* promoter as a model system, this work presents a detailed characterization of nucleosome disruption and provides a functional link between in vivo coactivator recruitment, chromatin remodeling, and transcriptional response. These studies employ cytosine-5 DNA methyltransferases (C5 DMTases) as highly sensitive and rapid in vivo probes of chromatin dynamics. Chapter I presents background on chromatin organization, transcriptional activation in the context of chromatin, and regulation of gene expression at the *S. cerevisiae PHO5* promoter. Two complementary uses for C5 DMTases in probing chromatin structure are outlined in Chapter II, including methods for constructing DMTase-expressing strains of *S. cerevisiae* and comprehensive protocols. In Chapter III, high-resolution chromatin mapping of the *PHO5* promoter enables us to relate in vivo site accessibility with nucleosome conformational stability. We show that *PHO5* promoter nucleosomes have different accessibilities/stabilities. Lastly, kinetic analysis of nucleosome disruption at the *PHO5* promoter, detailed in Chapter IV, demonstrates (i) a bidirectional and limited

---

This dissertation follows the format and style of Cell.

propagation of chromatin remodeling from enhancer-bound activators, and (ii) that interaction of SWI/SNF with the promoter localizes to the enhancer region.

SIGNIFICANCE

Early studies of the mechanisms by which activator proteins stimulate transcription demonstrated that the activation domains of a number of transcription factors interact directly with TATA-binding protein (TBP) or TBP-associated factors (TAFs) [reviewed in Tjian and Maniatis (1994)]. Subsequent studies suggested that the binding of TBP to the TATA-element in vivo is the rate-limiting step for transcriptional initiation and that activation domains increase the recruitment of TBP to promoters (Klein and Struhl, 1994; Xiao et al., 1995). Indeed, fusion of TBP to the DNA-binding domain of Gal4 resulted in transcriptional activation in the absence of interactions normally mediated by an activation domain.

A model for eukaryotic gene regulation emerged, termed "the triad model of transcriptional activation" (Struhl, 1996), and involves the interaction between an enhancer-bound transcription factor, complexes containing TBP and associated proteins bound to the TATA box, and RNA polymerase II (RNAP II) holoenzyme bound to the initiation site. This model was based in part on a series of experiments studying gene expression in *Saccharomyces cerevisiae* (Farrell et al., 1996). The protein Gal11 is a component of the mediator subcomplex of the RNAP II holoenzyme complex. In strains containing a single amino acid "P" (for potentiator) mutation in Gal11 (Gal11P), an activation-deficient version of the transcription factor Gal4 [lacking a classical activation

region (i.e., the protein domain of a transcriptional activator required for transcription)] was found to be a potent activator of transcription due to fortuitous interaction between the two mutant proteins. To explain the strong activation, it was proposed that the tethering of Gal11P to DNA via the interaction with the Gal4 derivative recruits RNAP II holoenzyme and activates transcription. Subsequent "activator bypass" experiments, artificially recruiting the transcriptional machinery by fusing a DNA-binding domain directly to components of mediator or RNA polymerase II holoenzyme (Barberis et al., 1995; Gaudreau et al., 1997; Keaveney and Struhl, 1998; Gaudreau et al., 1999), resulted in transcription in the absence of a classical activation region. While artificial recruitment of TBP in *S. cerevisiae* can result in transcriptional activation of some genes, at promoters where the TATA element is occluded by nucleosomes, artificial recruitment of TBP fails to activate transcription (Ryan et al., 2000). It was shown that a transcriptional activator can recruit the SWI/SNF complex and target chromatin remodeling activity independent of promoter sequence, TBP, or RNAP II holoenzyme (Yudkovsky et al., 1999).

Data from many systems now suggest that the mechanism of gene-specific transcriptional activation is ordered recruitment. Transcription and chromatin remodeling factors have been shown to be sequentially recruited to promoters (Cosma et al., 1999; Agalioti et al., 2000; Shang et al., 2000; Bhoite et al., 2001; Soutoglou and Talianidis, 2002; Bryant and Ptashne, 2003). The question arises as to how the staged process of gene activation employing an enhancer-bound transcription factor and likely involving the serial recruitment and activity of coactivators is able to result in the

subsequent assembly of the large transcribing complex. Enhancer-bound factors can directly target chromatin remodelers to and disrupt adjacent nucleosomes (Agalioti et al., 2000; Hassan et al., 2001). By contrast, little is known about the disruption of more distal nucleosomes at natural promoters in vivo. Thus, the method by which multiple factors gain access to and communicate across a promoter region in the context of chromatin is poorly defined. How does TBP bind a site in DNA constrained by a nucleosome that may be located hundreds of base-pairs away from an enhancer-bound transcription factor? Is there a difference in the extent of remodeling of several remodeled nucleosomes in a promoter region? Does the disruption of multiple, neighboring promoter nucleosomes occur simultaneously or sequentially?

Utilizing the *S. cerevisiae PHO5* promoter as a model system, this work illuminates some of the events that occur throughout the staging process of gene activation, presenting a detailed characterization of nucleosome disruption and providing a functional link between in vivo coactivator recruitment, chromatin remodeling, and the transcriptional response. This research is significant in that a steadily increasing list of molecular aberrations has associated chromatin coactivators (Roux-Rouquie et al., 1999), specifically members of the SWI/SNF2 family of proteins, with several human diseases including ATR-X syndrome (α-thalassemia/mental retardation syndrome, X-linked), Cockayne syndrome, and most recently in Schimke immuno-osseous dysplasia (Boerkoel et al., 2002). Additionally, a growing number of genetic developmental disorders, including Rett, Rubeinstein-Taybi, and Coffin-Lowry syndromes (Ausio et al., 2003), arise from a general dysregulation of transcription and

involve mutations in genes encoding histone-modification enzymes that modify chromatin structure and are thus referred to as chromatin remodeling disorders. All classes of multiprotein chromatin modification and remodeling activities are highly conserved, ranging from yeast to human. Thus, much of what is revealed in the simple budding yeast system should also be applicable to human cells and therefore relevant to our understanding and eventual treatment of human pathology.

CHROMATIN ORGANIZATION AND REGULATION OF GENE EXPRESSION

DNA, the double-stranded helical macromolecule located within the nucleus of every eukaryotic cell, contains almost all information necessary for living organisms to grow and function. It is responsible for preserving, duplicating, and communicating information within cells and passing this information from one cell generation to the next. DNA consists of repeating nucleotide molecules, composed of one sugar-phosphate moiety and a nitrogenous base. There are four nitrogenous bases in DNA: adenine (A); cytosine (C); guanine (G); and thymine (T). Weak chemical bonds between two bases on each of the two separate DNA strands form a base-pair (bp). Extended, the ~3,000,000,000 bp (3,000 Mbp) in a haploid human nucleus would be ~2 m in length (i.e., each base-pair is separated by 0.34 nm). All this hereditary material must be packaged into a nucleus of ~10 μm in diameter. Thus, eukaryotic genomes are found in a highly compact nucleoprotein complex called chromatin which, through several hierarchies of condensed structure, facilitates the packaging and organization of DNA

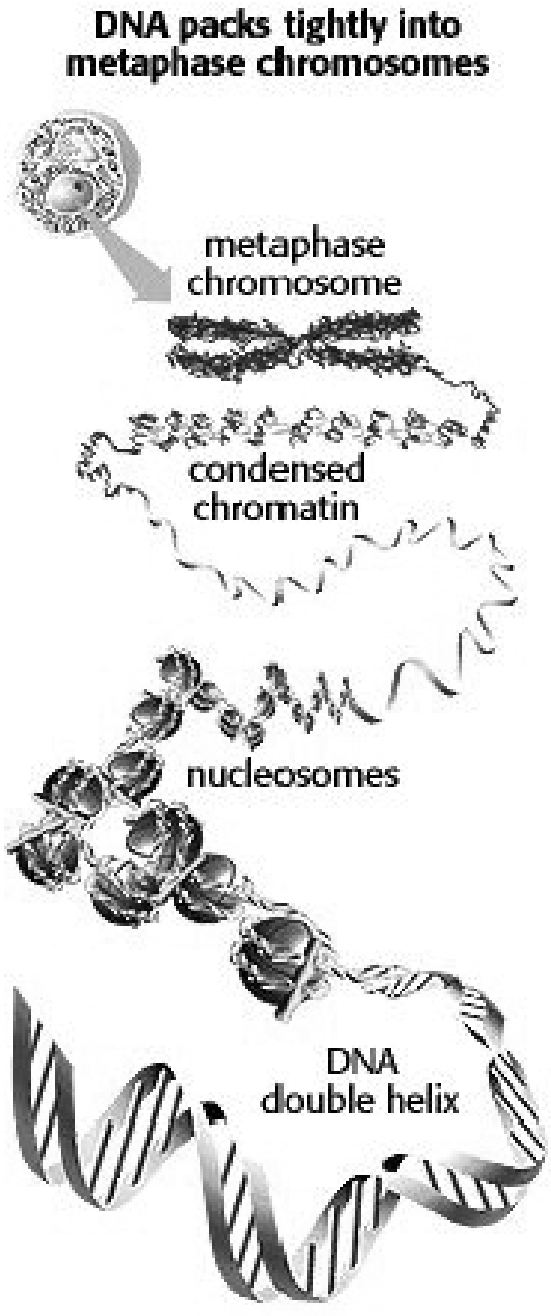

Figure 1-1. Hierarchies of Chromatin Structure

The DNA double helix is wrapped 1.67 times around a histone octamer to form a nucleosome. The resulting nucleosomal array (nucleosomes), often called “beads on a string”, is 10 nm in diameter. Further compaction coils the array into fibers that are 30 nm in diameter (condensed chromatin). Higher-order assemblies of unknown structure are organized into chromosomes (metaphase chromosome).

into chromosomes (Figure 1-1). Two forms of chromatin have been described; euchromatin and heterochromatin. Euchromatin is that portion of the genome most transcriptionally active. In contrast, heterochromatin is a densely packed form of chromosomes that is transcriptionally inactive, primarily made up of repeated sequences of non-coding DNA. The function of heterochromatin remains unknown. Heterochromatin can be distinguished from euchromatin by staining with the fluorescent DNA-binding dye DAPI. As heterochromatin consists of condensed DNA, DAPI-stained heterochromatin fluoresces brighter than euchromatin.

The fundamental repeating unit of chromatin is the nucleosome core particle, which occurs every 200 ± 40 bp (McGhee and Felsenfeld, 1980). The nucleosome core particle is comprised of a histone octamer core (two polypeptides each of histone H2A, H2B, H3, and H4) about which is wrapped 1.67 turns or 146 bp of DNA. The short stretches of histone-free DNA between nucleosomes in chromatin are referred to as linker regions. The crystal structure of the nucleosome core particle demonstrates a tripartite assembly (Figure 1-2) (Luger and Richmond, 1998). The tetrameric particle is a stable complex of two H3-H4 heterodimers having a handshake interlocking polypeptide fold, comparable in arrangement to that of the H2A-H2B heterodimers, and is referred to as the histone-fold motif. The histone-fold domain of all four histones is structurally similar and is constructed from three alpha-helices (α1, α2, and α3) connected by two loops, L1 and L2. The antiparallel arrangement of histones in the heterodimer places the L1 loop of one histone next to the L2 loop of the other, creating the DNA-binding site

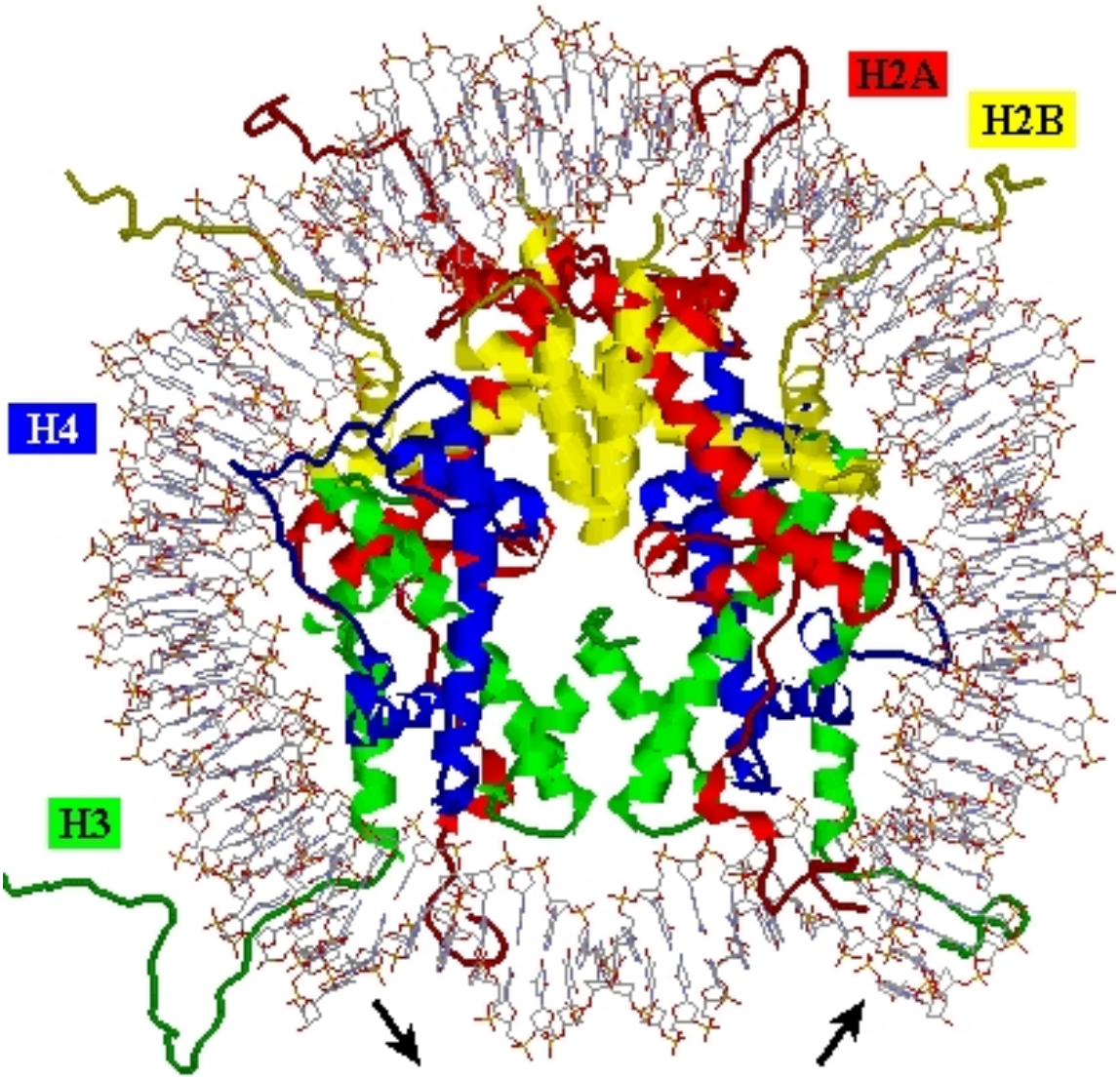

Figure 1-2. Crystal Structure of the Nucleosome Core Particle

The Oak Ridge 2.5 Angstrom (Å) nucleosome core particle structure containing native chicken histones and palindromic DNA (Harp et al., 2000). The tetrameric particle consists of two H3-H4 dimers (green and blue) and two H2A-H2B dimers (red and yellow) having a handshake interlocking polypeptide fold. The 146 bp of DNA is wrapped around the histone octamer 1.67 times in a left-handed superhelix. Arrows indicate the path of DNA onto and off of the histone octamer. PDB structure ID code 1EQZ.

L1L2 at each end of the dimer. A similar arrangement is seen for the α1 helix from each histone creating the central, second type of DNA-binding site α1α1.

While there are no observed direct interactions between the histone octamer and bases of DNA there are 116 observed hydrogen bonds made directly between protein and the DNA backbone (Davey et al., 2002). Water-mediated hydrogen bonds make up an additional 358 interactions. There are a total of 14 contact sites made where the minor groove of the double helix faces inward (every 10.2 bp). Accordingly, each histone-fold pair is associated with 27-28 bp of DNA separated by 4 bp linkers (Luger et al., 1997). A prominent feature on the histone octamer surface is a positively charged superhelical ramp about which the DNA is wrapped. The histone-fold domains organize the central 121 of 147 bp of nucleosomal DNA and, while overall curvature with bends into both major and minor grooves is distributed along the length of DNA, the diameter and bending are not uniform.

Direct analysis of the 1.9 Å resolution crystal structure of the nucleosome core particle (NCP147) reveals the conformation of DNA wrapped around the histone octamer (Richmond and Davey, 2003). While the overall superhelical parameters of nucleosomal DNA are sequence independent, the precise geometry of histone-DNA interactions and the local DNA structure depend subtly on the sequence of DNA. Intriguingly, NCP147 DNA has 2.2× the base-pair-step curvature necessary to generate the 1.67 superhelical turns around the histone octamer, bending the DNA 1,333.3˚ (opposed to the ideal superhelical fit of 600˚). Major groove bending, favored 1.3:1 per base-pair step (opposed to the 2:1 preference observed in oligonucleotides) is smooth

and all roll angles are positive (base-pair-step parameters are shown in Figure 1-3). The TA base-pair step appears only in major groove blocks and has the largest positive mean roll angle (11.8˚ vs. the next largest of 6.3˚ for GG = CC), correlating well with the observed conformational flexibility of TA in oligonucleotide DNA (el Hassan and Calladine, 1996). Synthetic DNA sequences selected for increased histone octamer affinity display a significant ~10 bp periodic placement of the dinucleotide TA (Thåström et al., 1999). Minor groove bending, almost exclusively at CA = TG base-pair steps, is kinked over each H2A-H2B dimer, never observed in crystallized oligonucleotides and rarely seen in protein-DNA complexes (Dickerson, 1998). Smooth bending is observed only over the H3-H4 tetramer with essentially all roll angles being negative. In oligonucleotide DNA, the base-pair step CA = TG has the lowest degree of propeller twist and hence is the most flexible step with respect to slide (the only base-pair step with a value larger than 1 Å) (Packer et al., 2000). Insertion of arginine side chains at 14 sites which are positioned towards the face of the histone octamer contributes to minor groove bending. Smooth bending is primarily due to a large alteration in shift values for GC, GG = CC, and AG = CT base-pair steps, relieving steric interference between bases. Curvature for both oligonucleotide and NCP147 DNA is primarily due to the base-pair-step roll parameter, favored over tilt (2:1 and 3:1, respectively). Analysis of structural components for both oligonucleotide and NCP147 DNA indicate significant base-pair-step parameter correlations between roll-slide-twist and tilt-shift with NCP147 DNA having increased values of both correlations, indicating that the conformational space occupied by NCP147 DNA is much smaller than for

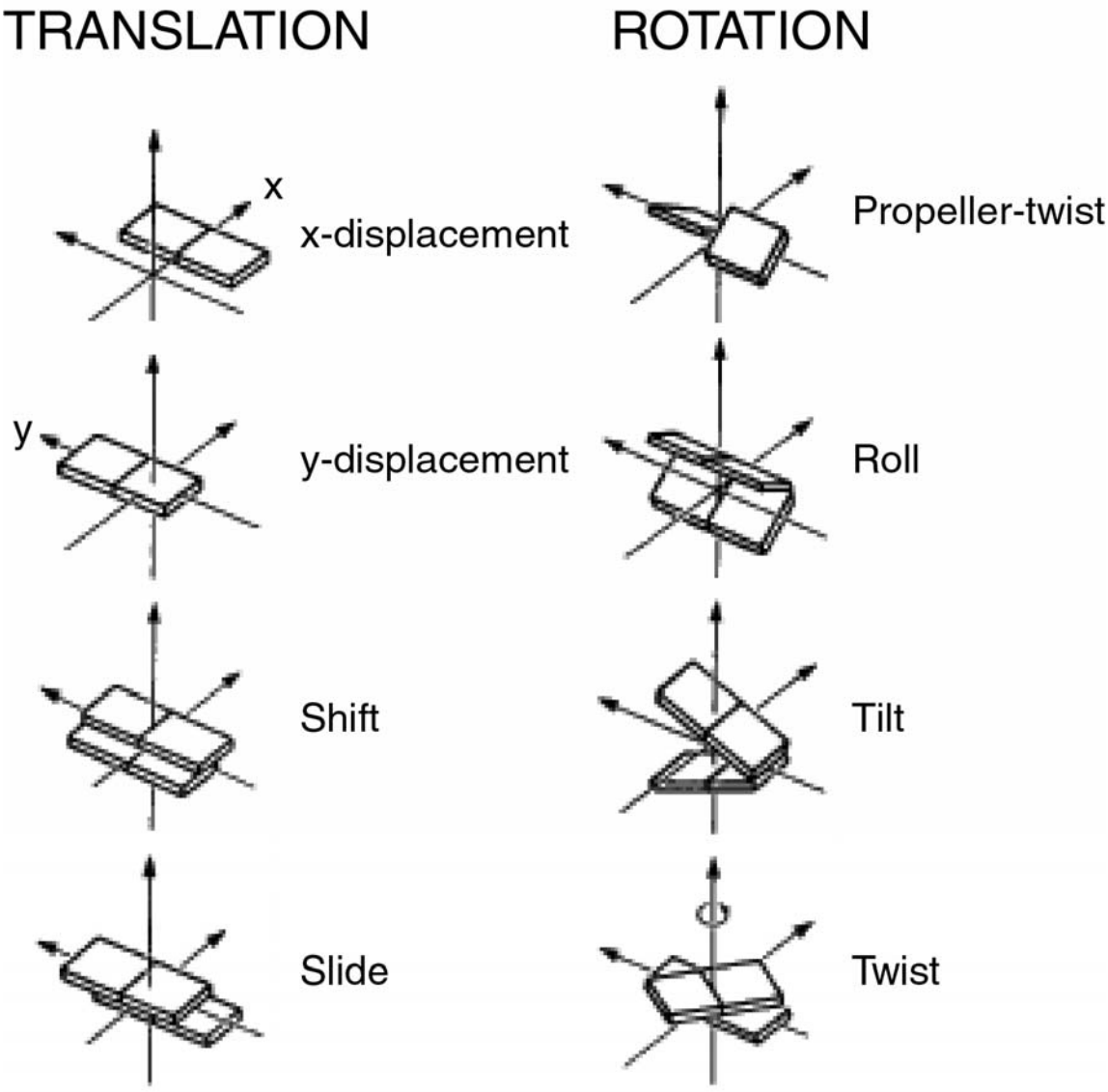

Figure 1-3. Definitions of Various Nucleic Acid Structure Parameters

Shown are four of eight possible translations involving two bases of a pair (upper left; x- or y-displacement) or two successive base-pairs (lower left; shift and slide) and four of eight possible rotations involving two bases of a pair (upper right; propeller twist) or two successive base-pairs (lower right; roll, tilt and twist).

oligonucleotide DNA. Thus nucleosomal DNA primarily utilizes the intrinsic mechanical properties of base-pair steps in order to bend DNA around the histone octamer. Base-pair-step flexibility in nucleosome positioning and stability appears to play a major role. Accordingly, base-pair step patterns observed in nucleosome positioning sequences may simply reflect the orientation of the major and minor grooves.

The amino termini of all the histones (15-30 residues) are unstructured and commonly referred to as the tails. The N-terminal tails of both histone H3 and H2B have random-coil segments that pass between gyres of DNA on the nucleosome surface. Histone H2A and H4 N-terminal tails also extend outward across the DNA. H2A is the only histone that also possesses a large, unstructured C-terminal tail. Although the electron densities for tail sequences exterior to the nucleosome core particle are weak (due to the lack of uniform structure) and not interpretable, a feature crucial for the role of the nucleosome in modulating DNA accessibility is that the histone tails are exposed. The histone tails serve as substrates for a variety of covalent, post-translational modifications by a growing list of transcriptional regulators. These modifications appear to modulate interactions between histone tails and other chromatin components, promoting unfolding of nucleosomal fibers and possibly exposing cis-regulatory regions in DNA for gene-specific transcription factors or transcriptional machinery. Thus, as the primary determinant of DNA accessibility, nucleosomes serve as the substrate for the essential biological processes of transcription, replication, cell division, recombination, and DNA repair.

NUCLEOSOME POSITIONING

The free energy of histone-DNA interactions serves to bias nucleosome positioning preferentially over specific DNA sequences. This DNA-sequence-dependent placement is referred to as nucleosome positioning (i.e., positioned nucleosomes refer to nucleosomes that are observed in all cells under identical conditions occupying the same position relative to the DNA). Two types of positioning are described; translational and rotational (Drew and Travers, 1985). Translational positioning is defined as the probability with which a histone octamer selects a specific contiguous sequence of 147 bp of DNA preferentially over other sequences of the same length. Rotational positioning is defined as a degenerate form of translational positioning in which the repetition of bendability signals due to base-pair composition defines a permissive rotational phase and favors the placement of the histone octamer onto a defined side of the DNA helix. Thus, rotationally positioned nucleosomes may be due to DNA sequences that are intrinsically bendable (anisotropically bendable) (Widom, 2001). Although the relative contributions of these parameters as well as additional constraints imposed by bound proteins and the organization of chromatin domains (Fedor et al., 1988) are not well defined, the increased affinity of histones for bendable DNA sequences suggests that anisotropic flexibility plays a role in the rotational positioning of nucleosomes.

Positioned nucleosomes have a direct consequence on the accessibility of trans-factors to their cognate DNA cis-regulatory regions. Transcriptional initiation is inherently repressed by this packaging of DNA and most transactivators bind

nucleosomes with greatly decreased affinity, especially at internal locations removed from the point of DNA entry/exit on the histone surface (Owen-Hughes and Workman, 1994; Xu et al., 1998b). Indeed, early studies using DNA methyltransferases (DMTases) as in vivo chromatin probes have shown that within the first two helical turns of nucleosomal DNA there is increased accessibility relative to the pseudo-dyad axis, but the observed accessibility is significantly lower than that seen in linker regions (Kladde and Simpson, 1994; Kladde et al., 1996; Xu et al., 1998b).

Nucleosomes are not static complexes and can undergo several conformational transitions. These transitions can be regulated by posttranslational modification and enzymatic function. Additionally, changes in the conformation of the nucleosome can be observed when the solution salt concentration is raised above 600 mM or lowered below 1 mM. With increased NaCl, initial dissociation of the nucleosome occurs with release of the H2A/H2B dimers (Yager et al., 1989). Lower salt concentrations also result in structural transitions of the nucleosome core and the nucleosome is thought to be in an elongated prolate structure that is partially unfolded (Czarnota and Ottensmeyer, 1996). Thus, while the interactions within the H2A/H2B and H3/H4 dimers is extremely stable, the interface between the dimers is much weaker. At NaCl concentrations of 100-300 mM, ~5-20% of nucleosome core particles spontaneously dissociate to free histone octamer and DNA. The free histone octamers do not dissociate further but instead bind as histone octamers to other nucleosome core particles (Hansen, 2002).

More recent studies of nucleosome dynamics come from kinetic studies of restriction enzyme access to nucleosomal DNA (Polach and Widom, 1995; Protacio et

al., 1997; Anderson et al., 2002). It is thought that DNA site exposure is a result of localized transient dissociation of nucleosomal DNA from the histone octamer surface. In vitro, the conformation equilibrium constant (K_{eq}^{conf}) can be used to describe the local nucleosomal DNA unwrapping transition and varies over two orders of magnitude from the nucleosome pseudodyad to the nucleosome edge (Anderson and Widom, 2000; Anderson and Widom, 2001). These studies support a model in which regions of DNA bound by the histone octamer are transiently released and freely accessible. This process is referred to as site exposure.

TRANSCRIPTIONAL ACTIVATION IN THE CONTEXT OF CHROMATIN

Transcriptional coactivators, acting with site-specific activators, comprise two general classes. The first class of coactivators are the ATP-dependent nucleosome remodeling complexes, containing the nucleic acid-stimulated ATPases of the Swi2/Snf2 subfamily, which utilize the energy derived from ATP hydrolysis to disrupt nucleosomes (Jones and Kadonaga, 2000; Wolffe et al., 2000). The Swi2/Snf2 subfamily, divided into four classes according to their domain structures, consists of ATPase complexes related to SWI/SNF, ISWI, CHD, or INO80 (Clapier et al., 2001; Tsukiyama, 2002). Each member in the Swi2 class of ATPases contains a bromodomain, found to be highly conserved in chromatin remodeling complexes (Haynes et al., 1992), and is thought to recognize acetyl-lysines in histone amino-termini (Owen et al., 2000). Eight proteins containing a total of 15 bromodomains are predicted to be encoded by the *Saccharomyces cerevisiae* genome (Winston and Allis, 1999) and include Swi2 and Gcn5 (see below).

Bromodomains are also found in human proteins, including TBP-associated factor 250 ($TAF_{II}250$, containing 2 bromodomains), the histone acetyltransferases CBP (CREB-binding protein) and P/CAF (p300/CBP associated factor). It has been shown in vitro that stable promoter occupancy by SWI/SNF (and SAGA, see below), in the absence of transcriptional activators, requires the Swi2 and Gcn5 bromodomains and nucleosome acetylation (Hassan et al., 2002).

The prototypical ATP-dependent nucleosome remodeling complex in *S. cerevisiae* is the SWI/SNF complex, consisting of 11 protein subunits (3 of which have more than one copy per complex) with an approximate mass of 1.14 MDa; in terms of the volume of occupied space, SWI/SNF is 55× larger than a single nucleosome (Smith et al., 2003). Other ATP-dependent nucleosome remodeling complexes of the Swi2/Snf2 subfamily include RSC (*S. cerevisiae*), brahma (*Drosophila*), and hBRM (Human brahma) and hBRG-1 (Human brahma-related gene 1) (Lusser and Kadonaga, 2003).

The second class of coactivators post-translationally modifies histones (Strahl and Allis, 2000). Modifications include acetylation, phosphorylation of serine and threonine residues, methylation and ubiquitination of lysine residues, and methylation of arginine residues (Fischle et al., 2003). The combinatorial effect of these post-translational modifications is thought to regulate the functional activity of the genome and is referred to as the histone code (Strahl and Allis, 2000). Among the second class of coactivators, histone acetyltransferases (HATs) have been the most extensively studied. Acetylation of histone H4 has been shown to increase the affinity of trans-activators for

nucleosomal DNA (Vettese-Dadey et al., 1996). Hyperacetylated histones are associated with actively transcribed chromatin; hypoacetylated histones are associated with inactive or silent chromatin (Jeppesen and Turner, 1993). In *S. cerevisiae*, five distinct multi-protein assemblies, Ada, NuA3, NuA4, SAGA, and SLIK (SAGA-like) acetylate specific lysines in the N-terminal tails of histones (Grant et al., 1997; Eberharter et al., 1999; Pray-Grant et al., 2002). However, to date only SAGA and NuA4 have been implicated in the regulation of transcriptional initiation. The SAGA (Spt-Ada-Gcn5 Acetyltransferase) complex, consisting of 13 subunits, primarily acetylates histone H3 on promoter proximal nucleosomes and is involved in recruitment of the general transcription machinery (Dudley et al., 1999; Eberharter et al., 1999). The catalytic subunit of SAGA, Gcn5, possesses HAT activity (Brownell et al., 1996) and is required for SAGA to transactivate and acetylate histones in vivo (Gregory et al., 1998; Kuo et al., 1998; Wang et al., 1998; Krebs et al., 1999; Syntichaki et al., 2000). NuA4 (Nucleosomal Acetyltransferase histone H4) contains 12 proteins, including the catalytic subunit Esa1, the only known essential HAT in yeast. NuA4 primarily acetylates histone H4 but over a much broader domain of nucleosomes than histone H3 acetylation by SAGA and has been shown to stimulate transcription from preassembled nucleosomal templates in an acetyl CoA-dependent manner (Smith et al., 1998; Steger and Workman, 1999).

TRANSCRIPTIONAL ACTIVATION BY RECRUITMENT

A substantial number of investigations have analyzed these two classes of coactivators and their role in gene expression. The triad model of transcriptional activation (also see Significance section) proposes that coactivators, which themselves do not appreciably bind DNA, act subsequent to activator binding (Ryan et al., 1998) and are recruited to target promoters by the transcriptional activator (Fry and Peterson, 2001). This model is supported by recent studies demonstrating that activators are able to bind their promoters in vivo in the absence of SWI/SNF, Gcn5, or Esa1 (Ryan et al., 1998; Cosma et al., 1999; Gregory et al., 1999; Reid et al., 2000). For SWI/SNF and Gcn5, gene promoters fall into three classes based on their coactivator requirements including genes that are: (i) dependent on both coactivators; (ii) affected by the loss of one or the other coactivator (i.e., coactivator activities that are functionally redundant); and (iii) independent of both SWI/SNF and Gcn5 (Biggar and Crabtree, 1999). The requirements for these coactivators at various promoters have been shown to vary depending on strain, media, influence of histone variants or corepressors, and the mitotic phase of the cell cycle (Holstege et al., 1998; Ryan et al., 1998; Biggar and Crabtree, 1999; Krebs et al., 2000; Sudarsanam et al., 2000). However, these investigations focused on the steady-state expression of a given gene in the presence or absence of a coactivator. More recent studies have identified effects on the rate of induction rather than the steady-state level of transcription for a variety of genes in the absence of a coactivator (Otero et al., 1999; Barbaric et al., 2001).

TRANSCRIPTIONAL ACTIVATION AT THE *PHO5* PROMOTER

In the yeast *Saccharomyces cerevisiae*, under repressive conditions of high inorganic phosphate (P_i), the *PHO5* promoter is organized into a series of positioned nucleosomes that constrain its TATA element and thereby repress transcription (Figure 1-4) (Bergman and Kramer, 1983; Almer and Hörz, 1986; Fascher et al., 1990; Barbaric et al., 1992). Furthermore, DNA binding by the site-specific transcription factors Pho4 and Pho2 (as heterodimers) to the second of two UASs in the *PHO5* promoter, UASp2, is blocked by its location at the center of a nucleosome (Venter et al., 1994). There are two hypersensitive regions (HSRs) in the *PHO5* promoter; HSR1, located upstream of nucleosome −5 and HSR2 (also known as the accessible UAS element for *PHO5*, UASp1) located between nucleosomes −2 and −3. It has been shown previously that transcriptional activation of *PHO5* requires the remodeling of positioned nucleosomes −1 through −4 (Almer et al., 1986). Nucleosome disruption of the *PHO5* promoter occurs under conditions of low P_i and leads to transcriptional activation (Han et al., 1988; Gregory et al., 1999). This disruption is effected by the recruitment of transcriptional coactivators by the site-specific transcriptional activators Pho4 and Pho2 (Figure 1-5). The transcription factor Pho4 activates expression of genes induced when cells are deprived of P_i. In high-P_i medium, Pho4 is phosphorylated by the Pho80/Pho85 cyclin/cyclin-dependent kinase (CDK) complex and exported to the cytoplasm. There are five serine-proline (SP) sites in Pho4, referred to as SP1-SP6, which are phosphorylated by Pho80/Pho85 and regulate nuclear import (SP4), nuclear export (SP2 and SP3), and Pho2 interaction (SP6) (Komeili and O'Shea, 1999). The function of SP1

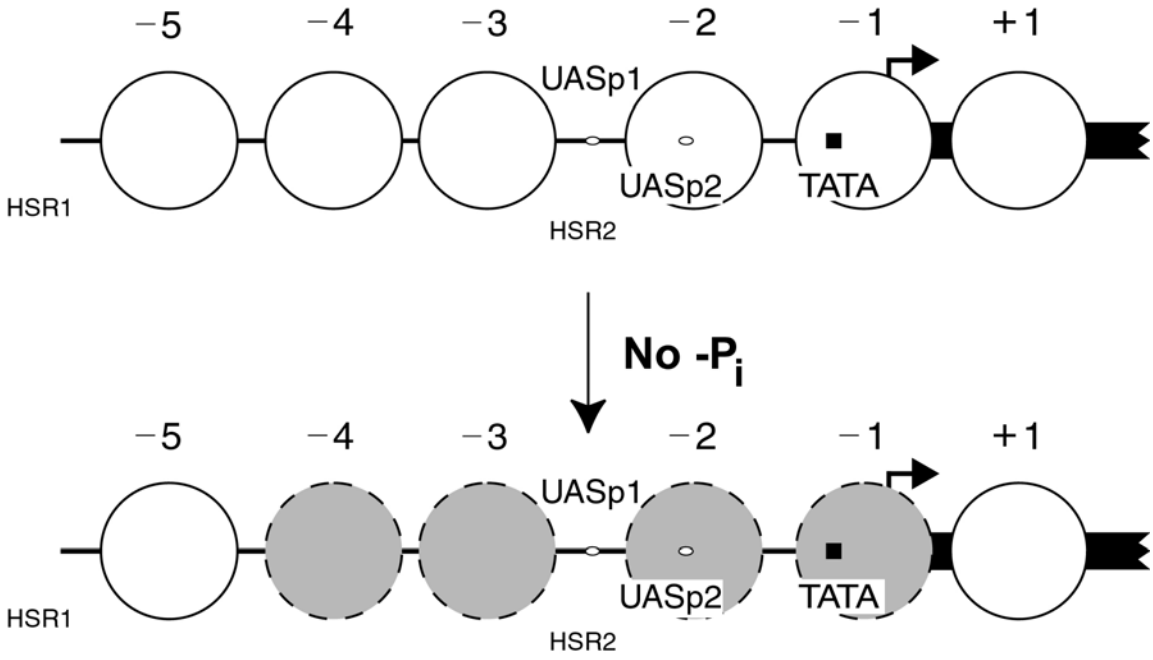

Figure 1-4. Structure of the *S. cerevisiae PHO5* Promoter

Phosphate (P_i) deprivation results in the remodeling of promoter nucleosomes −1 through −4 (grey dashed circles) concomitant with *PHO5* transcriptional activation. Large circles, positioned nucleosomes −5 to +1; open ovals, Pho4 binding sites UASp1 and UASp2; filled bar, TATA element; black arrowhead, major transcription initiation site; HSR1 and HSR2, hypersensitive regions 1 and 2, respectively; broken black rectangle, *PHO5* coding sequence.

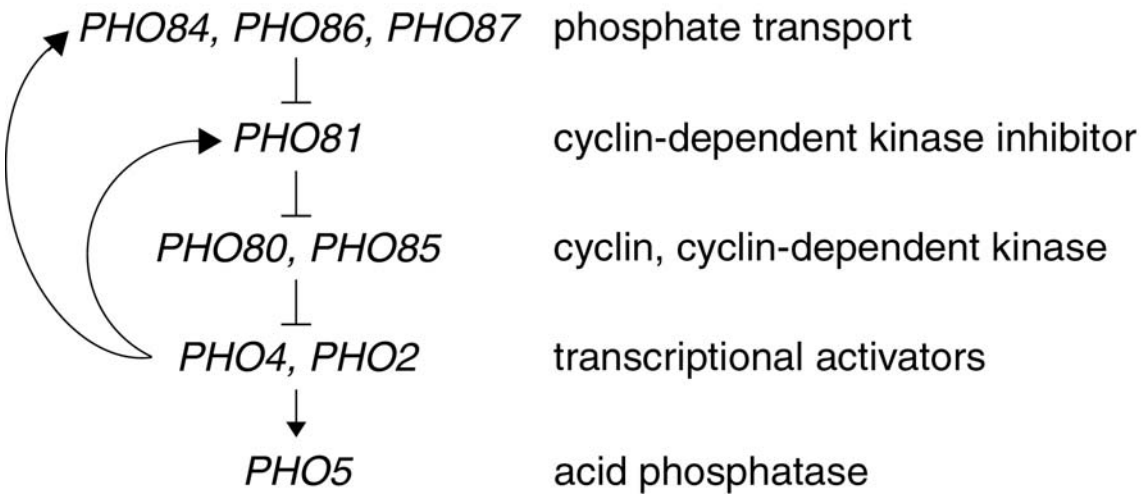

Figure 1-5. The *S. cerevisiae PHO5* Genetic Pathway

The repressible acid phosphatase *PHO5* is activated by the transcriptional activators Pho4 and Pho2. Under repressive conditions of high P_i the Pho80/Pho85 complex phosphorylates Pho4, signaling its export from the nucleus and preventing re-import. When cells are deprived of P_i, induction of *PHO5* is achieved by activation of the Pho80/Pho85 inhibitor *PHO81*. Activation of *PHO81* expression by Pho4 allows for positive feedback under activating conditions.

phosphorylation is unknown. The transcription factor Pho2 is required for maximal activation of *PHO5*. Pho2 is a pleiotropic activator, known to bind cooperatively with several acidic activators (Brazas and Stillman, 1993a; Brazas and Stillman, 1993b), including Pho4 at the *PHO5* promoter (Vogel et al., 1989; Barbaric et al., 1996; Barbaric et al., 1998).

Steady-state activation of the *PHO5* promoter is independent of both SWI/SNF and SAGA coactivators (Gregory et al., 1998), possibly due to recruitment of functionally redundant complexes (Biggar and Crabtree, 1999; Sudarsanam et al., 1999). Gcn5-dependent acetylation of histone H3 has been reported at *PHO5*, suggesting that SAGA is recruited even though it is not required for steady-state levels of activation (Krebs et al., 2000). Expression of *PHO5*, while independent of Gcn5 or SWI/SNF at the *PHO5* promoter under fully inducing conditions, becomes largely dependent on these remodelers when the promoters are weakened through mutation of UASs or when the nuclear concentration of Pho4 is low (e.g., in high P_i) (Gaudreau et al., 1997; Griffin-Burns and Peterson, 1997; Gregory et al., 1998; Holstege et al., 1998; Sudarsanam et al., 2000). Deletion of UASp2 at *PHO5* introduces an absolute requirement for *GCN5* in transcriptional activation at an otherwise coactivator independent gene (Gregory et al., 1998). More recently, it was established that, while the steady-state level of *PHO5* transcription was not affected by the deletion of *GCN5*, the rate of activation was significantly decreased (Barbaric et al., 2001). Indeed, SAGA does associate with the *PHO5* promoter (Barbaric et al., 2003). Moreover, deletion of *SNF2* has been found to significantly delay chromatin remodeling at the *PHO5* promoter (Reinke and Hörz,

2003). Thus, while fully-activating conditions of *PHO5* are independent of both SAGA and SWI/SNF, the rate at which steady-state activation is achieved is affected.

An alternative mechanism by which *PHO5* can be induced is the disruption of *PHO80*. Pho80 is a cyclin that acts with the CDK Pho85 (O'Neill et al., 1996). Disruption of *PHO80* leads to constitutive yet submaximal derepression of *PHO5* transcription under normally repressive conditions of growth in high-P_i medium. In a *pho80*Δ strain in high P_i, deletion of *GCN5* or mutation of residues critical for HAT function severely impair this constitutive submaximal activation of the *PHO5* promoter (Gregory et al., 1998; Gregory et al., 1999), displaying an altered remodeling state, with deoxyribonuclease I (DNase I) hypersensitivity localized to the UAS elements. This is consistent with data indicating that the binding of SWI/SNF and disruption of nucleosomes following activator targeting of the complex is restricted to promoter-proximal nucleosomes (Hassan et al., 2001).

In summary, the *PHO5* promoter is an excellent model system with which to characterize nucleosome disruption during promoter transactivation and to detail the changes that occur in nucleosome accessibility throughout the staging process of gene activation. Previous characterization of the *PHO5* chromatin transition and identification of DNA cis-regulatory regions establish a framework from which to begin our studies. Throughout this dissertation, DMTases are utilized as in vivo probes to study chromatin structure. Unusual for such a well-studied system as *PHO5*, the promoter chromatin structure has never been studied in detail. Thus, using both classical techniques as well as DMTases, a high-resolution structure of the *PHO5* promoter is presented in

Chapter III. *PHO5* promoter nucleosome accessibilities are examined and a correlate between nucleosome positioning and DNA curvature is discussed. Identification of SWI/SNF interaction with the promoter during the staging process of *PHO5* activation is shown in Chapter IV. Lastly, a temporal program of nucleosome disruption at *PHO5* during transcriptional activation is demonstrated.

CHAPTER II

MAPPING CHROMATIN STRUCTURE IN VIVO USING DNA METHYLTRANSFERASES*

SYNOPSIS

Cytosine-5 DNA methyltransferases (C5 DMTases) are effective reagents for analyzing chromatin and footprinting DNA-bound factors in vivo. Cytosine methylation in accessible regions is assayed positively by the PCR-based technique of bisulfite sequencing. In this chapter, we outline two complementary uses for the DNA methyltransferase CviPI (M.CviPI, GC specificity) in probing chromatin organization. First, we describe the use of the naturally occurring, free enzyme as a diffusible probe to map changes in nucleosome structure and to footprint factor interactions at cis-regulatory sequences. In a second application, termed Targeted Gene Methylation (TAGM), the DMTase is targeted via in-frame fusion to a DNA-binding factor. The rapid accumulation of DNA methylation enables highly sensitive detection of factor binding. Both strategies can be applied with any C5 DMTase, such as M.SssI, which also possesses short-recognition specificity (CG). A description of methods for constructing C5 DMTase-expressing strains of *S. cerevisiae* and analyzing chromatin regions is provided. We also include comprehensive protocols for the isolation and bisulfite treatment of genomic DNA as well as the subsequent bisulfite sequencing steps. Data demonstrating the efficacy of both DMTase probing techniques, theoretical

*Reprinted from Methods, *33*, Jessen W. J., Dhasarathy A., Hoose S. A., Carvin C. D., Risinger A. L., and Kladde M. P., Mapping chromatin structure in vivo using DNA methyltransferases, 68-80, Copyright 2004, with permission from Elsevier.

considerations, and experimental analyses are presented at *GAL1* and *PHO5*.

INTRODUCTION

Using C5 DMTases as in vivo probes of chromatin structure offers significant advantages over other more invasive methods: (i) the approach can be performed in living eukaryotic cells under physiological conditions; (ii) nuclear DNA is not damaged and is instead marked with a relatively innocuous methyl group; (iii) preparation of nuclei and cell permeabilization are not required, enabling detection of DNA-bound proteins that are often lost by these procedures, in addition to positioned nucleosomes; and (iv) only small culture sizes are needed, making it feasible to process many samples in a single experiment. Levels of 5-methylcytosine (m^5C) at potential DMTase target sites, and hence site accessibility, are positively displayed by bisulfite genomic sequencing (Frommer et al., 1992; Clark et al., 1994). DMTases are sterically occluded from their target sites located in nucleosomes and near or within factor-bound sequences. Thus, the differential access of free DMTases (probes in trans) to a region in different cell types (e.g., wild-type vs. mutant), cells grown under various conditions (e.g., induction vs. repression), or relative to protein-free DNA is used to detect the presence of chromatin or its alteration. Additionally, fusion of DMTases to DNA-binding proteins [TAGM probes, Targeted Gene Methylation, (Carvin et al., 2003a)] can be used to monitor factor binding, nucleosomal disruption, and to infer higher-order chromatin structure. Available DMTases with short specificities allow probing at resolutions on the order of 12-15 bp. We focus on DMTase CviPI [M.CviPI, GC specificity (Xu et al.,

1998a)], but identical methods apply to other C5 DMTases [e.g., M.SssI, CG specificity (Renbaum et al., 1990)].

MATERIALS AND METHODS

S. cerevisiae Strains and Growth Conditions

DMTase-expressing strains of *S. cerevisiae* were selected on complete synthetic medium (CSM) [6.7 g Bacto-yeast nitrogen base (YNB) with ammonium sulfate and without amino acids, 20 g glucose or galactose, and appropriate CSM supplement mix (Bio101, Vista, CA; the amount to add is indicated on the container label)].

The *S. cerevisiae* strain for probing *GAL1* was constructed by standard genetic methods from CCY694, *MAT***a**/*MAT*α *leu2*Δ0/*leu2*Δ0 *lys2*Δ0/*lys2*Δ0 *ura3*Δ0/*ura3*Δ0 *pho3*Δ::R/*pho3*Δ::R (S288C background), where R is a *Zygosaccharomyces rouxii* recombinase site that remains after intramolecular recombination. Cells were grown at 30˚C on plates or in liquid cultures of YPPD [2% glucose, 1% yeast extract (Difco), 2% peptone (Difco), 13.4 mM KH_2PO_4] or in liquid cultures of YPPG [1% yeast extract (Difco), 2% peptone (Difco), 2% galactose, 13.4 mM KH_2PO_4].

Yeast strains used in the TAGM analysis are derived from YPH500ΔL, *MAT*α *ade2-101 ura3-52 his3*-Δ200 *leu2*Δ1 *trp1*-Δ63 *lys2*-Δ1 (S288C background). Cells were grown in liquid cultures of high-P_i medium [2% raffinose, 20 mM 2-*N*-morpholino ethanesulfonic acid (MES), pH 5.5, 14 mM *L*-glutamine, 13.4 mM KH_2PO_4, and 0.7 g/l YNB without amino acids, $(NH_4)_2SO_4$, phosphate, or dextrose (Bio101, Vista, CA; cat #4029-622)] or P_i-free medium (substituting the 13.4 mM KH_2PO_4 with 13.4 mM KCl).

Medium for induction of free M.CviPI was high-P_i and P_i-free medium supplemented with 2% galactose to induce the *GAL1* promoter controlling DMTase synthesis.

Mapping chromatin structure in vivo using DMTases involves the following: (i) constructing DMTase-expressing strains of *S. cerevisiae*; (ii) screening for yeast strains with functional C5 DMTases; and (iii) in vivo analysis of chromatin structure and factor binding. Each step is outlined in detail.

Constructing DMTase-expressing Strains of *S. cerevisiae*

The M.CviPI plasmid is introduced into a strain of *E. coli* made competent for transformation. The strain must be completely deficient for methylation-dependent restriction (i.e., *mrr*$^-$ *mcr*BC$^-$, e.g., DH5α and XL1-Blue). Transformed cells are spread on a 2× YT plate containing 100 μg/ml ampicillin and incubated overnight at 37˚C. When individual colonies are visible, 7 ml of 2× YT medium containing 100 μg/ml ampicillin are inoculated with a single colony and incubated with shaking (300 rpm) for 8-12 hr at 37˚C. In practice, as C5 DMTases are toxic to *E. coli*, growth times are minimized to avoid accumulation of potential inactivating mutations. Most of our plasmids contain a strong, constitutive promoter that is downstream and transcribed oppositely of the DMTase gene, which limits expression of the DMTase in *E. coli* but not in yeast (Dorner and Schildkraut, 1994). It is recommended that the counter-transcribed promoter be included with the DMTase gene if subcloning of the DMTase to a different vector is required. Alternatively, the promoter can be added downstream of the ORF or transcriptional terminator by PCR amplification with a downstream primer

that contains the promoter sequence in a 5' extension. A stock of cells for cryogenic storage is made by pipetting 0.7 ml of culture into a suitable cryovial containing 0.35 ml 50% glycerol. Vortex well and store at −70˚C. Plasmid minipreps are prepared according to Ahn et al. (2000) or other suitable method. Plasmid DNA and DNA size-marker are electrophoresed on a 0.7% (w/v) Tris-acetate-EDTA (TAE) agarose gel containing 0.5 μg/ml ethidium bromide and viewed on a transilluminator to estimate the DNA concentration (Sambrook et al., 1989).

For chromatin analysis with a free DMTase, an integration plasmid (pSH1052) has been constructed with M.CviPI under control of an estrogen (17β-estradiol, E_2)-responsive promoter containing four LexA binding sites (*lex*O sites) located upstream of a minimal *GAL1* promoter. Induction is achieved by addition of E_2 in the presence of a chimeric activator, LexA-ER-VP16, a fusion of the *E. coli* LexA DNA-binding protein, human estrogen receptor α ligand-binding domain, and VP16 activation domain. LexA-ER-VP16 is expressed constitutively from the *ADH1* promoter (p*ADH1*) (Balasubramanian and Morse, 1999). pADH1-LexA-ER-VP16 is also present in pSH1052. Thus, a single transformation is sufficient to obtain yeast strains for probing the chromatin of a region of interest. More details of the construction of pSH1052 and its full DNA sequence are available on request. In the absence of E_2, LexA-ER-VP16 is transcriptionally inactive. Increased transcription of M.CviPI occurs in the presence of E_2, which is ectopic to yeast and thus does not affect normal yeast physiology (i.e., avoids heat shock, changes in carbon source, etc.). In particular, ectopic induction with E_2 enables the study of the chromatin structure of commonly studied inducible

promoters, such as *CUP1* and *GAL1*.

Approximately 0.5 μg of pSH1052 DNA are digested with AatII and AscI (as specified by the manufacturer) to release the plasmid backbone (colE1 origin of DNA replication and ampicillin resistance marker). Digestion also creates double-stranded breaks adjacent to *HO* sequences that facilitate integration at the *HO* locus by homologous, one-step gene replacement (Voth et al., 2001). A small aliquot of digested DNA is electrophoresed on an agarose gel in parallel with a DNA size-marker and uncut plasmid to verify complete plasmid digestion. A DMTase-expression plasmid for integration at *ADE2* is also available on request. Plasmids that express DMTases from the galactose-regulated *GAL1* promoter and/or integrate at the *LYS2* locus are also available.

Integration at the *HO* locus is achieved by inoculating 10 ml of appropriate medium (enough for 2 transformations) with freshly plated yeast cells and incubating with shaking (300 rpm) overnight at 30˚C. The following morning, dilute the culture to an optical density at 600 nm (OD_{600}) of 0.5 and incubate with shaking (300 rpm) at 30˚C. When the cell culture reaches an OD_{600} of 2, pellet the cells and resuspend them in 25 ml of sterile dH_2O. The cells are then pelleted, resuspended in 1 ml 100 mM lithium acetate ($LiC_2H_3O_2$), and transferred to a 1.7 ml microcentrifuge tube. Cells are pelleted again (5 sec in a microcentrifuge), resuspended in 80 μl 100 mM $LiC_2H_3O_2$, and divided into two 40 μl aliquots for individual transformations. Remove excess $LiC_2H_3O_2$ after pelleting the cells. Next, resuspend the cells in 240 μl 50% (w/v) polyethylene glycol. Add 36 μl 1 M $LiC_2H_3O_2$, 10 μl of 10 mg/ml single-stranded herring sperm DNA,

approximately 0.5 μg of digested plasmid DNA per transformation, bring to 50 μl total volume with dH_2O, and vortex well. Incubate for 30 min at 30˚C and then heat shock for 30 min in a 42˚C water bath. After pelleting the cells, remove the supernatant, resuspend the cells in 100 μl dH_2O, plate on appropriate selective medium (lacking lysine for pSH1052, which contains *LYS2* as a selectable marker), and incubate at 30˚C. A DMTase expression vector that contains a *LEU2* selectable marker is also available. Single colonies are picked after 2-3 days and streaked on a second selective plate to obtain single, pure colonies.

Probes for targeting DNA methylation are constructed by integrating M.CviPI directly at the gene coding for the DNA-binding protein of interest to create an in-frame fusion protein that is expressed from the endogenous yeast promoter. We have constructed a set of plasmids for PCR amplification of either M.CviPI or M.SssI (and selectable marker) and integration at either the N- or C-terminus by one-step gene replacement in yeast. The DMTase fusion protein can also be expressed from a plasmid or when integrated at an exogenous locus. Both N- and C-terminal fusions of M.CviPI (and M.SssI) retain DMTase activity (C. Carvin and M. Kladde, unpublished results). The DMTase and DNA-binding protein are separated by a flexible glycine-serine linker and a triple hemeagglutinin (HA) epitope tag. After transformation, correctly integrated DMTases are screened for by colony PCR and for DMTase activity by McrBC digestion.

Screening for Yeast Strains with Functional C5 DMTases

In order to screen for functional C5 DMTases, conditions for high-level expression of

DMTase and accumulation of m^5C are employed. Strains with integrated pSH1052 (free DMTase probe) are induced with 100 nM E_2; strains containing the TAGM probe (M.CviPI fused to *PHO4*) are induced by starvation for inorganic phosphate (P_i). Yeast cultures (5 ml) are first grown at 30˚C to an OD_{600} ~1, then pelleted and resuspended in 5 ml inducing medium at a similar density, and incubated at 30˚C overnight with shaking. By inoculating at such a high density, the cells will enter late log growth relatively quickly, slowing DNA replication and hence accumulating high levels of m^5C.

To isolate DNA, the cells are pelleted, resuspended in 0.7 ml 1× TE, pH 8.0, and transferred to 2 ml screw-cap microcentrifuge tubes. Acid-washed glass beads (0.3 g, 425-600 μm in diameter) are added and the cells are pelleted for 5 sec. Remove the supernatant and add the following reagents in order: (i) 0.2 ml 1× TE, pH 8.0; (ii) 0.2 ml smash buffer (10 mM Tris-HCl, pH 8.0, 2% Triton X-100, 1 mM EDTA, 1% SDS, 100 mM NaCl); (iii) 0.2 ml $CHCl_3$:IAA (24:1); and (iv) 0.2 ml equilibrated phenol. Vortex the samples for 8 min and then separate the phases by centrifugation at 14,000 rpm for 5 min, both at room temperature. Transfer the supernatant to a new 1.7 ml microcentrifuge tube containing 0.2 ml 10 M $NH_4C_2H_3O_2$, vortex, and incubate on ice for 2 hr to overnight. Pellet the samples for 5 min at 14,000 rpm at room temperature. Removal of the insoluble material, which is not RNA or DNA, increases the efficiency of subsequent procedures. Transfer the supernatant to a new 1.7 ml microcentrifuge tube containing 0.6 ml isopropanol and mix thoroughly. Pellet the nucleic acids by centrifugation at 14,000 rpm for 5 min at room temperature. Decant the supernatant, wash the pellet by the addition of 0.3 ml 70% EtOH:30% TE, pH 8.0, and

then pellet the nucleic acids for 2 min at 14,000 rpm at room temperature. Remove the supernatant, dry the pellet, and resuspend the samples in 50 μl of 0.1× TE, pH 8.0. It is not necessary to remove the RNA.

Screening for correct integration of DMTases by colony PCR requires two sets of primers. The first primer set is designed to amplify the protein of interest prior to fusion to the DMTase (negative control); the second primer set amplifies the newly created fusion gene. One primer, either in the ORF or terminator (C-terminal fusion) or promoter (N-terminal fusion) of the tagged gene of interest, may be shared between the two sets. The following reaction conditions (final concentrations) are used to amplify regions of interest: 0.5 μM each primer, 1.25 U Taq DNA polymerase, 1× Taq buffer, 1.5 mM $MgCl_2$, 0.2 mM dNTPs, dH_2O to 20 μl; prepare on ice. Add an amount of yeast cells that fits on the end of a P200 pipet tip directly to each PCR. Thermocycling parameters are: preheat to 94˚C; 1 cycle of 94˚C for 8 min; followed by 29 cycles of 94˚C for 1 min, 8˚C below the calculated T_m (Breslauer et al., 1986) for 1 min, 72˚C for 1 min per kilobase that is amplified; and a final extension of 72˚C for 4 min. PCR product (10 μl) and DNA size markers are electrophoresed on a 0.7% (w/v) TAE agarose gel containing 0.5 μg/ml ethidium bromide and viewed on a transilluminator.

Best results are obtained when the PCR fragment to be amplified is ≤ 1 kbp in length. If colony PCR analysis does not yield satisfactory product yields or larger fragments are to be amplified, standard PCR amplification using isolated yeast genomic DNA can be performed. Alternatively, correct integration can be determined by Southern analysis.

Rapid identification of functional C5 DMTases can be performed by McrBC endonuclease digestion. This type I endonuclease complex cleaves many sites between two (G/A)m^5C half-sites located between 32 bp and 2 kbp apart (Gasser et al., 1998). Thus, McrBC digestion of genomic DNA requires high levels of C5 methylation and results in a smearing pattern when electrophoresed on an agarose gel (Figure 2-1). For best results, we typically mix dH_20 (to bring to volume), the supplied enzyme buffer, GTP (1 mM), acetylated BSA (100 μg/ml), and ~0.2 μg genomic DNA. Next, the mixture is divided into two equal reactions, then 10 U McrBC enzyme (New England BioLabs) or an equal volume of 50% glycerol is added, followed by incubation for 1 hr at 37˚C. SDS (to 0.1%) is then added to disrupt McrBC-DNA binding. Add 1 μl 3 mg/ml RNase A, electrophorese on a 0.7% (w/v) TAE agarose gel containing 0.5 μg/ml ethidium bromide, and view on a transilluminator. If levels of m^5C are inadequate for efficient McrBC digestion, bisulfite sequencing provides increased sensitivity of m^5C detection. Once strains positive for DMTase expression have been identified, cells are grown under selection for the marker on the DMTase vector until an OD_{600} of ~1 is reached, and then a frozen stock is prepared.

In Vivo Analysis of Chromatin Structure and Factor Binding

Following construction of DMTase-positive strains, cells are cultured under the desired conditions and DNA is rapidly isolated. Levels of m^5C at accessed DMTase target sites are positively identified by bisulfite sequencing analysis. Best results are obtained when strains are freshly plated from frozen stocks under conditions that select for the DMTase

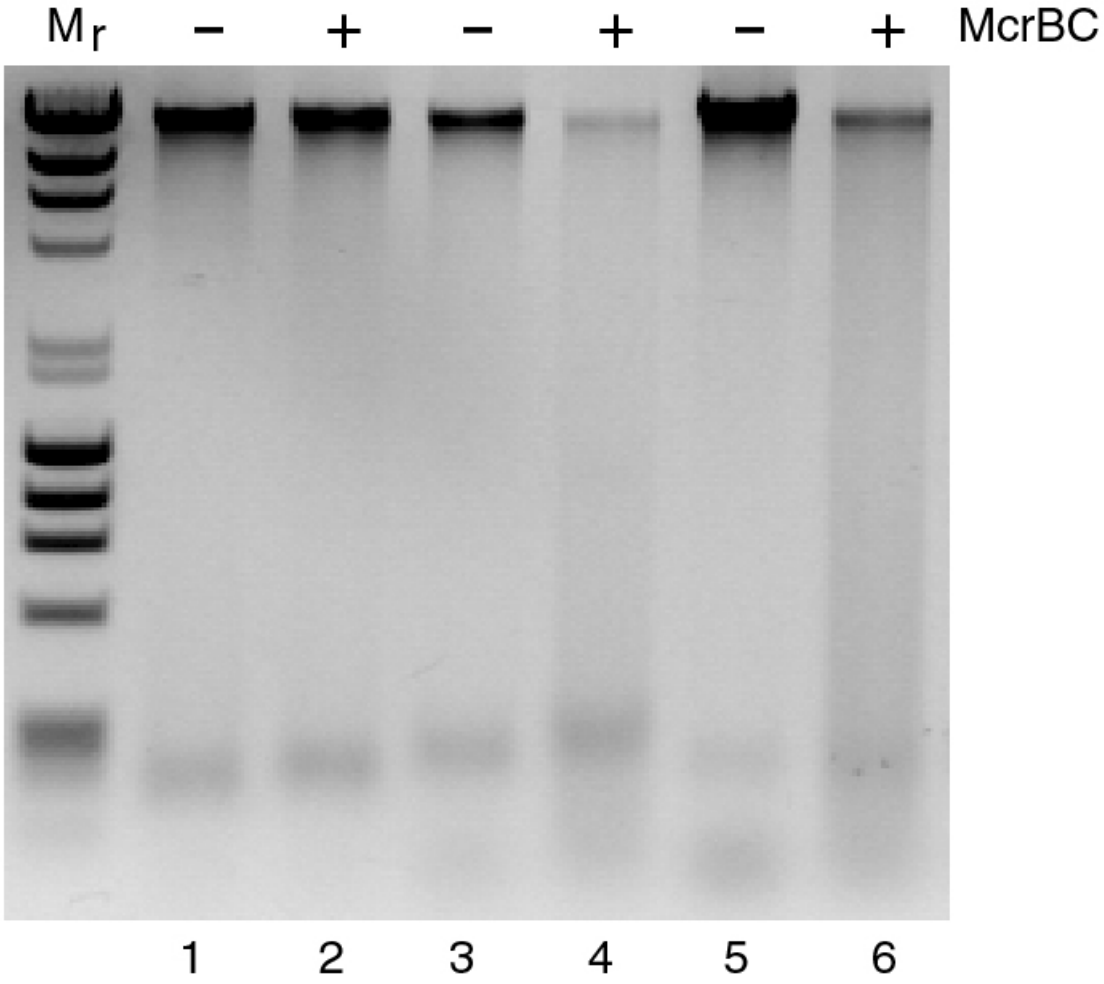

Figure 2-1. Identification of Functional M.CviPI by McrBC Digestion

Cells derived from three different M.CviPI transformants were treated with 100 nM E_2. Isolated genomic DNA was dissolved in the specified reaction conditions, divided equally, and treated with McrBC (+) or 50% glycerol (–) as indicated. Compared to the glycerol-treated control (lanes 3 and 5), McrBC thoroughly digested DNA from transformants 2 and 3 (lanes 4 and 6), producing a smear of lower molecular-weight fragments. DNA from transformant 1 (lanes 1 and 2) lacking M.CviPI activity serves as a negative control. M_r, HindIII-digested λ and HaeIII-digested ϕX174 RF DNA.

and are used as soon as possible (within two weeks). Also, avoid storage of these cells to 4˚C. Yeast cultures are grown under conditions specific for the region being studied using the appropriate inducer and/or media conditions for DMTase expression. It is not necessary to grow starter cultures under selective conditions if the DMTase is integrated. All cultures are kept in early log phase ($OD_{600} < 1$). Approximately 4 μg of genomic DNA is isolated per sample (equivalent to 20-25 ml of cells at an $0.5 < OD_{600} < 1$). For each sample, genomic DNA is isolated as outlined above.

Freshly prepare 3 N NaOH and 100 mM hydroquinone by dissolving each chemical in degassed dH_2O. Mix gently by inversion to avoid aeration. Pipet 20 μl total genomic DNA into a 0.65 ml microcentrifuge tube (which also fits in a thermocycler) containing 10 μl of 3× denaturation buffer (per sample, to be added to 20 μl genomic DNA: 3.0 μl 3 N NaOH, 0.7 μl 3 mg/ml sheared calf thymus DNA, 0.5 μl 0.5 M EDTA, pH 8.0, 5.8 μl degassed dH_2O). Saturated sodium metabisulfite solution is made as follows: to a 20 ml-capacity glass scintillation vial containing a small stir bar, add 0.1 ml of 100 mM hydroquinone, 5 g sodium metabisulfite [from previously unopened air-tight vial; we aliquot 0.5-1 kg sodium metabisulfite (Aldrich) and fill 5 g glass vials nearly to the brim in an oxygen- and H_2O-free chemical safety hood; vials are capped tightly and stored in the dark in a sealed vessel that contains Drierite], and 7 ml degassed dH_2O; the solution is immediately stirred and 1.0 ml 3 N NaOH is quickly added. The solution is adjusted to pH 5.0 at room temperature with additional 3 N NaOH and preheated to 50˚C in a water bath. At this point, the solution should be saturated with visible, undissolved crystals of sodium metabisulfite. A saturated solution is employed to promote

sulfonation of cytosine, the first step of bisulfite deamination, and to simplify reagent preparation. Samples of genomic DNA in 3× denaturation solution are heated at 98˚C for 5 min with the tube caps open in a thermocycler. With 1 min remaining in the denaturation step, transfer the preheated sodium metabisulfite solution to a stir-plate and stir gently. After 5 min denaturation, rapidly add 0.2 ml of sodium metabisulfite directly to each sample while in the thermocycler. Quickly cap the samples, vortex, and incubate for 6 hr in covered water bath at 50˚C. Overlaying each reaction with mineral oil can be omitted without affecting deamination efficiency.

After incubation, the samples are desalted. Transfer the samples to a 1.7 ml microcentrifuge tube and add 1 ml Promega Wizard PCR Preps resin. After mixing, transfer successive aliquots of the resin suspension directly to a minicolumn (no syringe) under vacuum until all of the resin is filtered. Then, attach syringe barrels and wash the resin 3× with 1 ml 80% isopropanol, ensuring complete evacuation of the column between washes. These procedures guard against residual contamination with guanidinium, which decreases subsequent yields of PCR product. Detach each minicolumn containing the resin from the syringe barrel and insert it into a new 1.7 ml microcentrifuge tube. Remove residual isopropanol by centrifugation at 14,000 rpm for 2 min in a microcentrifuge. Transfer the minicolumns to a new 1.7 ml microcentrifuge tube. Add 52 µl of 0.1× TE (preheated to 95˚C) and incubate for 5 min at room temperature. Elute the DNA by centrifugation of the minicolumns at 14,000 rpm for 20 sec.

Desulfonate the DNA (i.e., deaminated cytosines are uracil sufonate at this stage, Figure 2-2) by adding 8 µl desulfonation solution to each sample and incubating for 15 min at 37˚C. To neutralize the samples, add 18 µl 10 M $NH_4C_2H_3O_2$ and vortex. Add 0.2 ml of absolute ethanol and precipitate the DNA by incubation overnight at −20˚C (required for efficient recovery of deaminated DNA). The following day, pellet the DNA by centrifugation at 14,000 rpm for 30 min at room temperature. Remove the supernatant, add 0.3 ml 70% EtOH:30% TE, pH 8.0, and centrifuge the samples for 2 min at 14,000 rpm at room temperature. Remove the supernatant, dry the pellet, and resuspend the samples in 25 µl 0.1× TE, pH 8.0.

The efficiency of chemical conversion of unmethylated cytosine residues to uracil is on the order of 99.5-99.7% (Warnecke et al., 2002; our unpublished observations). Using the above deamination protocol, we routinely achieve 99.8% efficiency of cytosine conversion and have not observed artifacts reported for bisulfite sequencing (Warnecke et al., 2002).

Following bisulfite treatment, the upper and lower DNA strands are no longer complementary and separate primer sets are required to amplify each strand (Figure 2-3). Primers for PCR amplification of deaminated DNA are designed to anneal to sequences flanking a region of interest. Primer design is the most crucial aspect for achieving high-quality bisulfite sequencing results. It is critical that primers for PCR with deaminated DNA do not amplify the region from non-deaminated DNA. Thus, the initial primer that anneals to either the upper or lower DNA strand contains G to A or C to T transitions, respectively, and vice versa for the converging primer of each primer pair (Figure 2-3).

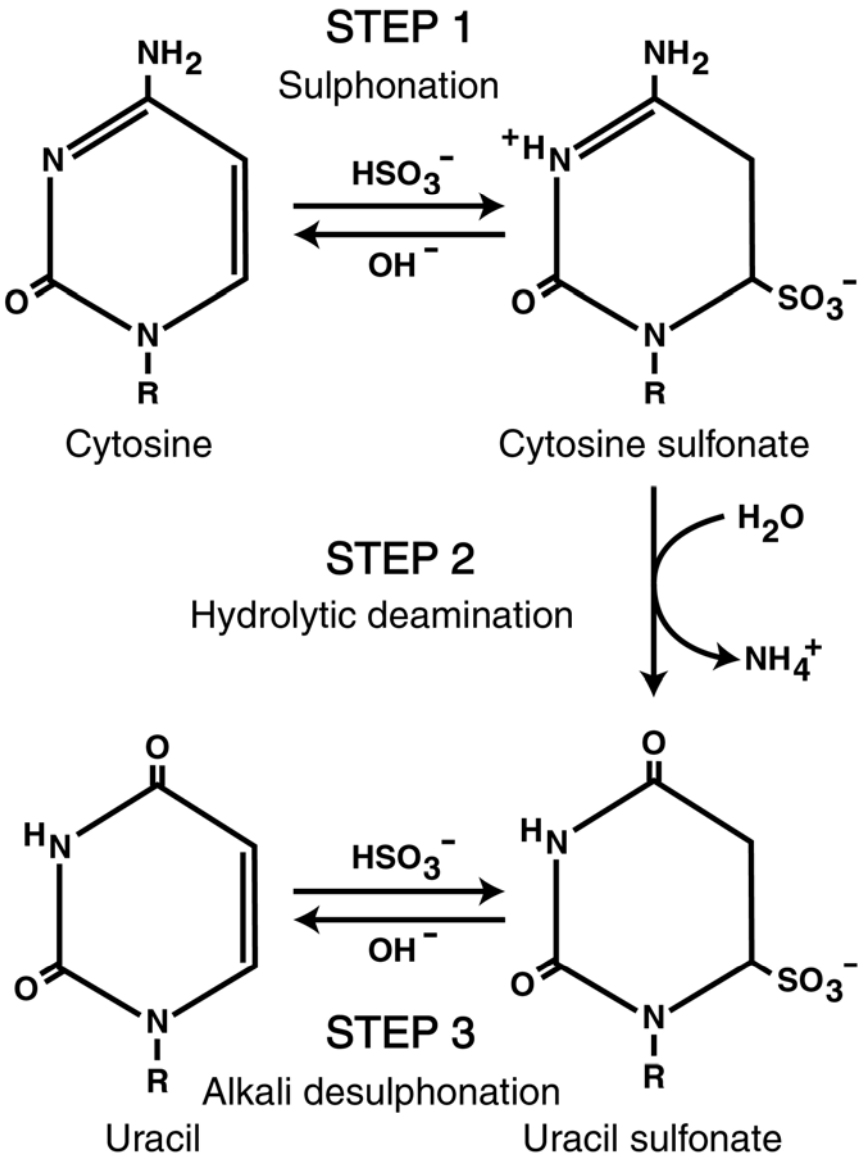

Figure 2-2. Sodium Bisulfite Modification of Unmodified Cytosine

Unmethylated cytosine is converted to uracil through a three-step process during sodium bisulfite modification. This conversion does not occur on cytosines that have been methylated.

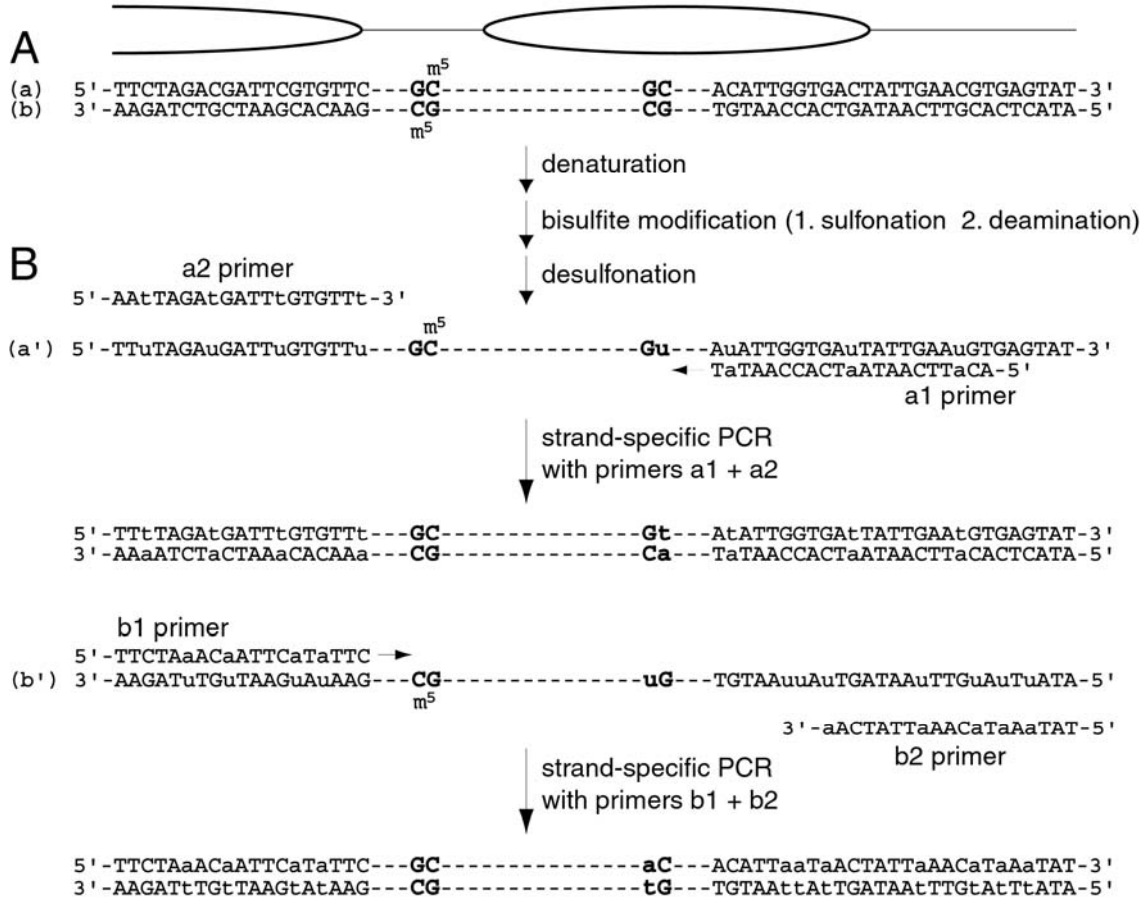

Figure 2-3. Detection of 5-Methylcytosine by Bisulfite Sequencing

(A) A hypothetical region with GC sites (bold) in a histone-free linker that is accessible to M.CviPI in vivo and thus methylated (m^5C) or at an inaccessible position in a nucleosome (ellipse). Total genomic DNA is denatured to upper (a) and lower (b) single-strands and treated with sodium metabisulfite. During bisulfite treatment, cytosines are sulfonated and then deaminated to produce a sulfonyl adduct of uracil. Subsequent treatment with alkali effects removal of the sulfonyl moiety (desulfonation).
(B) Strand-specific PCR amplification of bisulfite-treated DNA. Cytosine, but not m^5C, residues of the upper (a') and lower (b') DNA strands are deaminated and converted to uracil (lower case), resulting in DNA strands that are no longer complementary. The region of interest from each of the deaminated DNA strands is amplified in separate
reactions by the primer pairs 'a1' and 'a2' or 'b1' and 'b2'. In the design of the a2 and
b2 primers, all cytosines are changed to thymines (C to t). Conversely, the a1 and b1 primers are designed with guanine to adenine (G to a) transitions. The cytosines remaining in the population of amplified PCR products are detected by thermal cycle sequencing of the PCR product using ^{32}P-end-labeled primers a1 or b1 (or a primer internal to a1 or b1). Omission of dGTP and inclusion of ddGTP in the sequencing mix yields efficient termination at cytidines in the template strand.

Most importantly, disperse transitions as evenly as possible throughout the primer sequence to prevent amplification of non-deaminated DNA. One or two transitions can also be incorporated at the 3' end of each primer. Additionally, avoid: (i) long stretches of thymines or adenines (>7 bp), which destabilize binding and reduce specificity; and (ii) DMTase target sites. If avoiding DMTase target sites is not possible, potential amplification biases can be avoided by incorporating degenerate bases (G/A or C/T) in primers at the location of potentially methylated cytosines. In practice, amplification biases are only a concern in TAGM analysis as a high percentage of a DMTase target site can be modified. This is not a concern in analysis of chromatin structure by free DMTases – low levels of DMTase expression ensure that >90% of each DMTase target site is unmethylated (Kladde et al., 1996).

The reaction conditions (final concentrations) for 'hot-start' PCR amplification, which must be employed, are: 0.8 μM each primer, 1.25 U JumpStart Taq (Sigma), 1× JumpStart Taq buffer, 2.25 mM $MgCl_2$, 0.2 mM dNTPs, 1 μl of deaminated genomic DNA, dH_2O to 50 μl; prepare on ice. Cycling parameters are: 1 cycle of 94˚C for 2 min; followed by 29 cycles of 94˚C for 30 sec, 8˚C below the calculated T_m for 30 sec, 72˚C for 1 min per kilobase that is amplified; and a final extension of 72˚C for 4 min. PCR products are analyzed by 0.7% (w/v) TAE agarose-gel electrophoresis to ascertain the presence of a single amplification product. Products that are not full length will produce run-off primer extension products in the subsequent analysis that severely compromise data quality, i.e., can be mistaken for m^5C residues. PCR products are purified via Millipore Montage PCR Filters (cat. #UFC7PC250) as directed by the manufacturer,

since superior results are obtained compared to resin-based methods. PCR products are eluted with 15-20 μl 0.1× TE and their concentration is determined by analyzing 1 μl on a 0.7% (w/v) TAE agarose gel containing 0.5 μg/ml ethidium bromide.

A primer specific to the strand of interest is end-labeled: up to 20 pmole primer, 80 μCi [γ-^{32}P]ATP (6000 Ci/mmole), 1× T4 polynucleotide kinase buffer, 10 U polynucleotide kinase, dH_2O to 20 μl; incubate at 37˚C for 1 h. Unincorporated radionucleotide is removed with a Sephadex G-50 spin column. Primer is kept on ice or stored at −20˚C. As cytosines in the PCR product template are to be detected, always end-label the primer that contains the G to A transitions. While the initial PCR amplification primer can be end-labeled, a nested primer usually yields superior results.

Pipet 0.1 pmole of purified PCR product into a 0.65 ml microcentrifuge tube and place on ice. Each thermocycle sequencing reaction contains: 1 pmole radiolabeled primer specific to the strand of interest, 1× Sequitherm buffer, 1.25 U Sequitherm DNA polymerase (Epicentre, Madison, WI), 50 μM each of dATP, dCTP, and dTTP, 150 μM ddGTP, dH_2O to 8 μl. A mixture sufficient for the number of reactions being analyzed is prepared on ice. We have empirically determined that Pharmacia ultrapure ddGTP (cat. #27-2071-01) provides the best results. If absolute levels of methylation at each site are needed, the primer extension reaction should contain 5 μM each of dATP, dCTP, and dTTP, and 50 μM ddGTP (Kladde et al., 1996). However, typically, the data are superior in the presence of the higher nucleotide concentrations because less nonspecific primer extensions pauses occur. Sequencing ladders are obtained by transferring 4 μl of a mixture containing ~0.2-0.3 pmole PCR product DNA, 1-2 pmole ^{32}P-end-labeled

primer, 1.5× Sequitherm buffer, and 1.25 U Sequitherm DNA polymerase to tubes containing 2 μl of each sequencing mix. PCR parameters are: 1 cycle of 94˚C for 2 min; followed by 11 cycles of 94˚C for 30 sec, 8˚C below the calculated T_m for 15-30 sec, 70˚C for 1 min per kilobase that is amplified. When thermocycling is complete, add 0.5 volumes of 3× sequencing stop solution [containing 95% (v/v) deionized formamide, 10 mM EDTA, pH 7.6, 0.025% (w/v) bromophenol blue, 0.025% (w/v) xylene cyanole FF], vortex, and place on ice. Denature the samples at 70˚C for 5 min and quick chill on ice. Electrophorese 4 μl on a denaturing 4-6% polyacrylamide (19:1 acrylamide:bis-acrylamide), 50% urea gel. Gradient gels (top chamber buffer, 0.5× TBE; lower chamber buffer, 1-1.5 M $NaC_2H_3O_2$, 0.66× TBE) can be used to increase resolution in the upper part of the gel (Sheen and Seed, 1988). Note that lower molecular-weight products are not lost but are compressed at the bottom of the sequencing gel. As this includes excess primer, the end of the gel is highly radioactive and care should be taken to prevent personal exposure and contamination. Dry the gel and visualize by phosphorimager.

RESULTS

In bisulfite sequencing analysis, the intensity of each primer extension product on the resulting phosphorimage is directly proportional to the degree of m^5C incorporated at that site in vivo. If the chromatin structure is already known, product intensities are normalized to a histone-free linker region where m^5C levels will be equivalent between samples. Changes in relative methylation frequency are a function of probe accessibility; enhanced methylation is indicative of increased accessibility that accompanies

nucleosome disruption or direct targeting of m^5C by TAGM. In contrast, protection against methylation demonstrates site blockage by DNA-bound factors (i.e., factor footprints) or nucleosomes.

While the phosphorimage is often convincing by itself, quantitative analysis with ImageQuant software (Molecular Dynamics) using the "create graph" function is often informative. This analysis allows a visual comparison of the relative peak heights and areas that directly correspond to the relative frequencies of site methylation. Further analysis of absolute levels of m^5C at each site can be obtained by dividing the absolute number of radioactive counts (designated volume in ImageQuant) of a given band by all summed product intensities, including the run-off product at the top of the gel. Background is corrected using the local average setting. The run-off product is generated by primer extensions that do not terminate, either because a template is devoid of cytidines (i.e., was unmethylated in vivo) or ddGTP incorporation fails at one or more template cytidines. Using the lower specified nucleotide concentrations, termination efficiency at template cytidines is >96%, enabling determination of absolute m^5C levels (Kladde et al., 1996). At the higher concentration, dATP, dCTP, and dTTP are misincorporated at template cytidines, decreasing termination efficiency and leading to an underestimation of absolute m^5C frequencies. However, we usually employ 50 μM dATP, dCTP, and dTTP, since primer extension efficiency increases and higher quality data are obtained.

As in any footprinting analysis, rigorous, quantitative comparison of product intensities (volumes) requires single-hit kinetic levels of modification, which is governed

by Poisson statistics. Therefore, the sum of calculated absolute intensities of m^5C should be ≤ 37% if strict quantification is needed. Stated differently, in a given lane, relative levels of m^5C will be underestimated when the sum of lower molecular-weight products exceeds 37% of the total counts loaded.

The *GAL1* promoter is organized into positioned nucleosomes B and C located downstream of a histone-free region that contains four upstream activating sequences (UASs I-IV), sites of Gal4 binding that comprise the UAS_G region (Bash and Lohr, 2001). Analysis of the promoter chromatin under repressive and activating conditions on probing with free M.CviPI is shown in Figure 2-4. Strains were initially grown under repressive conditions in YPPD. The rich medium is supplemented with P_i as it is limiting for this nutrient (Neef and Kladde, 2003). Following overnight growth, cultures were pelleted, washed, and resuspended in galactose-containing medium (YPPG) to activate *GAL1*. After 5 hr activation, genomic DNA was rapidly isolated from cells before (0 min) or after (80 min) induction of M.CviPI synthesis by the addition of 100 nM E_2.

Under repressive conditions in glucose (Figure 2-4, lanes 1 and 2), methylation at most M.CviPI target sites in the UAS_G region (−453 to −336) increased with E_2 treatment. This is expected since UAS_G is located in a histone-free region of the *GAL1* promoter and hence m^5C levels should accumulate on induction of the DMTase probe. In contrast, relative to GC sites in UAS_G, those from −282 to −173 were protected against methylation by the B nucleosome.

Changes in the methylation pattern at the *GAL1* promoter were evident on activation by galactose. Methylation levels over the promoter can be normalized to those

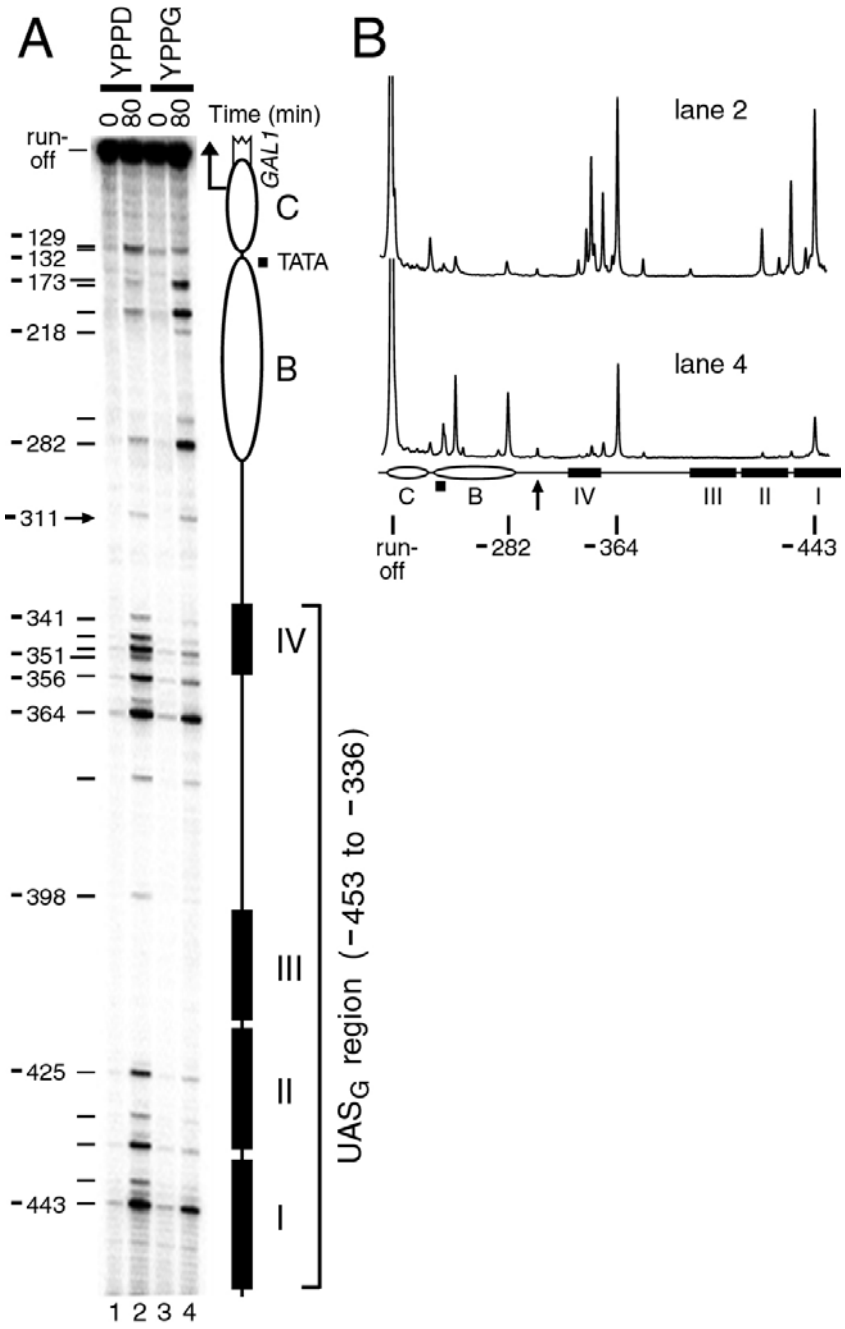

Figure 2-4. Analysis of *GAL1* Chromatin Structure in Living Cells Using Free M.CviPI

Cells grown under repressive (YPPD, dextrose, lanes 1 and 2) or activating conditions (YPPG, galactose, lanes 3 and 4) were subsequently untreated (0 min, lanes 1 and 3) or treated with 100 nM E_2 for 80 min (lanes 2 and 4) to induce M.CviPI synthesis. The bisulfite sequencing results are shown in the phosphorimage (A) or quantitative scans (B) of the indicated lanes. Ellipses, positioned nucleosomes B and C; black rectangles, Gal4 binding sites I-IV; filled bar, TATA element; black arrowhead, major transcription initiation site; broken open rectangle, *GAL1* coding sequence. Nucleotide distances relative to the *GAL1* ATG start codon of cytosines of select GC sites are indicated at the left.

of GC site −311 (straight arrow), which is not associated with a nucleosome and is located at a significant distance from the known Gal4 binding sites I-IV. The relatively high degree of m^5C at Gal4 sites I and II (GC sites −443 to −425) as well as IV (GC sites −351 to −341) in glucose is substantially diminished under activating conditions (compare lane 2 to 4). Protection in this region against methylation by M.CviPI is consistent with the known interaction of Gal4 homodimers. Protection of GC site −398 and sites −364 to −341 is likely due to steric occlusion of M.CviPI on Gal4 binding to sites III and IV, respectively. In vitro, purified Gal4-AH also protects sites next to a Gal4 UAS from modification by a DMTase (Xu et al., 1998b). In addition, protection near the TATA box is observed. Lastly, m^5C levels increase at several GC sites (−282 to −173) in galactose vs. glucose. This is in accord with the known perturbation of the B nucleosome that accompanies Gal4 binding and transactivation (Bash and Lohr, 2001).

More generally, as a first approximation, protection against methylation of GC (or CG if using M.SssI) sites spanning ~100 nucleotides suggests the presence of a positioned nucleosome. The protection of less than core particle-length DNA (147 bp) is due to increased access of DMTases to ~25 bp of DNA at nucleosomal termini (Kladde and Simpson, 1994; Kladde et al., 1996; Xu et al., 1998b). Regions of protection significantly less than 100 bp will typically correspond to binding of non-histone factors. Growth of cells under various conditions known to affect factor binding (e.g., glucose vs. galactose), deletion of genes coding for likely binding factors (e.g., *GAL4*), or binding site mutations will provide corroborative evidence for the identity of the bound factor. Finally, mapping the chromatin architecture of new regions requires comparison

of DMTase accessibility in chromatin to that in protein-free DNA, which is methylated in vitro. A hexahistidine-tagged version of M.CviPI is available for purification (Xu et al., 1998a) and M.SssI is commercially available (New England BioLabs).

Bisulfite sequencing analysis occasionally yields artifactual bands. Usually, these correspond to run-off primer extension products on templates that are not full length. Bands that do not map to known DMTase target sites can also arise due to paused polymerases as opposed to termination of extension by ddGTP incorporation. Lastly, albeit seldom in our experience, incomplete conversion of unmethylated cytosines during the bisulfite deamination procedure will yield ddGTP-dependent terminations at positions that do not correspond to cytosines in known GC sites. These primer extension artifacts can be discerned by processing a DMTase-negative strain in parallel throughout the bisulfite sequencing analysis.

An additional, powerful strategy for monitoring DNA-protein interactions in vivo relies on fusing the DMTase directly to a DNA-binding factor of interest, designated the targeting factor (Figure 2-5; Carvin et al., 2003a). Methylation is selectively increased at two classes of nucleosome-free, and hence accessible, sites in regions bound by the targeting factor. First, m^5C is enhanced proximal to the targeting factor binding site. Using glycine/serine-rich linker peptides of ~20 amino acids in length, this distance is typically about 10-40 nucleotides (Xu and Bestor, 1997; McNamara et al., 2002; Carvin et al., 2003a). Second, DNA methylation is also enhanced at distances up to several hundred nucleotides from the site of targeting factor interaction (van Steensel and Henikoff, 2000; Carvin et al., 2003a). Methylation at such distances is consistent with

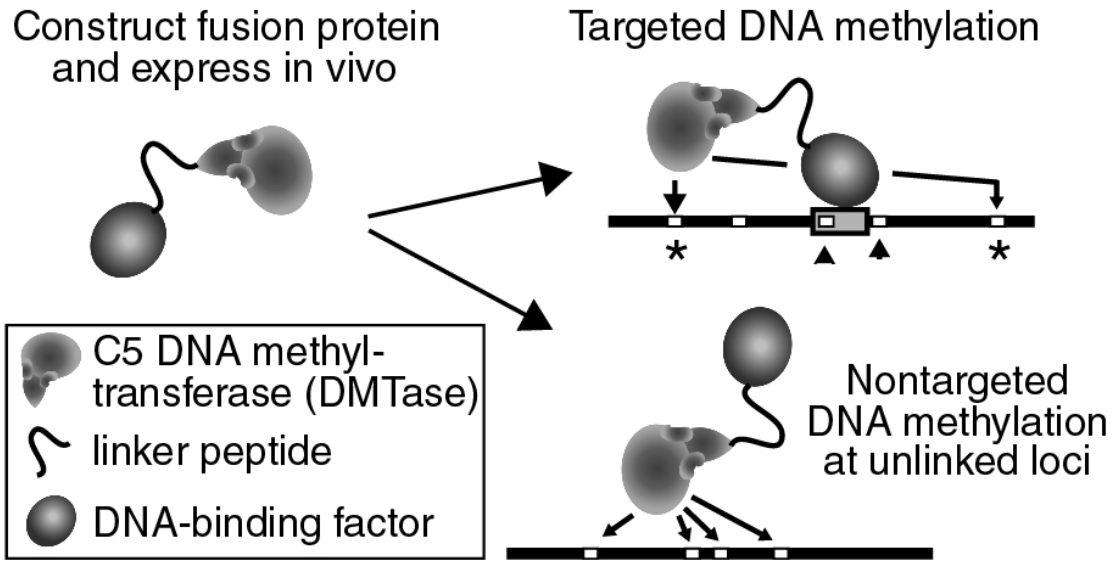

Figure 2-5. The Targeted Gene Methylation (TAGM) Strategy

Either M.CviPI or M.SssI is fused to the N- or C-terminus of a DNA-binding factor of interest (i.e., the targeting factor). On expression of the fusion protein in yeast under appropriate conditions, high-affinity binding at a cognate factor binding site leads targeted m^5C (asterisks, upper right). In addition, nontargeted DNA methylation occurs at unlinked loci (bottom right). Adapted from Carvin et al. (2003).

the juxtaposition of sites by nucleosomes and/or higher-order chromatin structure that would otherwise be more remote in protein-free DNA.

The identification of both proximally and distally targeted m^5C requires comparison of methylation patterns produced by the DMTase fusion and a suitable 'free' DMTase control. This control reveals preferences for nontargeted DNA methylation due to nearest-neighbor sequences and chromatin environment. As fusion of factors to DMTases can decrease the affinity of the DMTase for DNA (Xu and Bestor, 1997), the best-suited control is the fusion protein in which an amino acid substitution(s) inactivates the DNA-binding capability of the targeting factor. If no such mutant is available or there are concerns of residual targeting factor DNA binding, in practice, the free DMTase or equivalent (e.g., mut Zif-M.CviPI; see below) is adequate. In addition to detecting sites of targeted m^5C, the free DMTase control will usually identify the targeting factor binding site and any disrupted nucleosomes.

Application of TAGM using the transactivator Pho4 to target M.CviPI to the *PHO5* promoter, which expresses the major yeast acid phosphatase, is shown in Figure 2-6 (also see Carvin et al., 2003a). M.CviPI was integrated by site-specific recombination at the C-terminus of the endogenous *PHO4* gene. Control studies have been performed to ensure that fusion of the DMTase does not impair the function of the Pho4 targeting factor function (Carvin et al., 2003a). For the free DMTase control, M.CviPI was fused to a DNA-binding-deficient variant of Zif268, mutant (mut) Zif-M.CviPI, expressed from the *GAL1* promoter in medium containing galactose.

In Figure 2-6, the mut Zif-M.CviPI and Pho4-M.CviPI strains were grown overnight in high-P_i medium (+P_i) and then shifted to P_i-free medium (−P_i). After the indicated times, genomic DNA was isolated and m^5C at the *PHO5* promoter was assayed by bisulfite sequencing. When compared to the free DMTase control (lanes 1 and 2), m^5C and hence M.CviPI, is preferentially targeted to three GC sites near UASp1 (−343 and −330) and UASp2 (−240). These sites are readily identified by inspecting for alterations in relative band intensities in a given lane for the DMTase fusion as compared to the free DMTase control (Figure 2-6A, compare lanes 3-5 to lanes 1 and 2). Often, as shown in Figure 2-6B, quantitative scans of the phosphorimage with ImageQuant software are useful in discerning sites to which m^5C is directly targeted. For instance, with free mut Zif-M.CviPI, methylation at GC site −337 exceeds that at flanking sites −343 and −330. In contrast, expression of Pho4-M.CviPI leads to reversal of the relative band intensities; m^5C at both −343 and −330 surpasses that at −337. Remarkably, m^5C is clearly targeted upstream of UASp1 even in high P_i, which leads to predominant cytoplasmic localization of Pho4 (O'Neill et al., 1996). This basal level of Pho4 binding is not detectable by the commonly used technique of chromatin immunoprecipitation (ChIP) analysis (Carvin et al., 2003a).

DISCUSSION

DMTases are the least invasive of available chromatin mapping probes. As their use avoids DNA damage, cell permeabilization, or isolation of nuclei, experiments can be performed in living cells. The combined use of the C5 DMTases M.CviPI and M.SssI

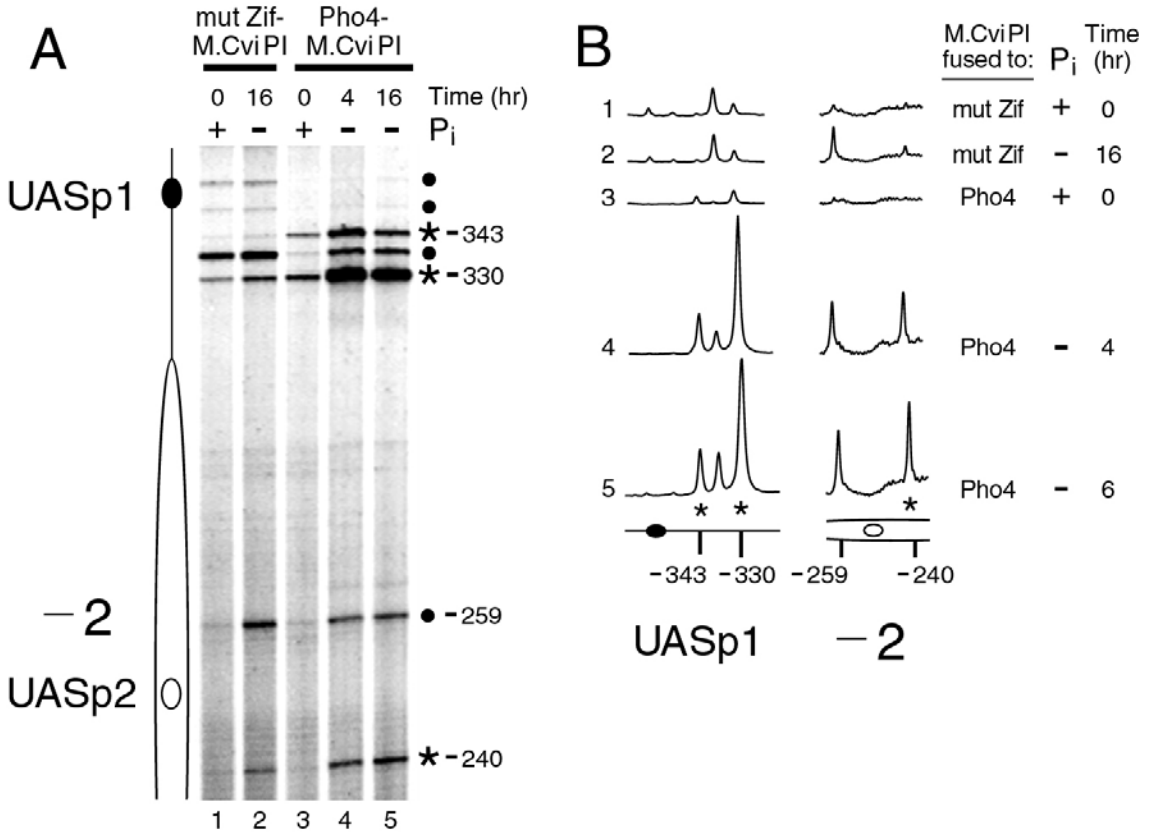

Figure 2-6. Targeting M.CviPI to *PHO5* by Fusion to the PHO Transactivator Pho4

Cells expressing the control free DMTase (mut Zif-M.CviPI, lanes 1 and 2) or Pho4-M.CviPI (lanes 3-5) were initially grown in the presence of high P_i (lanes 1 and 3). Under these conditions, the *PHO5* promoter is repressed and packaged into positioned nucleosomes (Almer and Hörz, 1986) due to the predominant cytoplasmic localization of Pho4 (O'Neill et al., 1996). After overnight growth, cells were either kept in high-P_i medium or *PHO5* transcription was activated by transfer to P_i-free medium as a result of accumulation of Pho4 in the nucleus (O'Neill et al., 1996). Both media also contained galactose to induce probe expression in the strain containing the free DMTase (and employ identical conditions for the *PHO4*-M.CviPI strain). Sites of targeted (*) and nontargeted (•) m^5C in the phosphorimage (A) or quantitative scans (B; lanes indicated at left). Ellipse, positioned nucleosome −2; filled oval, Pho4 binding site UASp1; open oval, UASp2. Nucleotide distances relative to the *PHO5* ATG of select GC sites are indicated at the right.

enable probing of the accessibility of one GC and CG site, respectively, on average every 12-15 bp. While sufficient to detect positioned nucleosomes and most DNA-bound factors, this resolution is inadequate for mapping the precise translational positions of nucleosomes. Until additional enzymes are discovered and implemented, conventional probes, such as micrococcal nuclease and deoxyribonuclease I, must be used for this purpose. The introduction of m^5C in accessible chromatin regions is sensitively monitored by PCR-based bisulfite sequencing, greatly reducing culture size and making it possible to process many samples simultaneously. Moreover, the DMTase probing systems in this chapter have distinct advantages over that previously available (Kladde et al., 1996): (i) sufficient levels of methylation accumulate within 30-80 min; and (ii) experiments can be performed with logarithmically growing cultures.

The choice between using a free DMTase and fusing the enzyme to a desired factor (TAGM) primarily depends on the biological question being addressed. Free DMTase probes are used to determine changes in nucleosome architecture and to map non-histone protein-DNA interactions (i.e., footprinting), thereby identifying cis-acting elements. Although we have focused on the in vivo use of DMTases, they are also effective for in vitro footprinting applications using purified factors or whole-cell extracts (Xu et al., 1998b; Jin et al., 1999; Li et al., 1999; Vyhlidal et al., 2000; Samudio et al., 2001). There is no foreseeable reason why chromatin remodeling could not be assayed in vitro as well. For most studies, probing with a free DMTase will suffice. However, if more than one factor is bound to a region, attributing protection of a given GC or CG site to one or the other factor may not be possible. In such cases, since the

identity of the DMTase-tagged factor is known, TAGM provides a positive signal for factor binding as opposed to loss of signal in a footprint. Moreover, the accumulation of targeted m^5C over time imparts exquisite sensitivity to TAGM, enabling detection of low factor occupancies. Enrichment of methylated over unmethylated sequences followed by hybridization to DNA microarrays could also allow TAGM to be used in genome-wide identification of factor binding sites.

CHAPTER III

NUCLEOSOME CONFORMATIONAL STABILITY AND THE ACCESSIBILITY OF NUCLEOSOMAL SITES AT THE *PHO5* PROMOTER IN VIVO

SYNOPSIS

Positioned nucleosomes in promoter regions are frequently found to regulate gene expression by obstructing the accessibility of DNA cis-regulatory elements to transactivators. However, the parameters contributing to the positioning and consequent stability of nucleosomes remain elusive. Here, we address the differences in histone-DNA interactions in vivo by examining the accessibility of nucleosomal sites in a natural array, the *S. cerevisiae PHO5* promoter in the absence of the transcriptional activator Pho4. High-resolution mapping of the *PHO5* promoter, required to relate in vivo site accessibility with nucleosome conformational stability, is presented. We find that nucleosomes 5' of the upstream activation sequence UASp1 (−3 to −5) are more accessible than downstream nucleosomes (−2 and −1). Nucleosomes −4 and −2 have the lowest and highest relative accessibilities of the five promoter nucleosomes examined, respectively. We further investigated the conformational stability of regulatory nucleosomes −2 and −1 by competitive mononucleosome reconstitution and show that nucleosome −2 is more stable than nucleosome −1, paralleling the differences in accessibility measured in vivo. These data illustrate a new method for measuring the differences in histone-DNA interactions in a nucleosomal array in living cells. We also show a correlation between DNA curvature and nucleosome positioning that is

consistent with the observed differences in accessibility, suggesting a model whereby intrinsic DNA curvature contributes to nucleosome positioning. Our analysis suggests that the affinity of histone-DNA interactions makes essential contributions to the chromatin organization of the promoter region and subsequent nucleosomal repression of *PHO5*.

INTRODUCTION

Modulation of chromatin accessibility is the primary mechanism for regulating site-specific access of protein factors to DNA in the context of transcription, replication, recombination, and repair. The fundamental repeating unit of chromatin, the nucleosome, occurs every 200 ± 40 bp along eukaryotic chromosomes (McGhee and Felsenfeld, 1980). Nucleosomes are frequently found in promoter regions obstructing access of transactivators and the transcriptional machinery to cis-regulatory sites in DNA (Han and Grunstein, 1988; Shimizu et al., 1991; Fascher et al., 1993; Wu, 1997; Flaus and Richmond, 1998; Soutoglou and Talianidis, 2002). Transcription factors that bind accessible regions in promoters contend with repressive chromatin structures by recruiting one or more multisubunit coactivators. Remodeled chromatin facilitates the loading of additional activators and, subsequently, the basal transcription complex as well as RNA Pol II at core promoters (Fry and Peterson, 2001). Thus, transcriptional control is tightly coupled to changes in nucleosome accessibility.

Nucleosomes have been suggested to exist in a conformational equilibrium, transiently exposing DNA at their termini in a process known as site exposure, allowing

site-specific factors cursory access to nucleosomal sites (Adams and Workman, 1995; Polach and Widom, 1995). Equilibrium constants describing conformational accessibility (K_{eq}^{conf}) decrease as one moves from the periphery of a nucleosome to the pseudodyad, indicating the increased difficulty of factors to access their cognate sites (Anderson and Widom, 2000). As shown in vitro by competitive nucleosome reconstitution studies in which radiolabeled tracer DNA competes with an excess of unlabeled competitor DNA for binding to limiting amounts of histone octamer, relative affinity equals relative equilibrium stability (Widom, 2001). Mechanical disruption of individual nucleosomes examined by stretching nucleosomal arrays using a feedback-enhanced optical trap has identified a staged release of DNA; the initial stage requires low force to remove 38 bp of DNA at each edge of the nucleosome (Brower-Toland et al., 2002). Consistent with increased histone-DNA interactions in the dyadic region, Widom and colleagues have recently identified that the central 71 bp of nucleosomal DNA appears to dominate the free energy of histone-DNA interactions in nucleosomes formed by competitive salt gradient dialysis (Thåström et al., 2004). The general conclusion of these studies is that, in vitro, nucleosomes have differential equilibrium stabilities with ~two helical turns of DNA entering and exiting the octamer surface exhibiting the lowest thermodynamic stability.

Examination of mononucleosome stabilities, while highly informative, do not address nucleosome stabilities in the context of an array. Further, synthetic nucleosomal arrays containing tandem repeats of a positioning sequence and thus homogeneous nucleosome conformational stabilities do not reflect the behavior of natural arrays

containing nucleosomes with diverse histone-DNA interactions. It would thus be of considerable value if approaches were developed to obtain similar information in vivo. Previously, we have shown that DNA methyltransferases (DMTases) can be used as probes of chromatin structure (Kladde and Simpson, 1994; Kladde et al., 1996; Xu et al., 1998b; Carvin et al., 2003a). In vitro, histone-DNA interactions are less stable within the first two helical turns entering and exiting a nucleosome than at the pseudodyad (Weischet et al., 1978; Lee et al., 1982; Simpson, 1990; Morse et al., 1992). Early in vivo work indicated that disruption of histone-DNA contacts beyond 25 bp into the nucleosome appears energetically unfavorable as determined by increased accessibility to nucleosomal DNA (Kladde and Simpson, 1994; Kladde et al., 1996; Xu et al., 1998b). These in vivo studies results faithfully reproduce the relative thermodynamic stabilities observed in vitro with the characteristic increase in accessibility of the nucleosome edge vs. center. We reasoned, therefore, that we should be able to extend these methods to study natural arrays in vivo, as DNA sequences having greater affinity for the histone octamer should form nucleosomes having commensurate conformational stability.

We have developed a novel DMTase-based system as a first approach to address nucleosome stabilities in vivo. As DMTases are sterically occluded from their target sites located in nucleosomes, expression in living cells allows us to assay nucleosome accessibility without damaging nuclear DNA and instead marking it with a relatively innocuous methyl group (Kladde and Simpson, 1994; Kladde et al., 1996; Xu et al., 1998a; Carvin et al., 2003a; Jessen et al., 2004b). The level of 5-methylcytosine (m^5C) at potential target sites and hence site accessibility is positively displayed and quantified by

bisulfite genomic sequencing (Frommer et al., 1992; Clark et al., 1994). We have chosen to investigate the in vivo conformational stabilities of the natural nucleosomal array of the *PHO5* promoter, a widely used model system for transcriptional regulation in the context of chromatin. In the absence of the transactivator Pho4, the *PHO5* promoter is organized into a series of five well-positioned nucleosomes (Almer and Hörz, 1986). The second of two UASs, UASp2, and the TATA element are obstructed by nucleosomes −2 and −1, respectively. High-resolution structural knowledge of the promoter is required in order to relate site accessibility with nucleosome conformational stability. Moreover, as the activation of *PHO5* is dependent upon Pho4 binding at UASp2 (Fascher et al., 1993) and the position of TATA-occluding nucleosome −1 dictates the dependency on the histone H4 tail and TFIID-associated bromodomain factor Bdf1 (Martinez-Campa et al., 2004), the position of promoter cis-elements relative to the edge of nucleosomes is biologically significant.

High-resolution structural information of *PHO5* promoter chromatin was therefore obtained by mapping the accessibility of nucleosomes −5 to +1 to both micrococcal nuclease (MNase) and the DMTase M.CviPI. Using a second DMTase, M.HhaI, we determined the relative accessibilities of upstream nucleosomes (−3, −4, and −5), each having a cognate site positioned within ~6 bp of the pseudodyad. We demonstrate that nucleosome −4 is significantly more accessible to M.HhaI than flanking nucleosomes −5 and −3. The HhaI site in downstream nucleosomes (−2 and −1) is positioned farther from the pseudodyad than those upstream and was expected be more accessible to M.HhaI. Surprisingly, downstream nucleosomes displayed *decreased*

accessibility to M.HhaI, suggesting that they are the most stable in the promoter region with the stability of nucleosome −2 > −1. This was confirmed by competitive mononucleosome reconstitution. Finally, we identify a distinctly conserved pattern of nucleosomal DNA curvature that is consistent with the observed differences in accessibility/stability. These findings further suggest a model in which intrinsic DNA curvature participates in the positioning of nucleosomes at *PHO5* promoter.

MATERIALS AND METHODS

S. cerevisiae Strains and Growth Conditions

For samples in which nuclei was isolated and digested with MNase, strain FY24 (*MAT*α *ura3-52, trp1*Δ63 *leu2*Δ1) was used (Gavin et al., 2000). All other *S. cerevisiae* strains were constructed by standard genetic methods from CCY694, *MAT***a**/*MAT*α *leu2*Δ0/*leu2*Δ0 *lys2*Δ0/*lys2*Δ0 *ura3*Δ0/*ura3*Δ0 *pho3*Δ::R/*pho3*Δ::R (S288C background), where R is a *Zygosaccharomyces rouxii* recombinase site that remains after intramolecular recombination. For probing *PHO5* promoter nucleosomes in vivo with M.HhaI [M.HhaI-Pho4 nuclear localization sequence/nuclear export sequence (NLS/NES), see below], strain WJY2410 (*MAT*α *can1*::M.HhaI-Pho4 NLS/NES-*LEU2 ho*::LexA-ER-VP16-*LYS2 PHO5*$^{\text{HhaI}}$ *pho4*::*lox*P, where *lox*P is a Cre recombinase site that remains after intramolecular recombination) was used. M.HhaI is expressed from an estrogen-inducible system (Balasubramanian and Morse 1999) and consists of an in-frame fusion of full-length M.HhaI, a TGLGIL linker peptide, the V5 epitope, and the NLS/NES of Pho4 [amino acids 2-199 with a D78P point mutation that abrogates the

Pho4 activation domain function; (McAndrew et al., 1998)]. The fusion gene was inserted into YIpM.HhaI-Pho4 under control of a minimal *GAL1* promoter containing four LexA binding sites (i.e., *lex*O sites) and integrated at the *CAN1* locus. The *PHO5* promoter in these strains (all *MAT*α *leu2*Δ0 *lys2*Δ0 *ura3*Δ0 *pho3*Δ::R) was modified to contain seven point mutations [original nucleotide (distance upstream of the translational start site) replacement nucleotide: T(−821)G, T(−638)G, G(−636)C, C(−513)G, C(−404)G, A(−336)G, and C(−238)G], creating the $PHO5^{HhaI}$ promoter. For footprinting with M.CviPI, the methyltransferase was expressed from the estrogen-inducible system in strains with an unaltered *PHO5* promoter; strains SHY1860 (*PHO4*) and SHY2490 (*pho4*::*kanMX4*), which are also *MAT***a** *leu2*Δ0 *lys2*Δ0 *ura3*Δ0 *pho3*Δ::R *ho*::M.CviPI-*LYS2*-LexA-ER-VP16.

Yeast were grown in YPPD [2% glucose, 1% yeast extract (Difco), 2% peptone (Difco), 13.4 mM KH_2PO_4] at 30˚C to mid-log phase and MNase digestion of chromatin from spheroplasted cells (Kent et al., 1993; Fazzio and Tsukiyama, 2003) was performed after ~1 min zymolyase (Seikagaku) treatment. Genomic DNA was purified using Qiagen Genomic Tip 20 columns.

Primer Extension Analysis of Chromatin

High-resolution mapping of MNase cleavage sites was performed as described previously (Shimizu et al., 1991; Gavin and Simpson, 1997). Following DNA purification, nuclease cleavage sites were detected by multiple-round primer extension with the ^{32}P-end-labeled oligonucleotides listed in Table 3-1 followed by electrophoresis

Table 3-1. Oligonucleotides Used for High-Resolution Mapping of *PHO5* Promoter Chromatin

^{32}P-End-Labeled Oligonucleotides for Primer Extension of MNase-Digested DNA.		
Primer	Sequence	Figure(s)
PHO5-976	ACGACGTCCGCTTACATG	3-2A
PHO5-1133	AGACTCCGTCCCTCTTT	3-2B
PHO5-1205	GATCCGAAAGTTGCATTCAACAAG AATGCG	3-3
Oligonucleotides for PCR Amplification of Bisulfite-Treated DNA.		
Primer[a]	Sequence	Figure(s)
*PHO5*b1-922	TTCAATTaCTAAATACAATaTTCCTT aaT	3-4 3-6A
*PHO5*b2-924	GAAAAtAGGGAttAGAATtATAAATT TAGTtT	3-4
*PHO5*b1-1047	ATATACCCATTTaaaATAAaaaTAAAC	3-5
*PHO5*b2-18	TGTAtTtTTGATAGTtTTAGttAGAtTG AtAGTAGG	3-5
*PHO5*b2-769	atatataagcttcAAtATTGGTAATtTtGAAT TTGtTTGtTGtTTGtT	3-6A
^{32}P-End-Labeled Oligonucleotides for Primer Extension of PCR Products Amplified from Bisulfite-Treated DNA.		
Primer[a]	Sequence	Figure(s)
*PHO5*b1-768	atatatctcgaggACTAATAaAAaAAAACA AaAaACTCCaT	3-4 3-6A
*PHO5*b1-1047	ATATACCCATTTaaaATAAaaaTAAAC	3-5

[a]Pairs of 'a' (a1 and a2) or 'b' (b1 and b2) are primers for the upper and lower DNA strands, respectively, from bisulfite-treated DNA. Nucleotides in lower case represent either G to a or C to t transitions.

on a polyacrylamide (acrylamide-bisacrylamide, 19:1)-50% urea gel buffered by an electrolyte gradient (Sheen and Seed, 1988). Protein-free DNA control samples were obtained by digesting either plasmid DNA or isolated genomic DNA containing the *PHO5* promoter with MNase to determine cleavage preferences in naked DNA.

Bisulfite Genomic Sequencing

Genomic DNA was rapidly isolated and m^5C levels were determined by bisulfite genomic sequencing as described (Jessen et al., 2004b). The oligonucleotides used for PCR amplification from bisulfite-treated DNA and multiple-round primer extension are listed in Table 3-1.

Secondary Structural Analysis

A bendability/curvature propensity plot calculated with DNase I-based trinucleotide parameters for the *PHO5* promoter region was calculated using the program bend.it (Vlahoviček et al., 2003).

Competitive Mononucleosome Reconstitution

Probes (~200 bp) were generated by cutting pPHO5 with MfeI and HaeII (nucleosome −2), ApoI and BspHI (−2 to −1 linker), and HindIII and BstEII (nucleosome −1). The 5S rRNA probe was produced by cutting a single copy of the *Lytechinus variegatus* 5S rRNA gene (Simpson et al., 1985) out of pUC19 with EcoRI and HindIII. The DNA fragments were purified by electrophoresis on an agarose gel. DNA fragments (50 ng)

were labeled with [α-^{32}P]ATP by end-filling. Labeled fragments (3 ng) were mixed with 1 ml of a 1:4 dilution of the Nap1p/core histone complex in the presence of 100, 200, and 400 ng competitor DNA (sheared yeast genomic DNA) and incubated at 30˚C for 45 min as described in Terrell et al. (2002). Prior to running on a 5% polyacrylamide gel (1/3x TBE) and visualized by exposure to a phosphorimager screen, 5 µl 10% glycerol was added to each sample.

RESULTS

High-resolution Chromatin Structure of the *PHO5* Promoter

A high-resolution map of the ~1 kb chromatin domain spanning the *PHO5* promoter, summarized in Figure 3-1, was assembled from primer extension analysis of MNase digests of both spheroplasts and isolated nuclei and is further supported by accessibility in vivo to the DMTase M.CviPI. The *PHO5* promoter, under repressive conditions of high phosphate (P_i), consists of five well-positioned nucleosomes (Almer and Hörz, 1986). Two nuclease hypersensitive regions, HSR1 and HSR2 (containing UASp1), are positioned upstream of nucleosome −5 and between nucleosomes −2 and −3, respectively (Almer and Hörz, 1986). Deprivation of P_i leads to the binding of Pho4 in conjunction with Pho2 (Barbaric et al., 1996) at UASp1. Extended P_i starvation leads to disruption of nucleosomes −1 to −4 concomitant with increased transcription (Almer and Hörz, 1986).

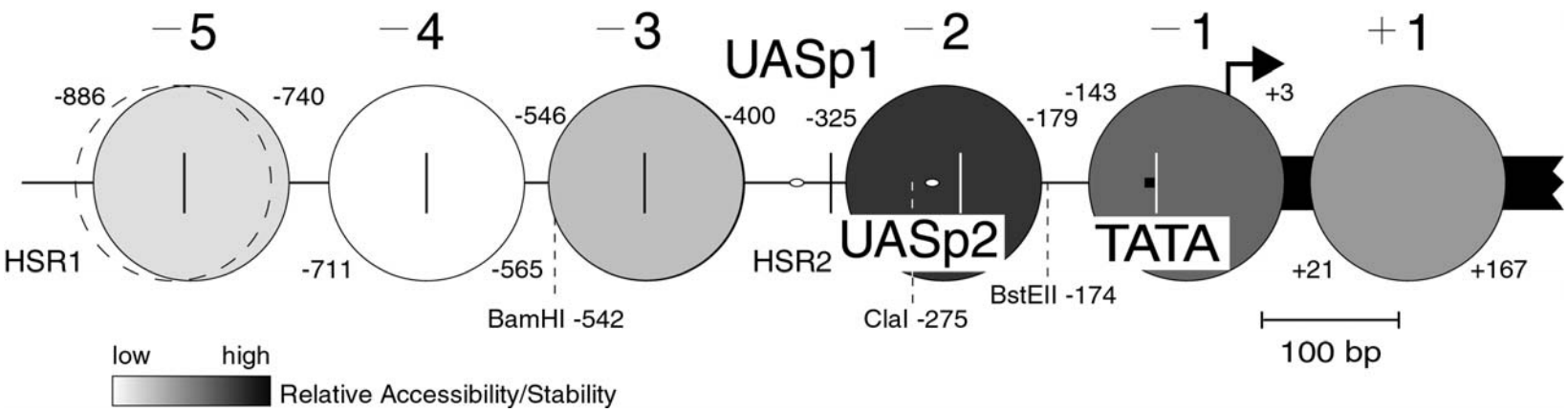

Figure 3-1. *PHO5* Promoter Nucleosome Positions and Relative Accessibilities/Stabilities Derived from This Study

The diagram (drawn to scale) shows the inferred position of nucleosomes −5 to +1 (circles), mapped by accessibility to MNase and M.CviPI. The position of nucleosome edges are indicated by nucleotide distances relative to the *PHO5* ATG. Nucleosome shading represents relative accessibilities/stabilities. Open ovals, Pho4 binding sites UASp1 and UASp2; filled bar, TATA element; black arrowhead, major transcription initiation site; HSR1 and HSR2, hypersensitive regions 1 and 2, respectively; broken black rectangle, *PHO5* coding sequence; vertical bars, HhaI sites introduced and existing in the $PHO5^{HhaI}$ promoter. Also indicated are restriction endonuclease sites commonly used to assay restriction endonuclease accessibility to *PHO5* promoter chromatin.

Positioned nucleosomes −5 to −3 are clearly visible following MNase digestion of the Watson strand of the upstream region of the *PHO5* promoter (Figure 3-2A). We describe how the positions of nucleosomes −5 to −3 were inferred as follows. In chromatin (Figure 3-2A, lanes 1-6), a nuclease hypersensitive region is present at −950 and demarcates the beginning of the *PHO5* promoter nucleosomal array. This hypersensitive region, known as HSR1, consists of repetitive dA and dT sequences spanning ~65 bp. The preferential digestion of the deproteinized template is consistent with the sequence preference of MNase for AT-rich regions with a 5' dC or dG (Drew, 1984; Flick et al., 1986). Immediately downstream there are two additional hypersensitive sites on the deproteinized template (−895 and −751) that display *decreased* digestion in chromatin (indicated by brackets). This protection is characteristic of a positioned nucleosome (nucleosome −5) obstructing access of MNase to the DNA. The distance between −895 and −751 is 144 bp, slightly less than the 147 bp of DNA in the nucleosome core particle. Increased accessibility of DNA entering and exiting the nucleosome to chromatin probes has been observed previously and likely reflects decreased histone-DNA interactions (Kladde and Simpson, 1994; Kladde et al., 1996; Weiss and Simpson, 1998; Xu et al., 1998b; Ravindra et al., 1999; Carvin et al., 2003a; Jessen et al., 2004a). Nucleosome −5 protects the region spanning at least −895 to −751 (145 bp). However, closer examination of the data shows a much greater fold protection of −751 vs. −895 relative to the deproteinized template suggesting that −751 is more internal to the nucleosome. Placing −751 ~one helical turn inside of nucleosome −5 positions the downstream edge near −740. Allowing the location of −895 to be 6 bp

Figure 3-2. Primer Extension Analysis of MNase-cut Sites in the Upstream *PHO5* Promoter Region

Protein-free DNA (lane D) and spheroplasts (lanes 1-6) were treated with increasing concentrations of MNase: lane D, 2.5 U/ml; lanes 1-6: 0, 6.25, 12.5, 25, 50, and 100 U/ml, respectively. The presence of undigested DNA at the top of the gel in the MNase-treated samples is due to the presence of unspheroplasted cells when the nuclease was added.
(A) Primer extension was performed using the Watson strand of isolated DNA as template. The diagram to the right shows the inferred position of nucleosomes −5 to −3 (ellipses). Asterisks, sites of increased nuclease cleavage; brackets, sites of protection relative to the deproteinized template. Lanes A, C, G, and T are sequencing reactions to facilitate site identification. Nucleosome −5 has a second, less populated translational position, indicated by the dashed ellipse.
(B) Primer extension was performed using the Crick strand of isolated DNA as template. The diagram to the right shows the inferred position of nucleosomes −5 to −1 (ellipses and circle). Open oval, Pho4 binding site UASp1; other symbols are as in (A).

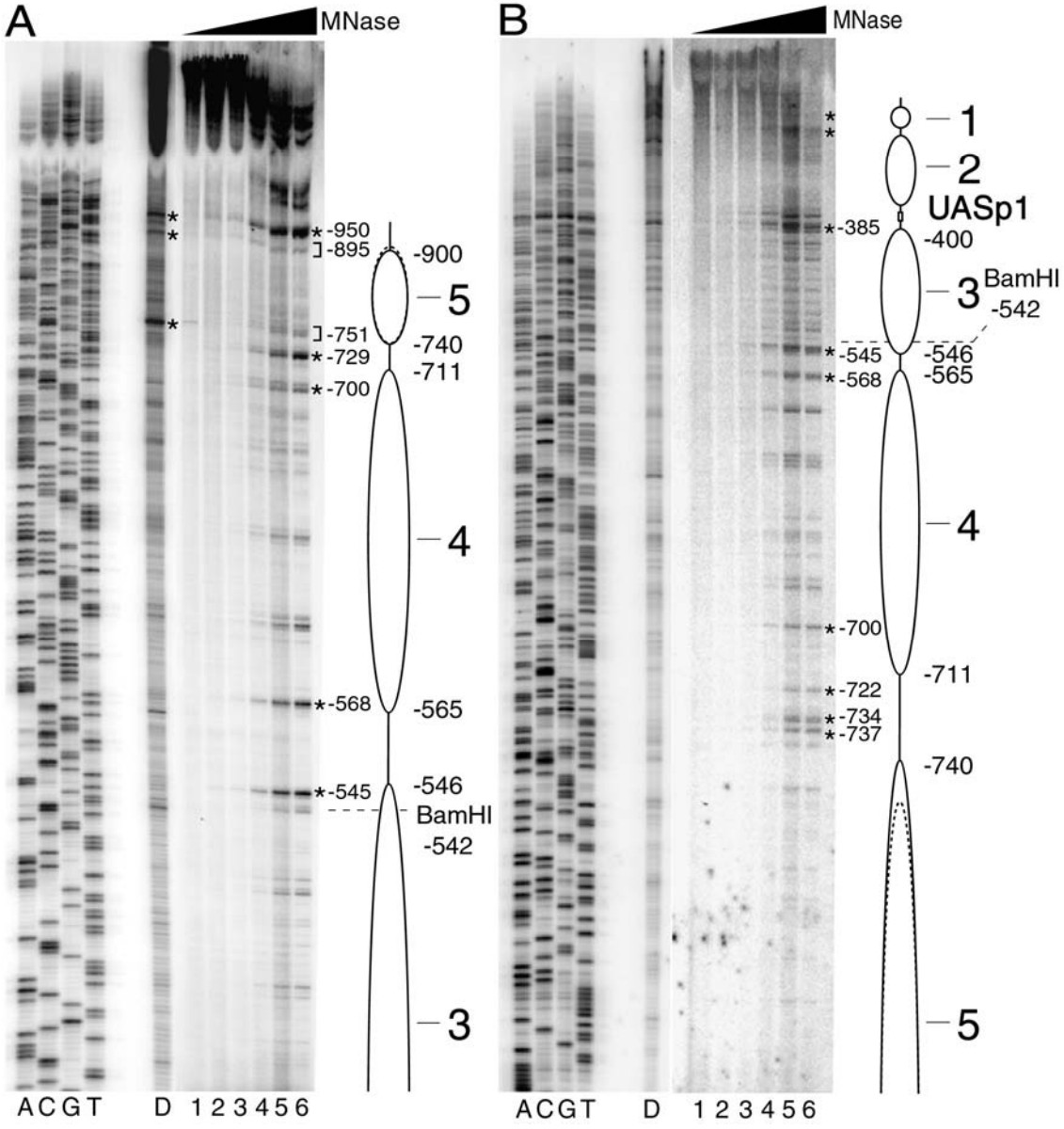
A
MNase
-950
-895
-900
5
-751
-740
-729
-711
-700
4
-568
-565
-546
-545
BamHI
-542
3
A C G T
D 1 2 3 4 5 6
B
MNase
1
2
UASp1
-385
-400
3
BamHI
-542
-545
-546
-568
-565
4
-700
-711
-722
-734
-737
-740
5
A C G T
D 1 2 3 4 5 6

internal to nucleosome −5 places the upstream edge at −900. With the region of protection now spanning 161 bp, it is possible that there is a second translational position for nucleosome −5 in a small fraction of cells, positioned further upstream by ~one helical turn. This is consistent with the view that poly(dA-dT) elements bias nucleosome positioning to favor, in the time average, positions where they lie outside the nucleosome (Iyer and Struhl, 1995; Anderson and Widom, 2001). In the absence of additional MNase cleavages between −950 to −895 and −751 to −729, our best estimate for the highest populated position of nucleosome −5 is between −886 and −740.

A hypersensitive site at −729 in chromatin (note the lack of digestion on the deproteinized sample) defines the linker region between nucleosomes −5 and −4. Digestion at −700 is less pronounced than at −729 indicating decreased accessibility of nucleosome −4 to MNase. Further downstream is a hypersensitive site around −568. The distance between −700 and −568 is 133 bp, less than the 147 bp of DNA in the nucleosome core particle. As −568 is digested by MNase to a greater extent than −700, suggesting that −700 is more internal to nucleosome −4 and thus more protected, we position the upstream edge of nucleosome −4 to be around −711 (upstream of −700 by ~one helical turn). MNase protection by nucleosome −4 spans 147 bp to −565, placing −568 internal to nucleosome −4 by 4 bp. We position the downstream edge of nucleosome −3 at −400 (see Figures 3-2B, 3-3, and 3-4), thus the upstream edge of nucleosome −3 is at −546. This is consistent with the observed hypersensitive site at −545 adjacent to the upstream edge of nucleosome −3.

Nucleosome positions were verified by primer extension across the same domain on the Crick strand of the upstream region of the *PHO5* promoter (Figure 3-2B). The accessible UASp1 region is readily identified near the top of the gel and consists of a cluster of hypersensitive sites around −385. Sites upstream of −400 are protected to −546 from MNase digestion by nucleosome −3. On the Crick strand, we again observe increased accessibility of −545 and −568 to MNase, further supporting our placement of nucleosomes −3 and −4. Sites located between −565 and −711 are protected by nucleosome −4. Increased accessibility of −700 to MNase identifies the upstream edge of nucleosome −4. Three hypersensitive sites at −722, −734, and −737 define the linker region between nucleosomes −4 and −5.

Nucleosomes −3 to +1 are identified in the map of MNase cuts on the Watson strand of the downstream region of the *PHO5* promoter (Figure 3-3). Two hypersensitive sites at −385 and −348 flank UASp1. The downstream edge of nucleosome −3 is established by the dramatic increase in accessibility of −407 to MNase relative to protein-free DNA. The edges of nucleosome −2 are indicated by strong protection of two pair of sites (−320, −312 and −204, −186, indicated by brackets) relative to the deproteinized template (Figure 3-3, compare lanes D and 1-4). The distance between −320 and −186 is 134 bp. We place the upstream edge of nucleosome −2 at −325, which allows 6 bp for protection of −320, positioning the downstream edge of nucleosome −2 at −179. Increased MNase digestion at −170, −154, and −137 establishes the linker region between nucleosomes −2 and −1, spanning ~36 bp. Strong nuclease protection is

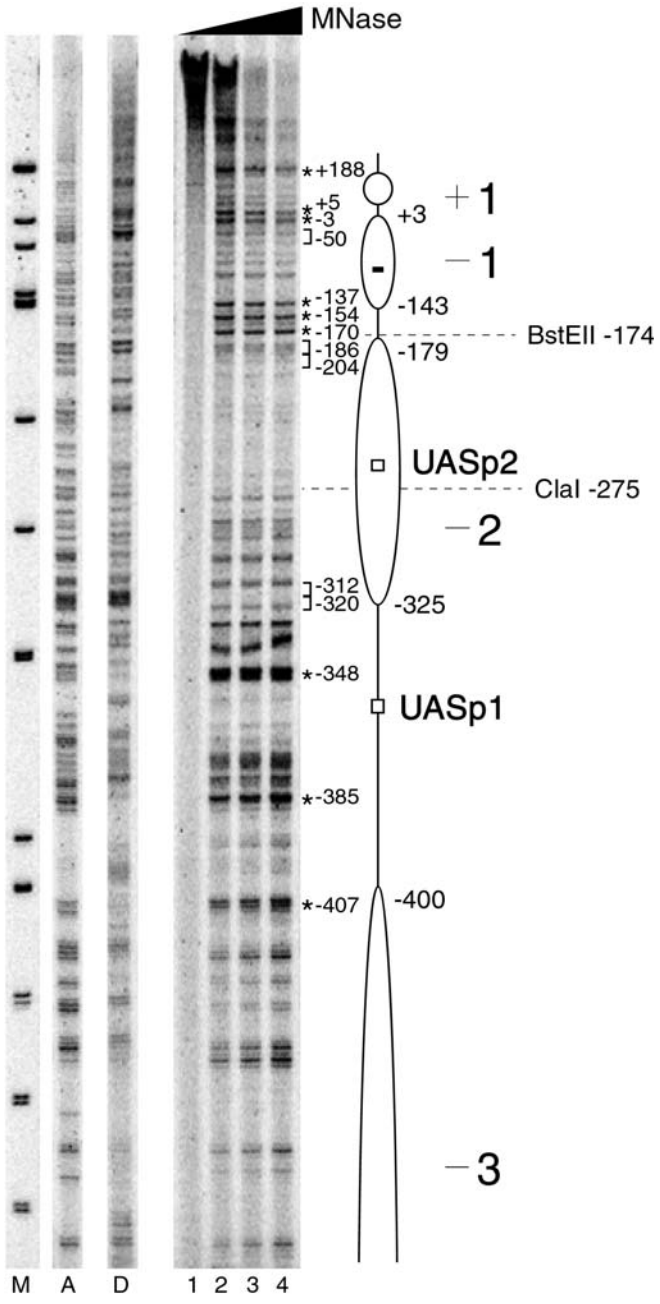

Figure 3-3. Primer Extension Analysis of MNase-cut Sites in the Downstream *PHO5* Promoter Region

Protein-free DNA (lane D) and nuclei (lanes 1-4) were treated with increasing concentrations of MNase: lane D, 0.3 U/ml; lanes 1-4: 0, 0.125, 0.25, 0.5 U/ml, respectively. Primer extension was performed using the Watson strand of isolated DNA as template. The diagram to the right shows the inferred position of nucleosomes −3 to +1 (ellipses and circle). Open bars, Pho4 binding sites UASp1 and UASp2; filled bar, TATA element; lane M, ^{32}P-end-labeled HinfI-digested ϕX174 RF DNA; lane A, sequencing reaction to facilitate site identification; asterisks, sites of increased nuclease cleavage; brackets, sites of protection relative to the deproteinized template. Nucleotide distances are relative to the *PHO5* ATG.

observed at −50 relative to the deproteinized template (Figure 3-3, compare lanes D and 2-4). Increased MNase accessibility is observed at −3 and +5, identifying the linker region between nucleosomes −1 and +1. The distance between hypersensitive sites −137 and −3 is 134 bp. Thus, placing the pseudodyad equidistant from each hypersensitive site positions nucleosome −1 between −143 and +3. A hypersensitive site at +188 indicates the linker region between nucleosomes +1 and +2 (also see Chapter IV for low-resolution mapping of nucleosomes −5 to +3). Thus, we conclude from the data shown in Figures 3-2 and 3-3 that the *PHO5* promoter nucleosome positions are: nucleosome −5 (−886 to −740); nucleosome −4 (−711 to −565); nucleosome −3 (−546 to −400); nucleosome −2 (−325 to −179); and nucleosome −1 (−143 to +3).

We also probed the *PHO5* promoter in a strain expressing the DNA methyltransferase M.CviPI, which recognizes GC sites (Xu et al., 1998a). Probing chromatin structure using DMTases can be performed in living cells and allows us to assay nucleosome accessibility without damaging nuclear DNA. As DMTases are sterically occluded from their target sites located in nucleosomes (Kladde and Simpson, 1994; Kladde et al., 1996; Xu et al., 1998b; Carvin et al., 2003a), the level of m^5C at potential target sites is directly proportional to the amount of site accessibility and can be positively displayed and quantified by bisulfite genomic sequencing (Jessen et al., 2004b), which converts all unmethylated cytosine residues to uracil and, subsequently via PCR, to thymine. Methylated cytosine residues resist deamination and remain cytosine in the template. Thus, the differential access of free DMTases to a region in different cell types (e.g., wild-type vs. mutant) or cells grown under various conditions

(e.g., induction vs. repression) is used to detect the presence of nucleosomes and alteration of their structure or position.

Accessibility of the upstream region of the *PHO5* promoter to M.CviPI was monitored after 14 hr of P_i deprivation in wild-type and *pho4*Δ strains (Figure 3-4). Pho4 is essential for *PHO5* chromatin remodeling and activation (Fascher et al., 1990). Accordingly, a decrease in band intensity at a given site and time point in *pho4*Δ relative to *PHO4*+ cells indicates the presence of a nucleosome. This is best seen by comparing band intensities at the pseudodyad of nucleosome −4 (Figure 3-4, compare −636 and 640, lanes 1-7 and 8-14). GC sites preferentially methylated in linker regions should be methylated at similar levels in both *pho4*Δ and *PHO4* cells. As the edges of nucleosomes are more accessible to DMTases than internal regions (Kladde and Simpson, 1994; Kladde et al., 1996; Xu et al., 1998b), the downstream edge of nucleosome −4 is identified by a modest increase in methylation of the *PHO4* strain relative to the *pho4*Δ strain at and near −578/582. Similar amounts of methylation are seen at −551 and −562 in both *pho4*Δ and *PHO4* strains indicating the location of the linker region between nucleosomes −4 and −3. This is consistent with the observed MNase hypersensitivity at −568 (see Figure 3-2) and confirms the position of the downstream edge of nucleosome −4 around −565. Increased methylation at −697 in the *PHO4* vs. *pho4*Δ strain indicates protection by nucleosome −4 and agrees well with the protection against MNase digestion at −700 (see Figure 3-2). Increased methylation in the *PHO4* strain at −747, −756, −762, and −770 relative to the *pho4*Δ strain indicates the downstream edge of nucleosome −5 and is consistent with the observed protection of −751 to MNase (see

Figure 3-4. Accessibility of *PHO5* Promoter Nucleosomes −2 to −5 to M.CviPI

Strains were grown in the absence of P_i for 14 hr prior to the induction of M.CviPI in *pho4*Δ (lanes 1-7) and *PHO4* (lanes 8-14) cells for the indicated times and then analyzed for m^5C levels by bisulfite sequencing. The diagram to the left shows the inferred position from MNase accessibility of nucleosomes −2 to −5 (ellipses). DNA migrates through the gel based on the log of the molecular weight, thus the nucleosomal pseudodyad (horizontal bars) indicated in nucleosomes −4 and −5 appears off center. Filled circles, GC sites recognized by M.CviPI. All bands that do not correspond to M.CviPI sites are due to non-specific pausing during primer extension. Open bar, Pho4 binding site UASp1. Pho4 binding protects two GC sites at UASp1 (−353/363) against methylation by M.CviPI [lanes 8-14, and (Carvin et al., 2003a)]. Note that DMTases access cognate sites located near the edges of nucleosomes more readily than sites near the nucleosomal pseudodyad (Kladde and Simpson, 1994; Kladde et al., 1996). Methylation at sites in *PHO4*+ cells that initially increase in intensity and then decrease at later times are due to masking of signal.

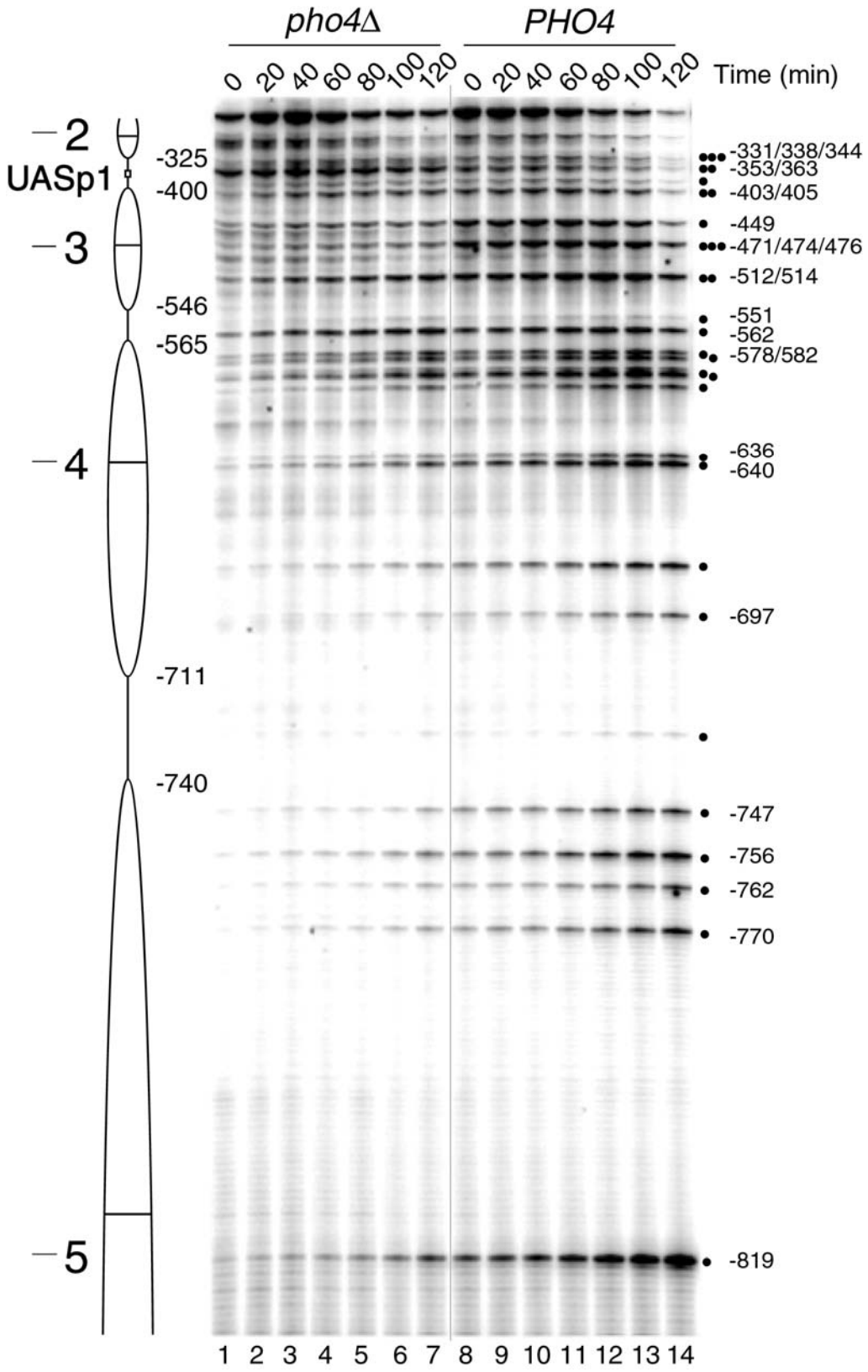
pho4Δ
PHO4
0 20 40 60 80 100 120 0 20 40 60 80 100 120
Time (min)
–2
UASp1
–3
–4
–5
-325
-400
-546
-565
-711
-740
-331/338/344
-353/363
-403/405
-449
-471/474/476
-512/514
-551
-562
-578/582
-636
-640
-697
-747
-756
-762
-770
-819
1 2 3 4 5 6 7 8 9 10 11 12 13 14

Figure 3-2). Note that the extent of protection from methylation at −819 in the *pho4*Δ strain relative to the *PHO4* strain, indicating its location near the nucleosome −5 pseudodyad. Similarly, at −471/474/476 there is a considerable degree of protection in the *pho4*Δ strain relative to the *PHO4* strain compared to either −449 or −512/514, indicating its location near the pseudodyad of nucleosome −3. Slight protection from methylation is observed at the downstream edge of nucleosome −3 at −403/405 in *pho4*Δ relative to *PHO4* cells. This is consistent with the increased accessibility of −407 to MNase (see Figure 3-3). Preferential methylation of the histone-free UASp1 region at −353/363 is observed in *pho4*Δ cells (Figure 3-4, lanes 1-7). Pho4 binding is observed in the *PHO4* strain by the protection against methylation by M.CviPI at −353/363 [Figure 3-4, lanes 8-14 and (Carvin et al., 2003a)]. The lack of increased methylation at −331/338/344 in the *PHO4* strain, consistent with accessibility of −348 to MNase (see Figure 3-3), confirms our placement of the upstream edge of nucleosome −2 at −325.

Lastly, accessibility of nucleosomes −1 and +1 to M.CviPI was monitored in wild-type and *pho4*Δ strains starved for P_i (Figure 3-5). Clear protection of GC sites immediately downstream of the TATA element is observed in the *pho4*Δ strain at −94 and −92 (Figure 3-5, compare lanes 1-3 and 4-6) relative to the *PHO4* strain. Protection from methylation at −61 in the *pho4*Δ strain relative to the *PHO4* strain is consistent with the decrease in accessibility at −50 to MNase (see Figure 3-3); reduced protection from methylation at −22 and −18 by M.CviPI identifies the downstream edge of nucleosome −1. Increasing protection from methylation at +31 and +43 delimits the

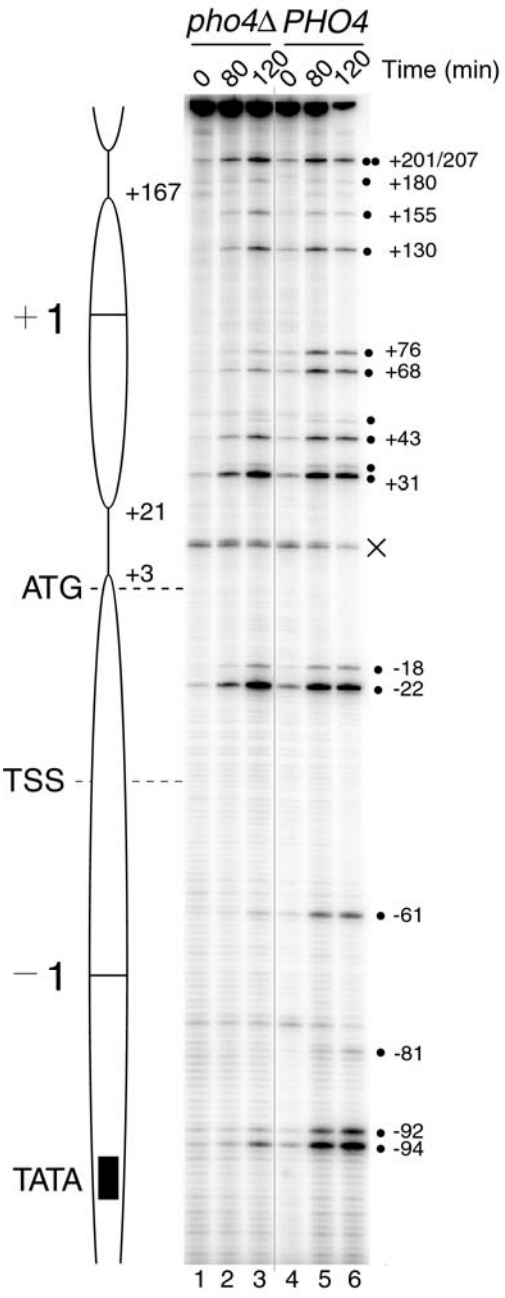

Figure 3-5. Accessibility of *PHO5* Promoter Nucleosomes −1 and +1 to M.CviPI

Strains were grown in the absence of P_i for 6 hr prior to the induction of M.CviPI in *pho4*Δ (lanes 1-3) and *PHO4* (lanes 4-6) cells for the indicated times and then analyzed for m^5C levels by bisulfite sequencing. The diagram to the left shows the inferred position from MNase accessibility of nucleosomes −1 to +1 (ellipses). Symbols are as in Figure 3-4; filled bar, TATA element; TSS, transcriptional start site; ATG, translational start site; ×, non-specific, major primer extension pause.

upstream edge of nucleosome +1 (Figure 3-5, compare lanes 2 and 5). Clear protection from methylation is observed at +68, +76, and +130 in the *pho4*Δ strain relative to the *PHO4* strain. Little difference in accessibility of +155 to M.CviPI is observed in both the *pho4*Δ and *PHO4* strains. The distance between +31 and +155 is 124 bp. Allowing ~one helical turn upstream of +31 places the upstream edge of nucleosome +1 at +21. The linker region between nucleosome +1 and +2 is identified by equivalent amounts of methylation in both strains at +180 and +201/207. In summary, the accessibility of the*PHO5* promoter to M.CviPI, consistent with the accessibility of the promoter to MNase, verifies the positions determined for nucleosomes −5 to −1. Additionally, we conclude from the data shown in Figures 3-3 and 3-5 that nucleosome +1 of the *PHO5* promoter is positioned between +21 to +167.

The Region Associated with Nucleosome −4 is the Most Accessible of the *PHO5* Promoter Nucleosomes

Accessibility of DNA associated with nucleosome −4 to MNase appears to be more than that of nucleosomes −3 and −5 (Figure 3-2). This is further evident from the M.CviPI probing of *pho4*Δ cells in Figure 3-4 (compare lanes 1-7 near the pseudodyad of nucleosomes −3, −4, and −5). The amount of methylation in *pho4*Δ cells as a percent of methylation achieved in *PHO4*+ cells is much greater at the pseudodyad of nucleosome −4 than −5 (Figure 3-4, compare −636/640 and −819, lanes 1-7 and 8-14). However, the abundance of sites and the departure from single-hit kinetics make quantification difficult. Our working hypothesis is that the differential accessibility of *PHO5* promoter

sequences associated with nucleosomes to each of the chromatin probes results from a difference in nucleosome stabilities. DNA sequences having increased affinity for the histone octamer should equate to nucleosomes having increased conformational stability. To more quantitatively assess the different stabilities of the *PHO5* promoter nucleosomes, we used a second DMTase, M.HhaI, as an in vivo probe to monitor chromatin dynamics (Jessen et al., 2004a). A modified version of the *PHO5* promoter was used that contains HhaI sites (GCGC) introduced by one or two point mutations into nucleosomes −2 to −5 (−1 was not altered) and in the histone-free UASp1 region, located 19 bp downstream of UASp1 (Figure 3-1). The customized promoter (*PHO5*^{HhaI}) is structurally and functionally indistinguishable from the wild-type promoter. In addition, cytosine methylation has no effect on promoter function, as has been shown previously for this and other promoters (Kladde et al., 1996; Carvin et al., 2003a; Jessen et al., 2004a). Moreover, M.HhaI methylates all six HhaI sites in protein-free *PHO5*^{HhaI} DNA at similar rates (Figure 3-6A).

In order to monitor the changes in *PHO5*-promoter chromatin kinetically, we devised a strategy that would allow for rapid increases in the nuclear concentration of M.HhaI. This was accomplished by an in-frame fusion of full-length M.HhaI to the nuclear localization sequence/nuclear export sequence (NLS/NES) of Pho4. The fusion gene is under control of an estrogen (17β-estradiol, E_2)-responsive promoter containing four LexA binding sites (*lex*O sites) located upstream of a minimal *GAL1* promoter. Induction is achieved by the addition of E_2 to the medium of cells expressing the chimeric activator, LexA-ER-VP16, a fusion of the *E. coli* LexA DNA-binding protein,

Figure 3-6. The Region Associated with Nucleosome −4 is the Most Accessible of the *PHO5* Promoter Nucleosomes

(A) All six HhaI sites in the *PHO5*^{HhaI} promoter are methylated at the same rate on naked DNA. M.HhaI methylation time course on protein-free plasmid DNA containing the *PHO5*^{HhaI} promoter. Time points were taken and m^5C levels were determined by bisulfite sequencing. HhaI sites for nucleosomes −5 to −1 and the histone-free UAS region (19 bp downstream of UASp1) are shown. Dashed ovals, in vivo translational position of promoter nucleosomes −5 to −1, shown for reference; open bar, Pho4 binding site UASp1.
(B) Methylation time course quantitatively comparing nucleosome accessibilities to M.HhaI in the absence of Pho4 by primer extension. M.HhaI was induced by the addition of 20 nM E_2 and methylation levels (mean ± standard deviation) in duplicate *pho4*Δ cultures were determined at the indicated times.
(C) Accessibility of the *PHO5*^{HhaI} promoter to M.HhaI during 12 hr of P_i starvation in a *pho4*Δ strain. M.HhaI synthesis was induced for 30 min prior to the indicated times of P_i starvation and m^5C levels were determined by bisulfite sequencing. The lower percentages of m^5C in this experiment reflect the shorter induction period of the DMTase and are not directly comparable to the percentages in (B). Methylation at the UAS site (19 bp downstream of UASp1) increases over time as a result of P_i starvation, which causes cell cycle arrest and thus stops the dilution of methylation.
(D) Cumulative derived in vivo apparent rate constants for methylation of HhaI sites in nucleosomes −3, −4, and −5 in a *pho4*Δ strain, plotted as a function of E_2 concentration.
(E) Accessibility of nucleosomes −5, −4, −3, and the UAS site to M.HhaI after 24 hr of P_i starvation in a *pho4*Δ strain. M.HhaI probe synthesis was induced in *pho4*Δ cells by the addition of 100 nM E_2 for 30- (grey bars) or 60-min (white bars) to induce a pulse of M.HhaI probe synthesis. The UAS site (19 bp downstream of UASp1) is shown as a reference for a HhaI site not bound by histones.

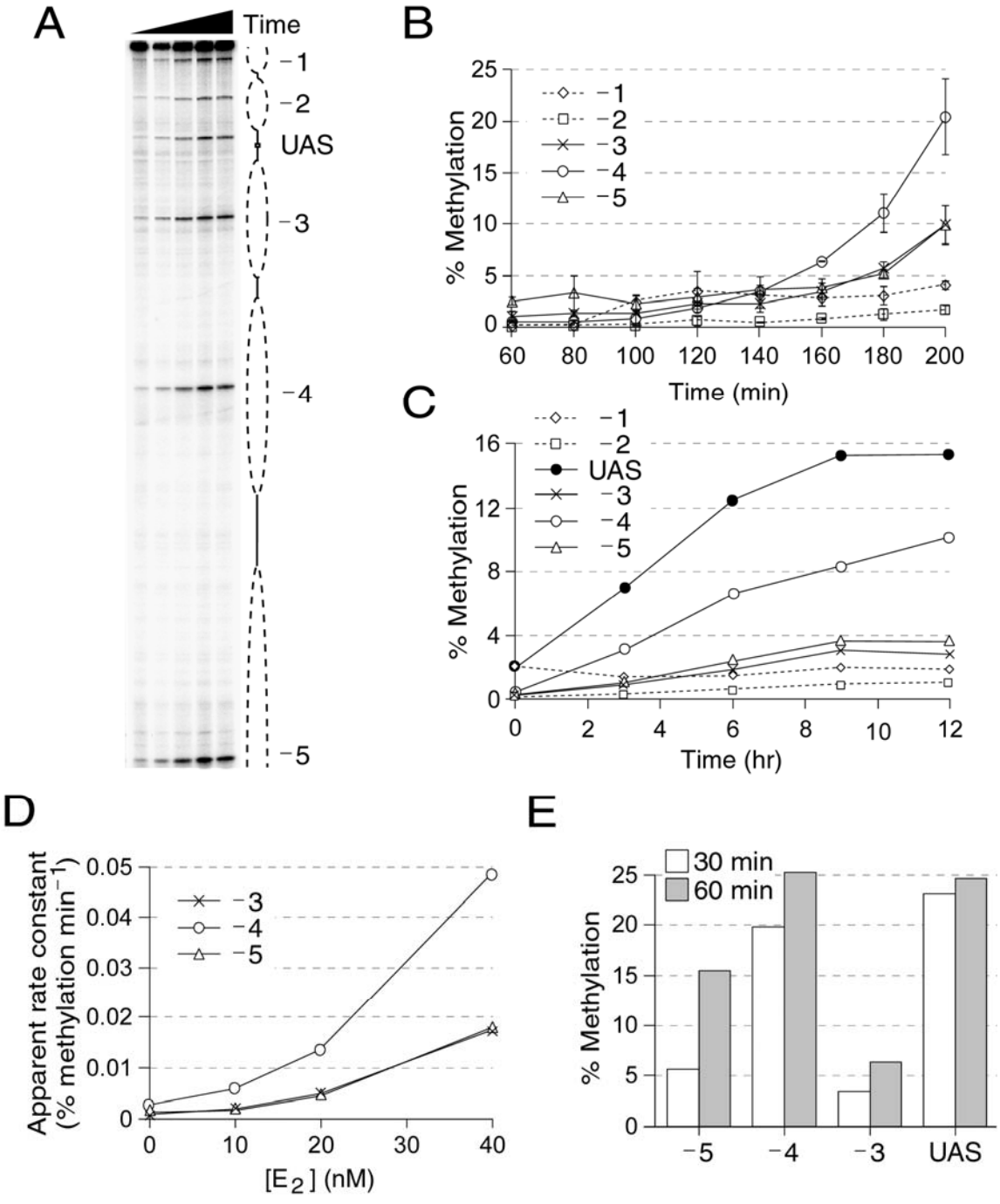
A
Time
−1
−2
UAS
−3
−4
−5
B
% Methylation
Time (min)
C
% Methylation
Time (hr)
D
Apparent rate constant
(% methylation min−1)
[E2] (nM)
E
30 min
60 min
% Methylation
−5
−4
−3
UAS

human estrogen receptor α ligand-binding domain, and VP16 activation domain. LexA-ER-VP16 is expressed constitutively from the *ADH1* promoter (Balasubramanian and Morse, 1999). Thus, high levels of the methyltransferase probe M.HhaI-Pho4 NLS/NES (hereafter referred to as M.HhaI) accumulate in the cytoplasm with the addition of E_2; subsequent deprivation of P_i allows for its rapid nuclear localization. Induction of M.HhaI in strains lacking *PHO4* therefore allows us to measure *PHO5* promoter nucleosome accessibility in the absence of transcriptional activation. In this way, accessibility of the $PHO5^{HhaI}$ promoter was monitored during an induction time course of M.HhaI in a *pho4*Δ strain under conditions of P_i starvation, which serves to allow M.HhaI to enter the nucleus.

Absolute frequencies of m^5C at each HhaI site in the $PHO5^{HhaI}$ promoter were rigorously quantified by primer-walking analysis with oligonucleotides that anneal immediately upstream of each HhaI site (Figure 3-6B). HhaI sites located 51 and 60 bp from the edge of nucleosomes −1 and −2, respectively, were highly refractory to methylation, consistent with the inability of *pho4*Δ cells to remodel the promoter region and activate *PHO5* transcription (Almer et al., 1986). The HhaI site in nucleosome −1 achieved ~2-fold more methylation at 200 min of M.HhaI expression than the site in nucleosome −2. In agreement with our working model, sites in nucleosomes −3, −4, and −5 displayed increased accessibility to M.HhaI over the methylation time course, with nucleosome −4 achieving 10-fold more methylation than the site in nucleosome –2 and 2-fold more than the sites in nucleosomes −3 and −5. As each of the HhaI sites are positioned within ~6 bp of the pseudodyad of each nucleosome, the differences in

accessibility to M.HhaI cannot be due to differences in site location (Anderson and Widom, 2000).

It is possible that the reduced accessibility of downstream nucleosomes to M.HhaI relative to nucleosomes upstream only occurs during initial, low-level expression and accordingly low concentration of the DMTase. Therefore, we extended the time of P_i deprivation and again probed the *PHO5* promoter. However, cell cycle arrest occurs as cells deplete intracellular pools of orthophosphate and polyphosphate (Pringle and Hartwell, 1981; Neef and Kladde, 2003). Consequently, the level of E_2-induced methylation increases well beyond conditions of single-hit kinetics, precluding quantification. For that reason, in this experiment, a pulse of M.HhaI expression was induced in *pho4*Δ cells in P_i-free medium 30 min prior to the indicated times (Figure 3-6C). Also shown is the amount of methylation at the UAS site (19 bp downstream of UASp1), indicating the level of accessibility at each time point at a site not bound by histones to M.HhaI. These 'snapshot' analyses show that Pho4-independent increases in accessibility of nucleosome −4 to M.HhaI at later times of P_i starvation still surpass those levels at nucleosomes −3 and −5. Similar to the differences in accessibility observed at early times following M.HhaI induction, nucleosome −4 accumulated 2.5-fold more methylation than nucleosomes −3 and −5 after 12 hr in P_i-free medium in *pho4*Δ cells.

Increased accessibility of nucleosome −4 relative to nucleosomes −3 and −5 was also observed following induction of M.HhaI over time by various doses of E_2. A significant increase the apparent rate constant for nucleosome −4 relative to nucleosomes

−3 and −5 was observed with increasing concentrations of E_2 (Figure 3-6D). Lastly, we tested whether the differences in accessibility between nucleosome −4 and nucleosomes −3 and −5 to M.HhaI remained after 24 hr of P_i starvation in a *pho4*Δ strain (Figure 3-6E). In this experiment, *pho4*Δ cells were deprived of P_i for 24 hr prior to the addition of a high concentration of E_2 for 30- or 60-min to induce a pulse of M.HhaI probe synthesis. Nucleosome −4, relative to nucleosomes −3 and −5, again displayed increased accessibility to M.HhaI irrespective of the time of probe induction, accumulating as much methylation as the histone-free UAS site.

Although unlikely, it remained a formal possibility that the higher accessibility of nucleosome −1 is due to its HhaI site being 9 bp closer to the nucleosomal edge than the site in nucleosome −2. To verify that the histone-DNA affinity of nucleosome −2 is greater than that of nucleosome −1, we performed native gel electrophoretic analysis of competitive mononucleosome reconstitutions (Figure 3-7). Short radiolabeled DNA fragments corresponding to each of the nucleosomes and a fragment centered at the linker region between them was mixed with limiting histones and various amounts of competitor yeast DNA as indicated. As a control, the 207 bp fragment of the *Lytechinus variegatus* 5S rRNA gene, known to contain a strong nucleosome-positioning sequence, was also used. The mononucleosome reconstituted from the DNA fragment centered at the linker region between nucleosomes −2 and −1 was clearly bound less well than either nucleosomes −2 or −1 (Figure 3-7, lanes 4-6). The mononucleosome reconstituted from the DNA fragment corresponding to nucleosome −1 was competed off at a lower concentration of competitor DNA than was the mononucleosome corresponding to

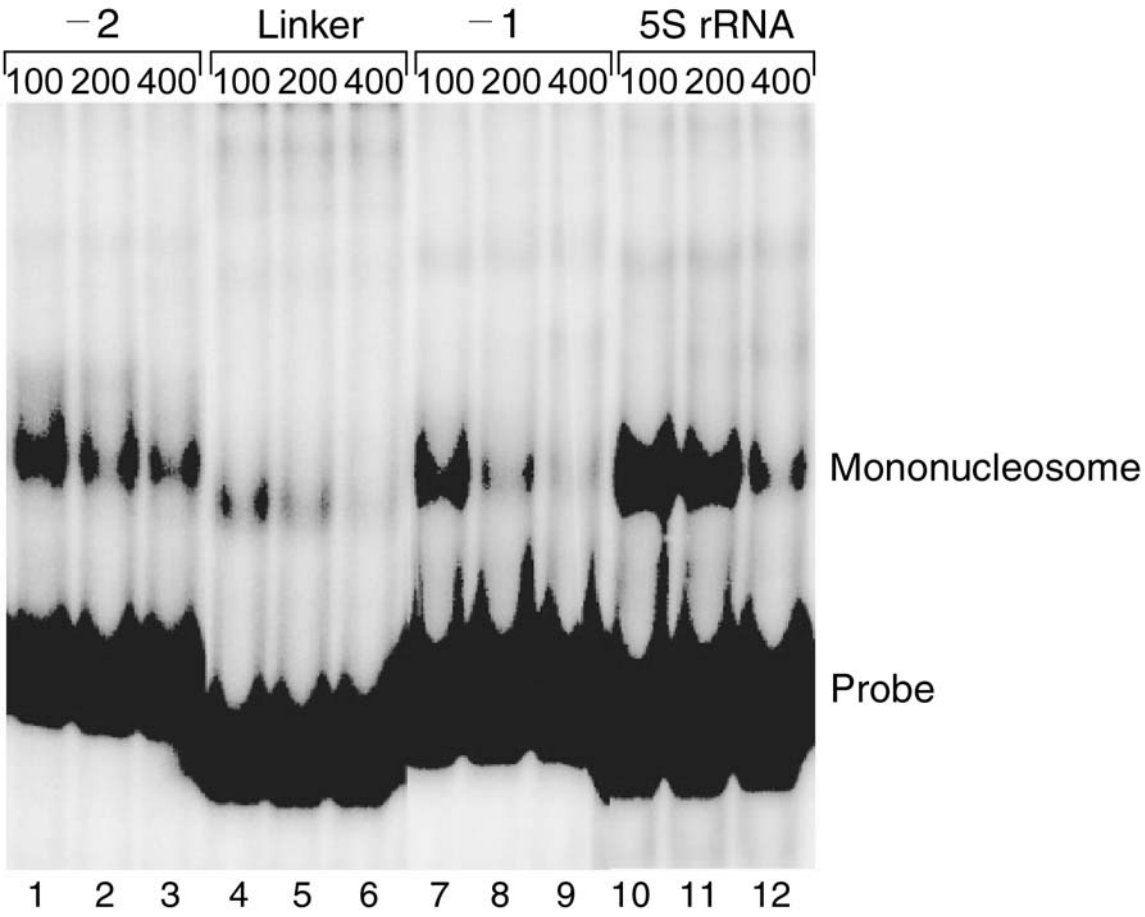

Figure 3-7. The Conformational Stability of Nucleosome −2 is Greater Than Nucleosome −1

Mononucleosomes were reconstituted onto short DNA fragments (~200 bp) corresponding to nucleosomes −2 and −1, a fragment centered at the linker region that spans ~35 bp between nucleosomes −2 and −1, nucleosome −1, and the 207 bp-fragment of the *Lytechinus variegatus* 5S rRNA gene that is known to contain a strong nucleosome-positioning sequence. Reconstitution was done in the presence of 100, 200, and 400 ng competitor DNA (fragmented yeast genomic DNA).

nucleosome −2 (Figure 3-7, compare lanes 2-3 and 8-9). We conclude from these data that the histone-DNA affinity and therefore the conformational stability of nucleosome −2 is greater than that of −1.

From the data presented in Figures 3-6 and 3-7, we conclude that the differential accessibility of nucleosomal sites to M.HhaI in vivo reflects relative histone-DNA interactions. Thus, we interpret these data to indicate that the *PHO5* promoter nucleosomes have varied conformational stabilities. Downstream nucleosomes −1 and −2 positioned over cis-regulatory elements posses the highest stabilities, even though their HhaI sites are located closer to the nucleosomal edge than sites in upstream nucleosomes. The accessibilities of nucleosomes −3 and −5 to M.HhaI, while higher than downstream nucleosomes, are nevertheless lower than that of nucleosome −4. Nucleosome −4 has the highest accessibility and therefore is likely to have the weakest histone-DNA affinity of the five nucleosomes in the *PHO5* promoter.

PHO5 Promoter Nucleosome Positioning Correlates with Predicted DNA Curvature

Recently it was proposed that the intrinsic curvature of a DNA sequence is the primary factor controlling nucleosome stability, acting positively at moderate levels of curvature and negatively at either high or low curvature (Scipioni et al., 2004). Alternatively, it has been suggested that DNA sequences that are anisotropically flexible rotationally position nucleosomes by reducing the free energy of DNA bending (Sivolob and Khrapunov, 1995; Widom, 2001). To investigate the contributions that each of these parameters

make to the positioning of nucleosomes at the *PHO5* promoter, secondary structural analysis was performed for the region of DNA associated with nucleosomes −5 to +1 (Figure 3-8) (Munteanu et al., 1998).

Bendability maxima are predicted for DNA sequences associated with nucleosomes −1 and −4 (Figure 3-8). There are three local bendability minima, two of which correspond to the *PHO5* promoter hypersensitive regions (HSRs) and a third upstream of the pseudodyad for nucleosome +1. These regions have increased AT content. The dinucleotide base-pair steps AT, AA, and TT have previously been shown to have poor conformational mobility due to lack of flexibility (el Hassan and Calladine, 1996; Packer et al., 2000). Moreover, poly (dA-dT) elements have been shown to decrease the affinity of histone-DNA interactions in nucleosomes (Anderson and Widom, 2001). The sequence of DNA associated with nucleosome −5 is predicted to have low bendability but a relatively moderate degree of curvature (1- to 6-degrees/10.5 bp helical turn), decreasing dramatically at the downstream edge. Similarly, the sequence of DNA associated with nucleosome −3 has a relatively moderate degree of curvature (0.5- to 4.5-degrees/10.5 bp helical turn) that increases sharply at the downstream edge. Inflexible or "kinked" DNA has recently been reported to impose a boundary constraint upon a nucleosome at the *AKY2* core promoter (Angermayr et al., 2002) and similarly, the large predicted transitions in DNA curvature could be acting as "bookends" to position nucleosomes −3 and −5. The region of DNA associated with nucleosome −4 is predicted to have a minimum value of curvature (< 2.5 degrees/10.5 bp helical turn). Consistent with DNA curvature contributing to the positioning of

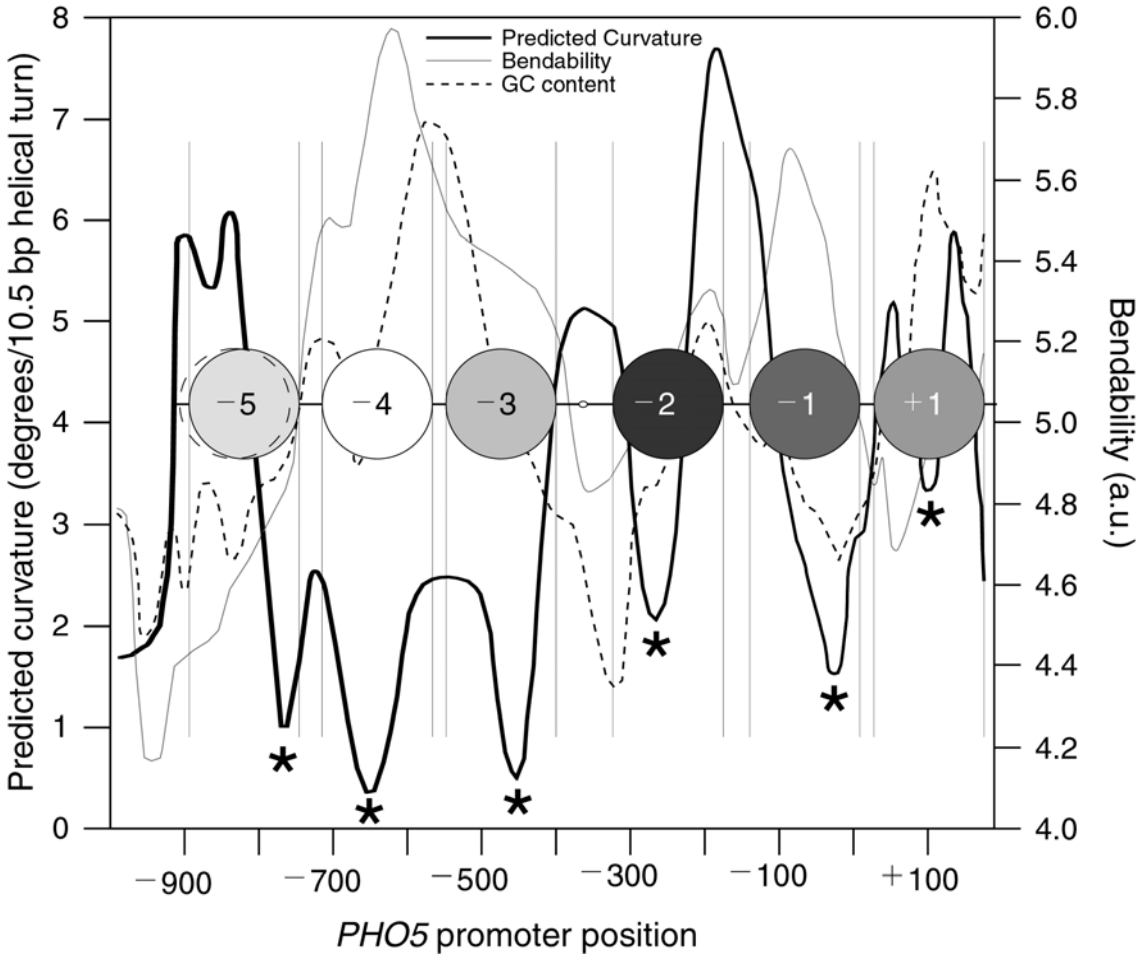

Figure 3-8. Curvature Propensity and Bendability Plot of the *PHO5* Promoter

The diagram of the *PHO5* promoter shows the inferred position of nucleosomes −5 to +1 (circles); open oval, Pho4 binding site UASp1. Nucleosome shading represents relative accessibilities/stabilities. The sequence associated with nucleosome −4 is identified as having a minimum of DNA curvature. Note the conserved pattern of DNA curvature; a minimum flanked by increasing curvature occurs within each nucleosomal sequence. Vertical bars demarcate the extent of curvature or bendability associated with each nucleosome; asterisks identify curvature minimums associated with each nucleosome. For clarity, the axis for %GC content has been omitted; the maximum, close to the downstream edge of nucleosome −4, is 0.53 and the minimum at the UASp1 region is 0.33.

nucleosomes, the low level of curvature correlates with the high level of accessibility of nucleosome −4 to M.HhaI (see Figure 3-6). Strikingly, a conserved pattern of predicted bending is observed with a region of decreased curvature located internal to each of the five promoter nucleosomes, flanked by elements of increased curvature. Nucleotide sequence patterns responsible for an analogous conserved pattern of curvature in heterochromatic satellite DNA have been shown previously to be similar for both satellite and nucleosome positioning DNA sequences (Fitzgerald et al., 1994). These results are consistent with the observed differences in accessibility of nucleosomes at the *PHO5* promoter to M.HhaI in vivo and support a model by which intrinsic DNA curvature participates in the positioning of nucleosomes at the *PHO5* promoter.

DISCUSSION

In this study, we have developed a means to quantitatively assess the relative accessibility of each nucleosome at the *PHO5* promoter in vivo. Unlike synthetic nucleosomal arrays containing tandem repeats of a single positioning sequence, natural arrays contain nucleosomes with diverse histone-DNA interactions and thus heterogeneous nucleosome conformational stabilities. Thus, our approach addresses the differences in histone-DNA affinities in the context of a native cellular chromatin environment. In vitro, equilibrium accessibility is dependent upon both site position (i.e., edge vs. center) and DNA sequence (Anderson and Widom, 2000). High-resolution mapping of the *PHO5* promoter allowed us to position HhaI sites in nucleosomes −3 to −5 within ~6 bp of the pseudodyad and thus measure the relative affinity of histone-

DNA interactions in vivo independent of site position. We demonstrate that nucleosomes at the *PHO5* promoter have varying levels of accessibility to M.HhaI. Importantly, accessibility of the regulatory nucleosomes −2 and −1 containing cis-elements essential for activation parallels the results of mononucleosome reconstitution with the stability of nucleosome −2 > −1. This result is consistent with the requirement for the overexpression of Pho4 needed to overcome nucleosomal protection of UASp2 and activate *PHO5* in either the absence of UASp1 (Venter et al., 1994) or the activity of the histone acetyltransferase Esa1 (Nourani et al., 2004). We infer from these data that the increased accessibility of upstream *PHO5* promoter nucleosomes to M.HhaI suggests decreased conformational stability. Nucleosome −4 has the highest accessibility of the five promoter nucleosomes examined, reflecting decreased histone-DNA affinity. This is surprising given that nucleosomes −3 and −5 are thought to contribute to the positioning of nucleosome −4 by imposing boundary constraints (Fascher et al., 1993). Perhaps, in conjunction with nucleosomal boundary constrains, the positioning of nucleosome −4 is due to the high degree of bendability observed for that region. Nevertheless, our analysis of the accessibility of nucleosomal sites indicates that the affinity of histone-DNA interactions make essential contributions to the chromatin organization of the promoter region and consequently nucleosomal repression at *PHO5*. This has been suggested by others (Fascher et al., 1993; Haswell and O'Shea, 1999; Terrell et al., 2002) as in vivo depletion of histone H4 causes derepression of *PHO5* under otherwise repressive conditions of high-P_i (Han et al., 1988).

At *PHO5*, the differences in observed nucleosome accessibility/stability parallel the differences in DNA curvature for regions encompassing each of the nucleosomes. Intrinsic DNA curvature has been proposed to be a primary factor controlling nucleosome stability and thus nucleosome positioning (Scipioni et al., 2004). Similarly, it has also been suggested that translational positioning of nucleosomes can be assisted by intrinsic DNA curvature (Bash and Lohr, 2001). Given that the overall levels of predicted DNA curvature are similar for nucleosomes −3 and −5 and that they have similar levels of accessibility to M.HhaI, these results are consistent with a model in which DNA curvature participates in the translational positioning of nucleosomes at the *PHO5* promoter. This is further supported by the finding that deletion of the UASp1 region (−345 to −392) had no effect on the positions of adjacent nucleosomes, ruling out the possibility that additional factors, bound at UASp1, exert a boundary constraint on nucleosome −3 (Fascher et al., 1993). Nucleosome −2 has the lowest measured accessibility to M.HhaI (see Figures 3-3, 3-6B, and 3-6C) and the highest degree of intrinsic DNA curvature. Nucleosome −1 has slightly lower levels of curvature and consequently lower stability than nucleosome −2 (see Figures 3-3, 3-6B, and 3-6C). In light of these analyses as well as our competitive mononucleosome reconstitution, we maintain that the stability of nucleosome −1 is a reflection of histone-DNA interactions and not a result of boundary constraints from nucleosomes −2 and +1 (Fascher et al., 1993).

The position of the *PHO5* promoter nucleosomes correlate with a pattern of local DNA curvature. Each nucleosome is positioned over an element of decreased curvature,

flanked by tracts of increasing curvature. An analogous pattern of bending has been observed previously, shown to be similar for both satellite and nucleosome positioning DNA sequences, consisting of two 50-60 bp bending elements separated by a 20-30 bp region of low curvature (Fitzgerald et al., 1994). These data suggest that an energetic bias for the positioning of a nucleosome at *PHO5* may be defined by a local curvature minimum. However, other determinants such as interactions between nucleosomes and higher-order chromatin structure likely contribute to the overall stability and positioning of nucleosomes.

In summary, our results are most consistent with a model of nucleosome accessibility in vivo whereby the affinity of histone-DNA interactions determines the probability with which factors can gain access to nucleosomal sites in chromatin. As a consequence, nucleosomes with a high degree of conformational stability require either high concentrations of factor to drive binding of nucleosomal targets or the continuous targeted recruitment of chromatin remodelers such as SWI/SNF. By this model, disruption of nucleosome-occluding cis-elements requires persistent SWI/SNF function (Biggar and Crabtree, 1999) and ATP-driven nucleosome remodeling is highly reversible (Logie and Peterson, 1997; Jaskelioff et al., 2000). Finally, the high level of stability of nucleosome −2 at the *PHO5* promoter may explain the requirement for coactivators at early times of activation (Barbaric et al., 2001; Reinke and Hörz, 2003).

CHAPTER IV

BIDIRECTIONALLY PROPAGATED CHROMATIN REMODELING DURING TRANSCRIPTIONAL ACTIVATION IN VIVO

SYNOPSIS

Promoter transactivation is accompanied by the remodeling of nucleosomes in chromatin. However, the molecular mechanisms by which promoter elements communicate across a promoter region to effect transcriptional activation at a distance remain unclear. Here, we present kinetic studies of the chromatin remodeling program at the *Saccharomyces cerevisiae PHO5* promoter. Our results show that nucleosomes proximal to the upstream activating sequences (UASs), relative to distal nucleosomes, are remodeled earlier in time during the initial stages of transcriptional induction and achieve higher levels of disruption at steady-state activation of *PHO5*. Consistent with this temporal program of chromatin reorganization, association of the Pho4 transactivator at the *PHO5* promoter increases over time, localizing SWI/SNF preferentially at the UAS region. These results support a novel mechanism of upstream activation by which chromatin remodeling propagates in a stepwise, bidirectional, and finite manner.

INTRODUCTION

Enhancers are DNA elements in metazoans that activate gene expression from distances as far as several thousand base-pairs upstream or downstream of a gene (Khoury and Gruss, 1983). In yeast, UASs are functionally similar to enhancers but appear to have a

substantially reduced ability to activate transcription at large distances and when located downstream of TATA elements (Guarente and Hoar, 1984; Brent and Ptashne, 1985). The current view of transcriptional regulation in eukaryotes involves enhancer- or UAS-bound activators that, via protein-protein interactions, effect the ordered recruitment of multi-protein complexes that participate in the ultimate assembly of the transcription preinitiation complex (PIC) at the core promoter (Lemon and Tjian, 2000; Fry and Peterson, 2001). A central, albeit poorly understood, feature of the recruitment model of transcriptional activation concerns the mechanisms by which enhancers (or UASs) and basal promoter elements communicate with each other at a distance (Wang and Giaever, 1988).

Within the eukaryotic nucleus, communication between upstream and downstream gene regulatory regions occurs in the context of chromatin. In promoter regions, nucleosomes inhibit transcription by obstructing DNA binding by activator proteins and the basal transcription machinery (Owen-Hughes and Workman, 1994). Accordingly, activators binding at one or more accessible cis-regulatory regions contend with repressive chromatin by recruiting a series of multisubunit coactivators, which lack sequence-specific DNA binding (Kadonaga, 1998; Fry and Peterson, 2001; Narlikar et al., 2002). In *S. cerevisiae*, these include SAGA, which contains the Gcn5 histone acetyltransferase, and the SWI/SNF chromatin remodeling complex, which hydrolyzes ATP to disrupt nucleosomal histone-DNA contacts (Howe et al., 1999; Vignali et al., 2000). The coordinated recruitment of multiple coactivator complexes by DNA-bound activators has been shown to target immediately adjacent, TATA-occluding

nucleosomes for chromatin remodeling (Agalioti et al., 2000; Lomvardas and Thanos, 2002). By contrast, little is known about how chromatin remodelers are targeted over larger distances, often spanning hundreds of base-pairs, to effect the disruption of multiple nucleosomes for PIC assembly. Moreover, at promoters where multiple, neighboring nucleosomes are targeted for disruption, it is not known whether there are differences in the extent of disruption between nucleosomes or if their remodeling occurs simultaneously or sequentially.

The *PHO5* promoter of *S. cerevisiae* has been used extensively to address the role of chromatin structure in the regulation of transcription. An extended region of the *PHO5* promoter, encompassing at least four positioned nucleosomes, is rendered hypersensitive to nucleases upon activation by phosphate (P_i) starvation (Bergman and Kramer, 1983; Almer et al., 1986). Recent studies suggest that the hypersensitivity is due, at least in part, to histone loss (Boeger et al., 2003; Reinke and Hörz, 2003; Adkins et al., 2004; Boeger et al., 2004; Nourani et al., 2004). Paradoxically, detailed structural analyses by Boeger et al. (2003, 2004) indicate a modest loss of nucleosomes from the induced *PHO5* promoter, approximately one-half of the expected number. It is currently unclear whether this reflects the remodeling of all *PHO5* promoter nucleosomes in a fraction of cells or if different nucleosomes along the promoter are disrupted to varying extents in all cells. These and other studies have addressed the initial repressive and final activated states of *PHO5* promoter chromatin. However, none have examined intermediate states of nucleosomal perturbation along the promoter, which should reveal important aspects of the activation process.

Here, we find a distinct temporal program of chromatin remodeling during the initial stages of *PHO5* transcriptional activation. Nucleosomes proximal to the *PHO5* UAS region are disrupted earlier and to a greater extent than nucleosomes located more distal. Consistent with these temporal changes in chromatin structure, SWI/SNF preferentially localizes at the UAS region, coincident with increases in Pho4 activator binding. A local maximum of UAS-associated SWI/SNF provides an in vivo mechanism for the preferential remodeling of UAS-proximal nucleosomes. Our results indicate that chromatin remodeling can be propagated bidirectionally to encompass a variable number of nucleosomes within different cells in a population. Moreover, our results support a novel mechanism of UAS-core promoter communication by which SWI/SNF recruitment leads to the stepwise disruption of multiple nucleosomes to facilitate downstream PIC assembly.

MATERIALS AND METHODS

S. cerevisiae Strains and Growth Conditions

All *S. cerevisiae* strains were constructed by standard genetic methods from CCY694, *MAT***a**/*MAT*α *leu2*Δ0/*leu2*Δ0 *lys2*Δ0/*lys2*Δ0 *ura3*Δ0/*ura3*Δ0 *pho3*Δ::R/*pho3*Δ::R (S288C background), where R is a *Zygosaccharomyces rouxii* recombinase site that remains after intramolecular recombination. For probing chromatin in vivo with M.HhaI [M.HhaI-V5-Pho4 nuclear localization sequence/nuclear export sequence (NLS/NES), see below], the methyltransferase was expressed from an estrogen-inducible system (Balasubramanian and Morse, 1999). The *PHO5* promoter in these strains (all *MAT*α

*leu2*Δ0 *lys2*Δ0 *ura3*Δ0 *pho3*Δ::R) was modified to contain seven point mutations [original nucleotide (distance upstream of the translational start site) replacement nucleotide: T(−821)G, T(−638)G, G(−636)C, C(−513)G, C(−404)G, A(−336)G, and C(−238)G], creating the *PHO5*^{HhaI} promoter. Strains WJY2280 (*PHO4*) and WJY2410 (*pho4*::*lox*P, where *lox*P is a Cre recombinase site that remains after intramolecular recombination) were used for probing nucleosome disruption. The relevant genotype of both strains is also *MAT*α *can1*::M.HhaI-V5-Pho4 NLS/NES-*LEU2 ho*::LexA-ER-VP16-*LYS2 PHO5*^{HhaI}. For footprinting with M.CviPI, the methyltransferase was expressed from the estrogen-inducible system in strains with an unaltered *PHO5* promoter; strains SHY1860 (*PHO4*) and SHY2490 (*pho4*::*kanMX4*), which are also *MAT***a** *leu2*Δ0 *lys2*Δ0 *ura3*Δ0 *pho3*Δ::R *ho*::M.CviPI-*LYS2*-LexA-ER-VP16. The M.CviPI probe (mut Zif-M.CviPI) was constructed as previously described (Carvin et al., 2003a). Essentially, it is a 'free' methyltransferase that contains the full-length, wild-type M.CviPI with its N-terminus fused to a DNA-binding-deficient version of the zinc-finger protein Zif268. For ChIP analysis, strains LFY1617 (*MAT***a** *leu2*Δ0 *lys2*Δ0 *ura3*Δ0 *pho3*Δ::R *SWI2*-13Myc::*kanMX4*) and ADY2724 (*MAT***a** *leu2*Δ0 *lys2*Δ0 *ura3*Δ0 *pho3*Δ::R 3Myc-*PHO4*) were used. The methyltransferase probe M.HhaI-V5-Pho4 NLS/NES consists of an in-frame fusion of full-length M.HhaI, a TGLGIL linker peptide, the V5 epitope, and the NLS/NES of Pho4 [amino acids 2-199 with a D78P point mutation that abrogates the Pho4 activation domain function; (McAndrew et al., 1998)]. The fusion gene was inserted into YIpM.HhaI-Pho4 under control of a minimal *GAL1* promoter containing four LexA binding sites (i.e., *lex*O sites) and integrated at the *CAN1* locus.

Cells were grown at 30˚C on YPPD plates [2% glucose, 1% yeast extract (Difco), 2% peptone (Difco), 13.4 mM KH_2PO_4] or in liquid cultures of defined high-P_i medium [2% glucose, 20 mM 2-*N*-morpholino ethanesulfonic acid (MES), pH 5.5, 14 mM *L*-glutamine, 13.4 mM KH_2PO_4, 0.7 g/l YNB without amino acids, $(NH_4)_2SO_4$, phosphate, or dextrose, 0.77 g/l CSM supplement mix (Bio101)] or P_i-free medium (substituting the 13.4 mM KH_2PO_4 with 13.4 mM KCl). When P_i starvation was employed, the cells grew for only two to three additional generations after being washed and resuspended in P_i-free medium.

rAPase Activity Assays

After growth under the specified conditions, the cells were chilled to 4˚C, washed twice, and resuspended with cold 0.1 M sodium acetate, pH 3.6. After a 10 min preincubation of 500 μl of cell suspension at 30˚C, acid phosphatase activity was assayed by the addition of 500 μl of 20 nM *p*-nitrophenylphosphate (Roche) and incubation at 30˚C for 10 min. Enzymatic activity was terminated by the addition of 250 μl of 1 M Na_2CO_3 and quantified by measuring the absorbance at 420 nm. Activities are reported in Miller units [(A_{420} × 1,000)/(OD_{600} × volume (in milliliters) of cells assayed × 10 min)].

Bisulfite Genomic Sequencing

Genomic DNA was rapidly isolated after the addition of sodium azide to 0.015% and 5-methylcytosine (m^5C) levels were determined by bisulfite genomic sequencing as described (Jessen et al., 2004b). The final concentrations of dNTPs (A, C, T) and ddGTP

in the primer extension reactions were 50 μM and 150 μM, respectively, enabling >96% efficiency in detection of methylated cytosines. Therefore, the absolute frequencies of non-methylated templates (run-off product at the top of the gel; generated on templates lacking m^5C) and site methylation were calculated by dividing the intensity of a given band by all summed product intensities. For cumulative quantification of Pho4-dependent increases in nucleosome accessibility, the absolute frequencies of m^5C at each HhaI site in the *PHO5*^{HhaI} promoter were rigorously quantified by primer walking on PCR products amplified from bisulfite-treated DNA. The oligonucleotides used in these PCR amplification reactions as well as those used for primer walking are listed in Tables 4-1 and 4-2. For primer walking, each HhaI site was rigorously quantified independent of the others by digesting PCR-amplified products with restriction enzymes prior to primer extension. Thus, each extension either terminates at the HhaI site or runs off the end of the PCR product, enabling strict quantification of methylation frequencies. The software package Kaleidagraph was used to generate curve fits and to derive times of half-maximal remodeling ($t_{½}$).

ChIP Analysis

After growth in defined high-P_i medium, cell cultures were washed twice and resuspended in P_i-free medium for the times indicated prior to treatment with 1% formaldehyde for 15 min at room temperature. ChIP analysis was performed as described (Hecht et al., 1995) using 2 μl of rabbit A-14 anti-Myc antibody (Santa Cruz Biotechnologies). Samples from two independent time courses of P_i starvation were quantified by PCR in triplicate in real time using an ABI PRISM 7900HT Sequence

Detection System (Applied Biosystems) for continuous SYBR Green I fluorescence detection. Finnzymes DyNAmo HS SYBR Green qPCR master mix was used in a 10 µl reaction volume. Serial dilutions of input DNA were used to generate a standard curve for each genomic region that was analyzed using primers listed in Table 4-3 (R^2 values for each linear curve fit are indicated): *PHO5* UAS (−492 to −191 bp), $R^2 = 0.985$; *PHO5* nucleosome −1 (−174 to −7 bp), $R^2 = 0.984$; *PHO5* nucleosome −5 (−877 to −765 bp), $R^2 = 0.981$; and the control *WHI4* locus (+1152 to +1314 bp), $R^2 = 0.997$.

Micrococcal Nuclease (MNase) Analysis

MNase digestion (4 min with 0, 15, 30, and 60 U/ml) of chromatin from spheroplasted cells was performed (Kent et al., 1993) after 20 min zymolyase (Seikagaku) treatment of 1.5×10^9 cells grown overnight in high-P_i medium. Isolated genomic DNA was then digested with ApaI, electrophoresed on a 1.6% agarose-TAE gel, transferred to a membrane, and hybridized with a probe corresponding to a 498 bp upstream region of the *PHO5* promoter (PCR amplified using the primers described in Table 4-1).

Table 4-1. Oligonucleotides for PCR Amplification

Oligonucleotides for PCR Amplification of the MNase Hybridization Probe.		
Primer	Sequence	Figure(s)
PHO5-771	GGCCCCAAAAAGTATTGTCTTC	4-1B
PHO5-566	TTTGCGCAAAGATGGACAAAAACCATC	4-1B
Oligonucleotides for PCR Amplification of Bisulfite-Treated DNA.		
Primer[a]	Sequence	Figure(s)
*PHO5*b1-922	TTCAATTaCTAAATACAATaTTCCTTaaT	4-2A,B,E 4-3 4-4A,B 4-5A,B
*PHO5*b2-769	atatataagcttcAAtATTGGTAATtTtGAATTTGtTTGtTGtTTGtT	4-2A,B,E 4-3 4-4A,B
*GAL1*b1-1007	CAATTTTAaAAaTACTTTCACTTTaTAAC	4-2D
*GAL1*b2-95	GtAtTTTTtGGttAATGGTtTTGGTAA	4-2D
*PHO5*a1-20	aaCTAaTTTaCCTAAaaaAATaaTACCTaCATTaaCC	4-2C
*PHO5*a2-1132	AtTTtAAAtGAAGGTAAAAGGTTtATA	4-2C
*PHO5*b1-751	TaTTTTCTCATaTAAaCaaACaTCaTCT	4-2B 4-4B 4-5C
*PHO5*b2-968	GATATtTTTTTGGGTAttAATtTTGTtGAtAT	4-5C
*PHO5*b2-924	GAAAAtAGGGAttAGAATtATAAATTTAGTtT	4-4B 4-5A,B

[a]Pairs of 'a' (a1 and a2) or 'b' (b1 and b2) are primers for the upper and lower DNA strands, respectively, from bisulfite-treated DNA. Nucleotides in lower case represent either G to a or C to t transitions.

Table 4-2. Bisulfite Genomic Sequencing Primers

^{32}P-end-labeled Oligonucleotides for Primer Extension of PCR Products Amplified from Bisulfite-treated DNA.

Primer[b]	Sequence	Figure(s)
*PHO5*b1-768	atatatctcgaggACTAATAaAAaAAAACA AaAaACTCCaT	4-2A,E 4-3 4-4B 4-5A
*PHO5*b1-751	TaTTTTCTCATaTAAaCaaACaTCaTCT	4-2B 4-3 4-4A,B
*GAL1*b1-1067	TCTCTTTaaAACTTTCAaTAATAC	4-2D
*PHO5*a1-1053	AACAaATTTAAACATTaaTAATCT	4-2C
*PHO5*b1-1100	TAATAATTaCaAaAAACaTaACCCAA CT	4-2E 4-3
*PHO5*b1-1101	CTCTCTTTACAaaACaCCaaAaAC	4-2E 4-3
*PHO5*b1-1102	AATaCCAAAAAAAaTAAAAaTAATT AAAAaAaTT	4-2E 4-3 4-5C
*PHO5*b1-1047	ATATACCCATTTaaaATAAaaaTAAA C	4-5C
*PHO5*b1-1103	aTCACCTTACTTaaCAAaaCATATA	4-3
*PHO5*b1-922	TTCAATTaCTAAATACAATaTTCCTT aaT	4-5B

[b]Pairs of 'a' (a1 and a2) or 'b' (b1 and b2) are primers for the upper and lower DNA strands, respectively, from bisulfite-treated DNA. Nucleotides in lower case represent either G to a or C to t transitions.

Table 4-3. Oligonucleotides for Quantitative ChIP Analysis		
Oligonucleotides for Quantitative ChIP Analysis.		
Primer[c]	Sequence	Figure(s)
PHO5-272 (−1)	GGTCACCTTACTTGGCA	4-6
PHO5-237 (−1)	TCTCGAATTTGCTTGCT	4-6
PHO5-1133 (−5)	AGACTCCGTCCCTCTTT	4-6
PHO5-1134 (−5)	ATGTGCAGTAGTAACTTATCA	4-6
WHI4-1169 (*WHI4* ORF)	TAGCCAGGATGTTCCACA	4-6
WHI4-1170 (*WHI4* ORF)	CAAATTGGAAGGAACATTCG	4-6
PHO5-1172 (UAS)	GGAAGTCATCTTATGTGCGCTGCTT	4-6
PHO5-1173 (UAS)	ATGTGCGATCTCTTCGAAAACAGGG	4-6
[c]The region amplified by each primer is indicated in parentheses.		

RESULTS

Temporal and Bidirectional Disruption of *PHO5* Promoter Chromatin

To reveal chromatin remodeling intermediates that form during *PHO5* activation, we have undertaken a novel kinetic approach in living cells. Relative to the *PHO5* coding region, five upstream and three downstream nucleosomes are positioned in the presence of high repressive concentrations of inorganic P_i [Figure 4-1 and (Almer and Hörz, 1986)]. The UASp1 region is histone free but is flanked by positioned nucleosomes. Following extended P_i deprivation, at least four upstream nucleosomes are remodeled concomitantly with increased transcription (Almer et al., 1986), however, the kinetic details of the chromatin reorganization are unknown. Remodeling of nucleosomal arrays by the SWI/SNF complex has been reported to be a highly reversible process (Logie and Peterson, 1997; Biggar and Crabtree, 1999; Jaskelioff et al., 2000). Therefore, to avoid the loss of metastable remodeling intermediates while preparing nuclei or permeabilizing cells, we have employed a cytosine-5 (C5) DNA methyltransferase (M.HhaI) as a highly sensitive and rapid probe of in vivo chromatin dynamics [Materials and Methods and (Kladde et al., 1996; Jessen et al., 2004b)].

In order to use M.HhaI as an in vivo chromatin probe, the *PHO5* promoter was modified at its endogenous location to contain a single HhaI site (GCGC) in the histone-free UASp1 region and in the central region of each positioned nucleosome, creating the *PHO5*^{HhaI} promoter [Figure 4-1 and (Almer and Hörz, 1986; Terrell et al., 2002; our unpublished data)]. One or two point mutations were introduced in nucleosomes −2 to −5 (−1 was not altered) and in the UASp1 region. As expected, the minor sequence

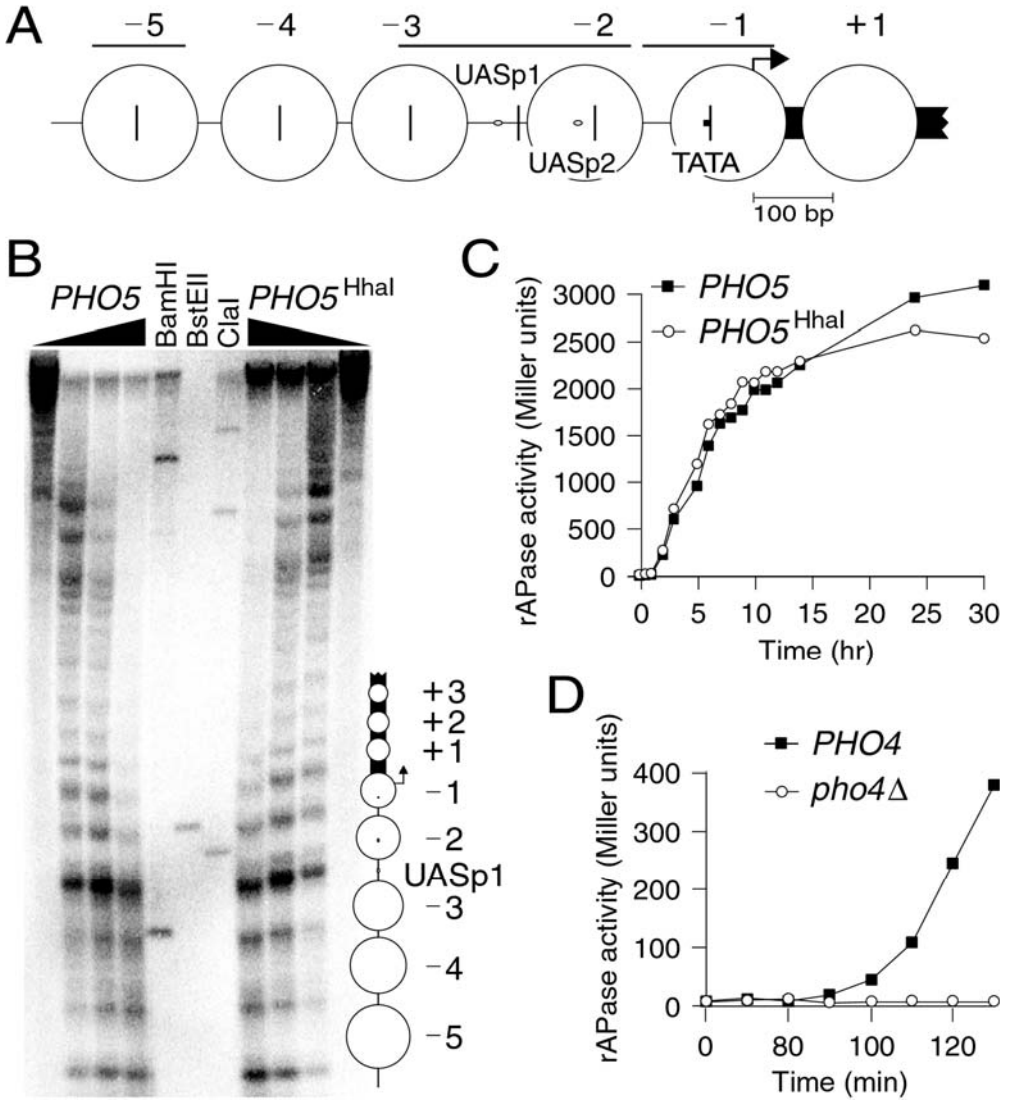

Figure 4-1. System for In Vivo Kinetic Analysis of *PHO5* Chromatin Remodeling

(A) The *PHO5*^{HhaI} promoter. Large open circles, positioned nucleosomes −5 to +1 as determined in (B) and (Almer and Hörz, 1986). Vertical bars, HhaI sites; horizontal bars, regions assayed by ChIP analysis in Figure 4-6; open ovals, Pho4 binding sites UASp1 and UASp2; filled bar, TATA element; black arrowhead, major transcription initiation site; broken black rectangle, *PHO5* coding sequence.
(B) MNase analysis of the *PHO5* and *PHO5*^{HhaI} promoters. Samples in the first and last lanes were not digested with MNase. The presence of undigested DNA at the top of the gel in the MNase-treated samples is due to the presence of unspheroplasted cells when the nuclease was added. In the middle lanes, genomic DNA was digested with the indicated restriction enzyme prior to indirect end-labeling to generate fragments that serve as molecular weight markers. Symbols as in (A).
(C) Extended time course of activation of the *PHO5* and *PHO5*^{HhaI} promoters upon P_i starvation. rAPase, repressible acid phosphatase.
(D) Initial rates of *PHO5* activation in *PHO4* and *pho4*Δ strains following transfer from high- to no-P_i medium. The mean ± standard deviation for duplicate cultures is shown (errors are too small to be visible).

alterations do not compromise the normal regulation of the *PHO5* promoter since the chromatin structure (Figure 4-1B) and activation kinetics (Figure 4-1C) of the *PHO5* and *PHO5*^{HhaI} promoters are extremely similar, if not identical. Additionally, induction of M.HhaI synthesis and hence methylation of HhaI sites in the *PHO5* or *PHO5*^{HhaI} promoter does not affect their repressed or activated levels of expression (data not shown). These results demonstrate that *PHO5*^{HhaI} is structurally and functionally indistinguishable from the wild-type promoter and is not influenced by the introduction of 5-methylcytosine (m^5C).

M.HhaI accessibility was monitored during induction of the *PHO5*^{HhaI} promoter in wild-type and *pho4*Δ strains (Figure 4-2). Pho4 is essential for *PHO5* chromatin remodeling and activation (Fascher et al., 1990), thus repressible acid phosphatase (rAPase) activity increases only in the *PHO4*$^{+}$ strain (Figure 4-1D). As nucleosomes occlude the access of DNA methyltransferases to their cognate sites (Kladde and Simpson, 1994; Kladde et al., 1996), bisulfite sequencing analysis (Frommer et al., 1992; Clark et al., 1994; Jessen et al., 2004b) shows preferential methylation of the histone-free UASp1 region in *pho4*Δ cells (Figure 4-2A, lanes 1-8). By 80-100 min of activation, access of M.HhaI to each nucleosomal site is significantly greater in *PHO4* vs. *pho4*Δ cells (Figure 4-2A, compare matched time points in lanes 1-8 and 9-16), demonstrating Pho4-dependent changes in nucleosome position (sliding or displacement) and/or conformation, collectively defined as activator-dependent chromatin remodeling (Aalfs and Kingston, 2000). The data in Figure 4-2A suggest that

Figure 4-2. *PHO5* Chromatin Remodeling Propagates Bidirectionally from UASp1-Proximal to -Distal Nucleosomes

Initial increases in M.HhaI accessibility at the upstream (A) and downstream (B) regions of the *PHO5*^{HhaI} promoter in *pho4*Δ (lanes 1-8) and *PHO4* (lanes 9-16) strains. At the indicated times of P_i starvation, genomic DNA was rapidly isolated and m^5C levels at each HhaI site on the bottom DNA strand were determined by bisulfite genomic sequencing, which yields a positive signal in proportion to the level of m^5C at a given site. The most abundant product at the top of the gel is the run-off product generated by primer extension on unmethylated templates. Ellipses, positioned nucleosomes −1 to −5; horizontal lines, HhaI sites. All bands on the gel that do not correspond to a HhaI site result from non-specific pausing during primer extension.
(C) M.HhaI accessibility of the upper strand of the *PHO5*^{HhaI} promoter. The downstream region is analyzed and symbols are as in (A). Two non-specific products due to primer extension pausing are visible near the run-off product.
(D) Similar levels of M.HhaI activity are expressed in the *pho4*Δ and *PHO4* strains. Internal samples used in (A-C) were analyzed by bisulfite sequencing, demonstrating the same rate of m^5C accumulation at a histone-free HhaI site in the *GAL1* promoter.
(E) Cumulative quantification of Pho4-dependent increases in nucleosome accessibility. Methylation levels (mean ± standard deviation) in duplicate *pho4*Δ and *PHO4* cultures were determined at the indicated times of P_i starvation. Values have been corrected by subtracting the background methylation in *pho4*Δ from the methylation in *PHO4* cells. Statistically significant levels of m^5C (P-value < 0.05; t-Test, two-sample assuming equal variances) in *PHO4* relative to *pho4*Δ strains occur at 60 min for nucleosomes −3 and −4, 80 min for nucleosome −2, 100 min for nucleosome −5, and 120 min for nucleosome −1. Pho4-dependent remodeling of nucleosome −4 is underestimated at later times due to its significant accessibility in *pho4*Δ cells.

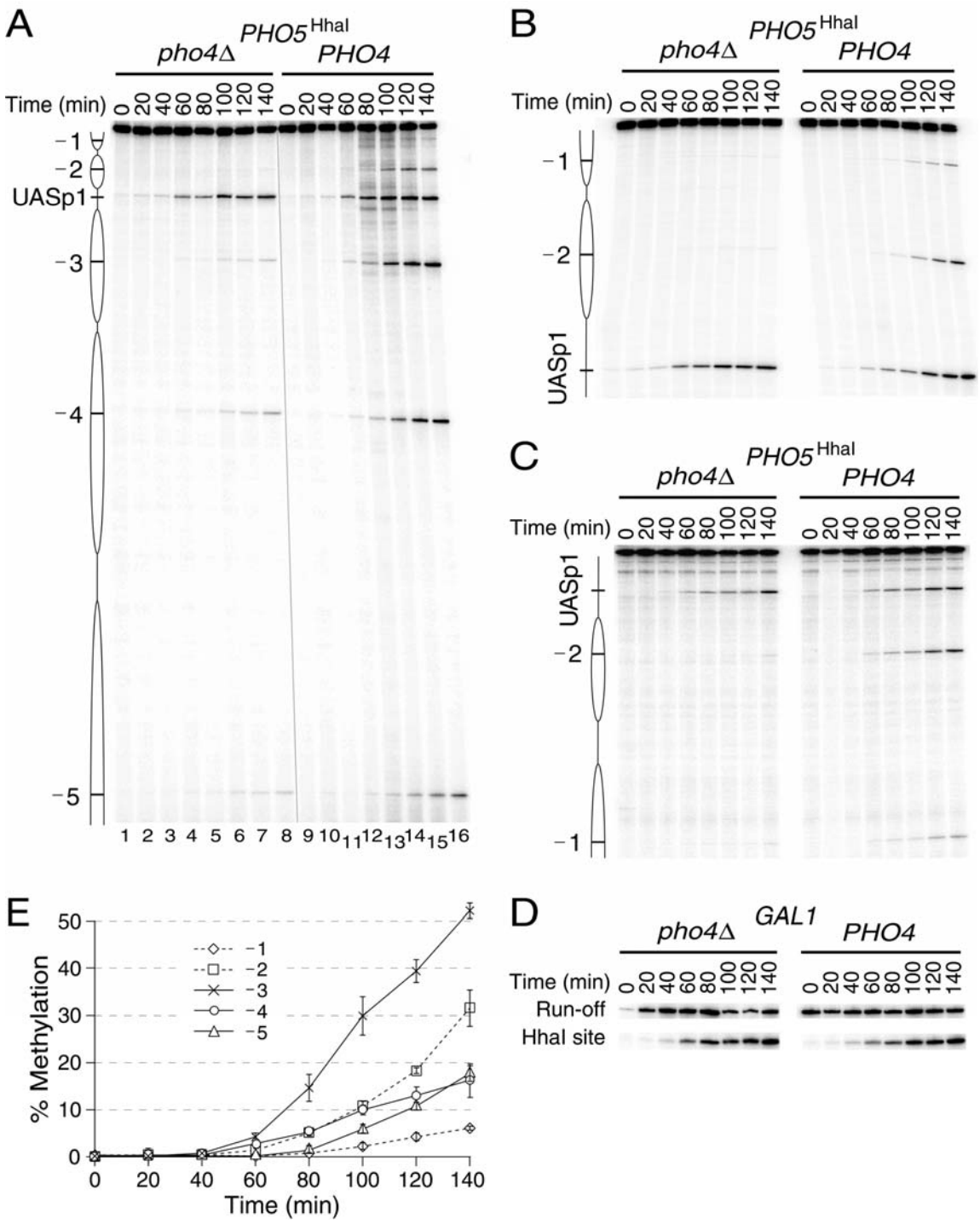
A
PHO5 HhaI
pho4Δ
PHO4
Time (min)
0 20 40 60 80 100 120 140 0 20 40 60 80 100 120 140
−1
−2
UASp1
−3
−4
−5
1 2 3 4 5 6 7 8 9 10 11 12 13 14 15 16
B
PHO5 HhaI
pho4Δ
PHO4
Time (min)
0 20 40 60 80 100 120 140 0 20 40 60 80 100 120 140
−1
−2
UASp1
C
PHO5 HhaI
pho4Δ
PHO4
Time (min)
0 20 40 60 80 100 120 140 0 20 40 60 80 100 120 140
UASp1
−2
−1
D
GAL1
pho4Δ
PHO4
Time (min)
0 20 40 60 80 100 120 140 0 20 40 60 80 100 120 140
Run-off
HhaI site
E
% Methylation
50
40
30
20
10
0
−1
−2
−3
−4
−5
0 20 40 60 80 100 120 140
Time (min)

Pho4 targets nucleosome −3 for remodeling earlier than nucleosome −4, which is perturbed before nucleosome −5.

Absolute frequencies of m^5C at each HhaI site in the *PHO5*^{HhaI} promoter were rigorously quantified by re-analysis with primers that anneal just upstream of each HhaI site (i.e., primer walking). Representative results using the UASp1 primer show that nucleosome −2 is remodeled earlier and to a greater extent than is nucleosome −1 during promoter activation (Figure 4-2B). This result was confirmed by the analysis of accessibility of *PHO5*^{HhaI} chromatin to in vivo-expressed M.HhaI on the upper DNA strand (Figure 4-2C). These temporal differences in accumulation of m^5C in Figures 4-2A to 4-2C are due to specific remodeling of the *PHO5*^{HhaI} promoter chromatin because they depend on Pho4, which recruits SWI/SNF (see Figure 4-6). Further, the *PHO4* and *pho4*Δ strains display similar amounts of M.HhaI activity, since, at each matched time point, similar levels of m^5C are present at the UASp1 region (Figures 4-2A to 4-2C) as well as at a single, accessible HhaI site in the UASg region of the *GAL1* promoter (Figure 4-2D). The cumulative, quantitative primer extension data presented in Figure 4-2E indicate that statistically significant levels of methylation occur earlier in time at nucleosomes flanking UASp1 (−2 and −3) than at distal nucleosomes (−1 and −5). A replot of each curve in Figure 4-2E as the percentage of methylation achieved at 140 min indicates that the rates of remodeling of each nucleosome are quite similar (data not shown). Thus, Figure 4-2E reflects the time at which the remodeling process initiates at each nucleosome as opposed to the rate at which each nucleosome is remodeled. In contrast, M.HhaI methylates all six cognate sites in protein-free *PHO5*^{HhaI}

DNA at nearly identical rates, further supporting our conclusion that disruption of UAS-proximal nucleosomes occurs earlier in time and is preferential to that of distal nucleosomes upon activation (Figure 4-3).

Preferential Disruption of UAS-Proximal Nucleosomes Persists at Full Promoter Activation

It was possible that the reduced remodeling of distal nucleosomes occurs only during initial promoter induction (Figure 4-2) or under conditions of constitutive but submaximal transcription that occur in a *pho80*Δ strain (Gregory et al., 1998; Komeili and O'Shea, 1999; Boeger et al., 2003; our unpublished observations). Thus, at later times of activation, perhaps the level of disruption of nucleosomes distant from the UAS reaches that of nucleosomes flanking the UAS. We tested, therefore, whether remodeling of nucleosomes neighboring UASp1 is favored when the *PHO5*^{HhaI} promoter is activated for longer periods of time (Figure 4-4A) or approaches steady-state activation (Figure 4-4B). In Figure 4-4A, over 5 hr of activation, it remains evident that nucleosome −2 is remodeled before and to a greater extent than is nucleosome −1. We then analyzed the changes that occur in chromatin accessibility at the promoter when cells were starved for P_i for 24 hr. In this latter experiment, a pulse of M.HhaI probe synthesis was induced in cells in P_i-free medium 30 min prior to the indicated times. This 'snapshot' analysis shows that the Pho4-mediated increases in nucleosome accessibility plateau at different levels with times of half-maximal ($t_{½}$) remodeling, again increasing from UAS-proximal to -distal nucleosomes (Figure 4-4B). These results

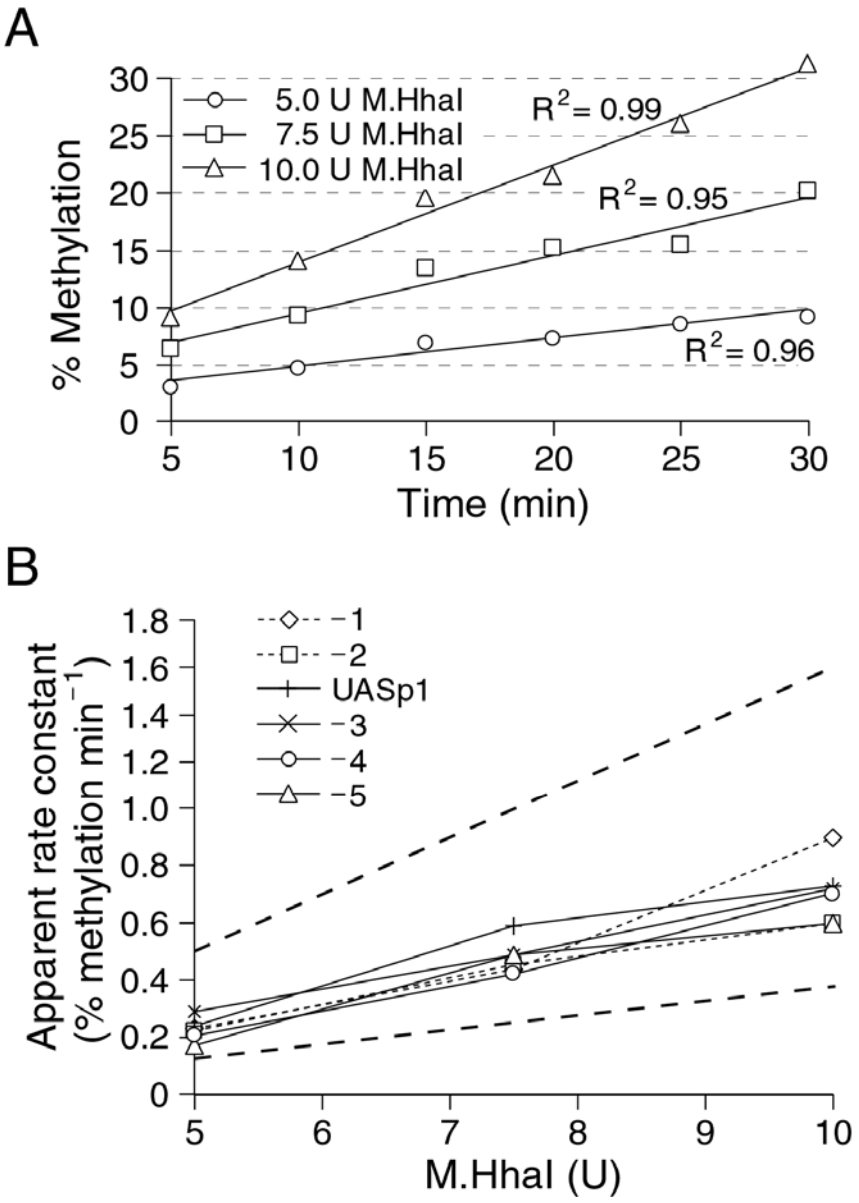

Figure 4-3. M.HhaI Methylates All Cognate Sites on Naked *PHO5*^{HhaI} DNA at Similar Rates

Protein-free plasmid DNA containing the *PHO5*^{HhaI} promoter was methylated over time in vitro with the indicated amounts of M.HhaI activity. Aliquots were removed at 5-min intervals and m^5C levels were quantitatively determined by bisulfite sequencing with primers that anneal immediately upstream of each HhaI site. In (A) representative results for the HhaI site in nucleosome −4 are shown and in (B) the cumulative derived apparent rate constants for all six HhaI sites are plotted. In (B) the upper and lower heavy dashed lines represent slopes that are 2-fold more or less, respectively, than the mean slope of the six data curves.

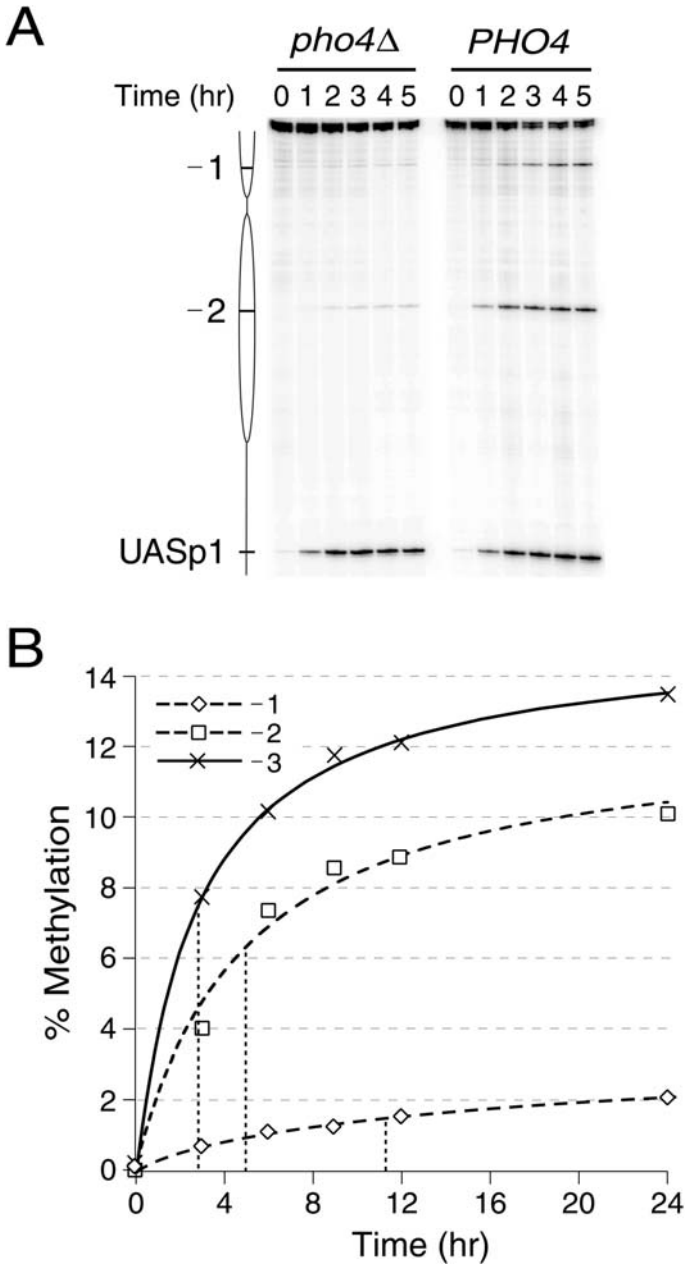

Figure 4-4. Preferential Disruption of Nucleosomes Neighboring UASp1 Persists at Extended Times of Activation

At the indicated times of P_i deprivation, *pho4*Δ and *PHO4* cells were harvested and the m^5C level at each HhaI site (horizontal lines) was determined by bisulfite sequencing of the bottom DNA strand as in Figure 4-2B. M.HhaI accessibility during the first 5 hr (A) or 24 hr (B) of activation. In (B) M.HhaI synthesis was induced for 30 min prior to the indicated times of P_i starvation and m^5C levels were determined by bisulfite sequencing. The lower percentages of m^5C in this experiment reflect the shorter induction period of the DNA methyltransferase to maintain single-hit kinetics throughout the time course and do not correspond to the absolute levels of nucleosome remodeling. The $t_{½}$ values as derived from the fitted curves are 2.8, 5.0, and 11 hr for nucleosomes −3, −2, and −1, respectively.

confirm that Pho4 targets nucleosomes adjacent to the UAS region for remodeling prior to more distal nucleosomes. Moreover, the data suggest that UAS-proximal nucleosomes are remodeled more effectively, reform less readily than distal nucleosomes, or both, even under conditions of full promoter activation. We re-emphasize that these data reflect the differences in the time at which the remodeling process initiates at each nucleosome. Normalization of the increased accessibility in each nucleosome to the level achieved at 24 hr demonstrates similar rates of remodeling.

We also probed the wild-type *PHO5* promoter as activation progresses in a strain expressing a second DNA methyltransferase, M.CviPI, which recognizes GC sites [Figure 4-5 and (Xu et al., 1998a)]. As the edges of nucleosomes are more accessible to DNA methyltransferases than internal regions (Kladde and Simpson, 1994; Kladde et al., 1996; Xu et al., 1998b), in this experiment it is best to compare m^5C levels at M.CviPI sites near each nucleosomal pseudodyad (center, marked by horizontal lines). As all HhaI sites (GCGC) are also sites for M.CviPI, the sites near the pseudodyad correspond to the same sites that are assayed above in Figures 4-2 and 4-4. The data of Figure 4-5A verify that nucleosome −3, which lies next to UASp1, is favored for disruption over nucleosomes −4 and −5.

It remained a possibility that structural features of the chromosome upstream of nucleosome −5 prevent a high degree of remodeling of this nucleosome. However, this is unlikely as a constitutive nuclease hypersensitive region (HSR1) is present immediately upstream of nucleosome −5 (Almer and Hörz, 1986). Indeed, in comparison to the GC site located near the pseudodyad of nucleosome −5, a GC site located in HSR1 was

Figure 4-5. Chromatin Remodeling of the Wild-Type *PHO5* Promoter Spreads from UASp1

(A) Accessibility of the upstream *PHO5* promoter region to M.CviPI. *PHO4* cells, expressing M.CviPI, were grown in the presence (+) or absence (−) of P_i for the indicated times and then analyzed for m^5C levels by bisulfite sequencing. Ellipses, positioned nucleosomes −5 to −2; horizontal bars, HhaI sites; L, linker region; filled circles, GC sites recognized by M.CviPI. All bands that do not correspond to M.CviPI sites are due to non-specific pausing during primer extension. Pho4 binding protects two GC sites at UASp1 against methylation by M.CviPI (Carvin et al., 2003a). Note that DNA methyltransferases access cognate sites located near the edges of nucleosomes more readily than sites near the nucleosomal pseudodyad (Kladde and Simpson, 1994; Kladde et al., 1996). Thus, it is most informative to compare methylation intensities over the time course between GC sites located near each nucleosomal pseudodyad (i.e., the location of the HhaI site).
(B) The upstream hypersensitive region 1 (HSR1) is highly accessible under both repressive and activating conditions. Cells were treated as in (A) for bisulfite sequencing analysis. For the sake of comparison, the GC site near the pseudodyad of nucleosome −5 is also shown.
(C) Binding of Pho4 at UASp2 (left panel) and TATA-binding protein (TBP) at TATA (right panel) do not protect against methylation. Bisulfite sequencing analysis of *pho4*Δ and *PHO4* strains starved for P_i for 6 hr prior to the induction of M.CviPI synthesis via the addition of estrogen for the indicated times. Open circle, Pho4 binding site UASp2; filled bar, TATA element; other symbols are as in (A).

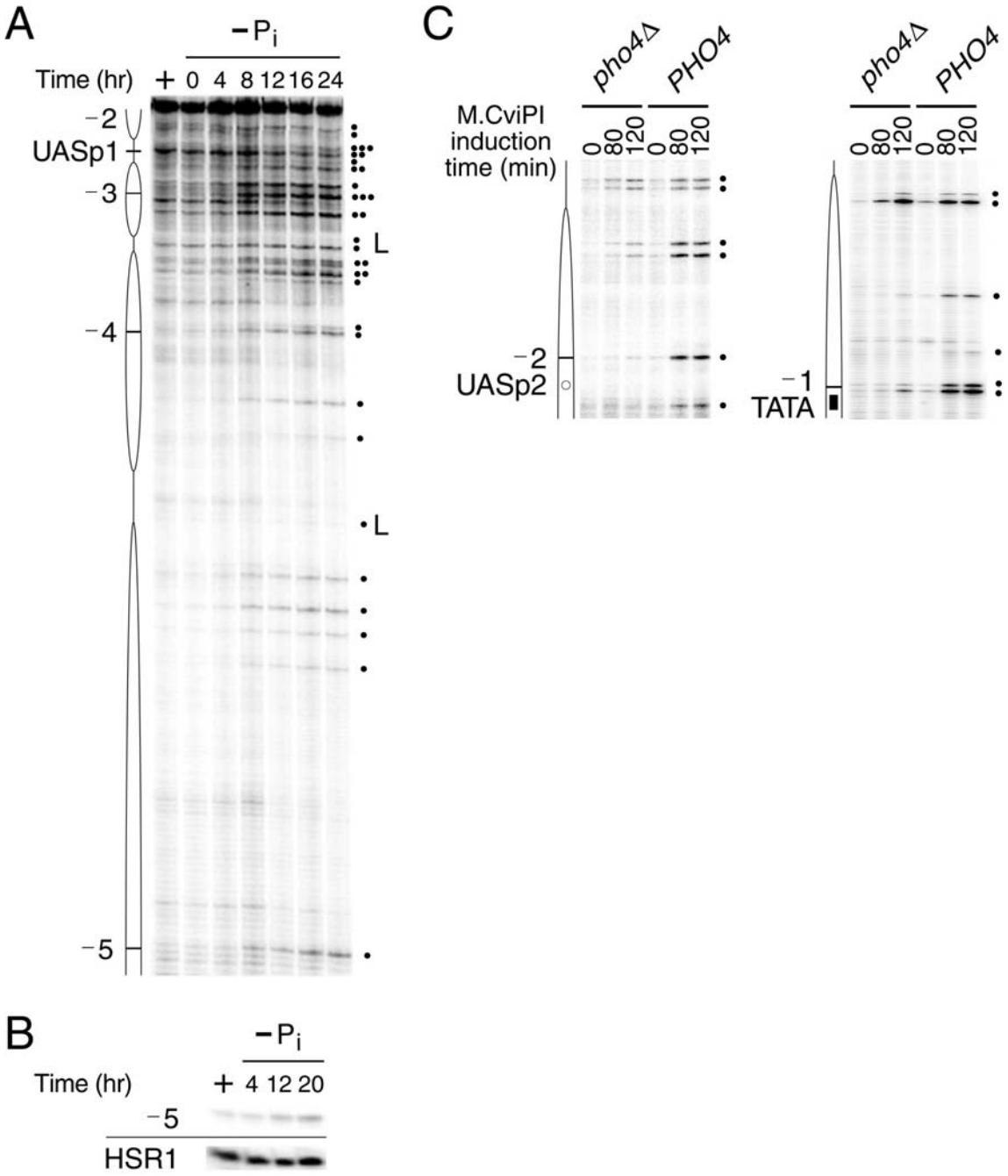
A
−Pi
Time (hr) + 0 4 8 12 16 24
−2
UASp1
−3
L
−4
L
−5
B
−Pi
Time (hr) + 4 12 20
−5
HSR1
C
pho4Δ
PHO4
M.CviPI induction time (min)
0 80 120 0 80 120
−2
UASp2
−1
TATA

highly methylated under both repressive and activating conditions (Figure 4-5B). Thus, our results suggest that the propagation of chromatin remodeling likely attenuates as a function of distance from the UAS as opposed to being counteracted by a repressive region of chromatin that is present upstream of nucleosome −5.

Since M.CviPI recognizes the same M.HhaI site near the pseudodyad of both nucleosomes −2 and −1, we could also evaluate whether DNA-binding proteins that assemble on the induced promoter are potentially protecting against methylation. For example, upon activation, Pho4/Pho2 or TBP might occlude access to UASp2 and TATA, respectively, which would delay methylation by M.HhaI at nucleosomes −2 and −1 relative to −3. This is clearly not the case as, in Figure 4-5C, the HhaI sites in both nucleosomes −2 and −1 are highly accessible to M.CviPI even after 6 hr of P_i starvation, when promoter cis-elements have substantial factor occupancy [see Figure 4-6 and (Dhasarathy et al., 2004)]. We conclude that the temporal increases in accessibility of M.HhaI (−3 > −2 > −1) at each nucleosome reflect differences in the time at which they are targeted for chromatin remodeling during induction.

SWI/SNF Localizes Preferentially at the UAS Region of the Induced *PHO5* Promoter

To investigate the mechanistic basis for propagating chromatin remodeling from proximal to distal nucleosomes, we analyzed the time course of Pho4 binding and recruitment of SWI/SNF to the wild-type *PHO5* promoter by chromatin immunoprecipitation (ChIP) in Myc-tagged strains (Figure 4-6). Tagging either Pho4 or

Figure 4-6. Activation Localizes SWI/SNF Preferentially at the UAS Region of the *PHO5* Promoter

(A) Initial *PHO5* induction rates of duplicate experiments. Activities were measured internally for select samples analyzed in (B).
(B) Time course of association of 3Myc-Pho4 and Swi2-13Myc. Cells were cross-linked at the indicated times of P_i starvation and analyzed by ChIP analysis with PCR in real time at the *PHO5* UAS and at nucleosomes −1 and −5 (regions indicated in Figure 4-1A). No tag control (wild-type), 3Myc-Pho4, and Swi2-13Myc strains were analyzed in parallel. The graphs show ratios (region *n*/control *WHI4* coding region) for the duplicate experiments (mean ± standard deviation).

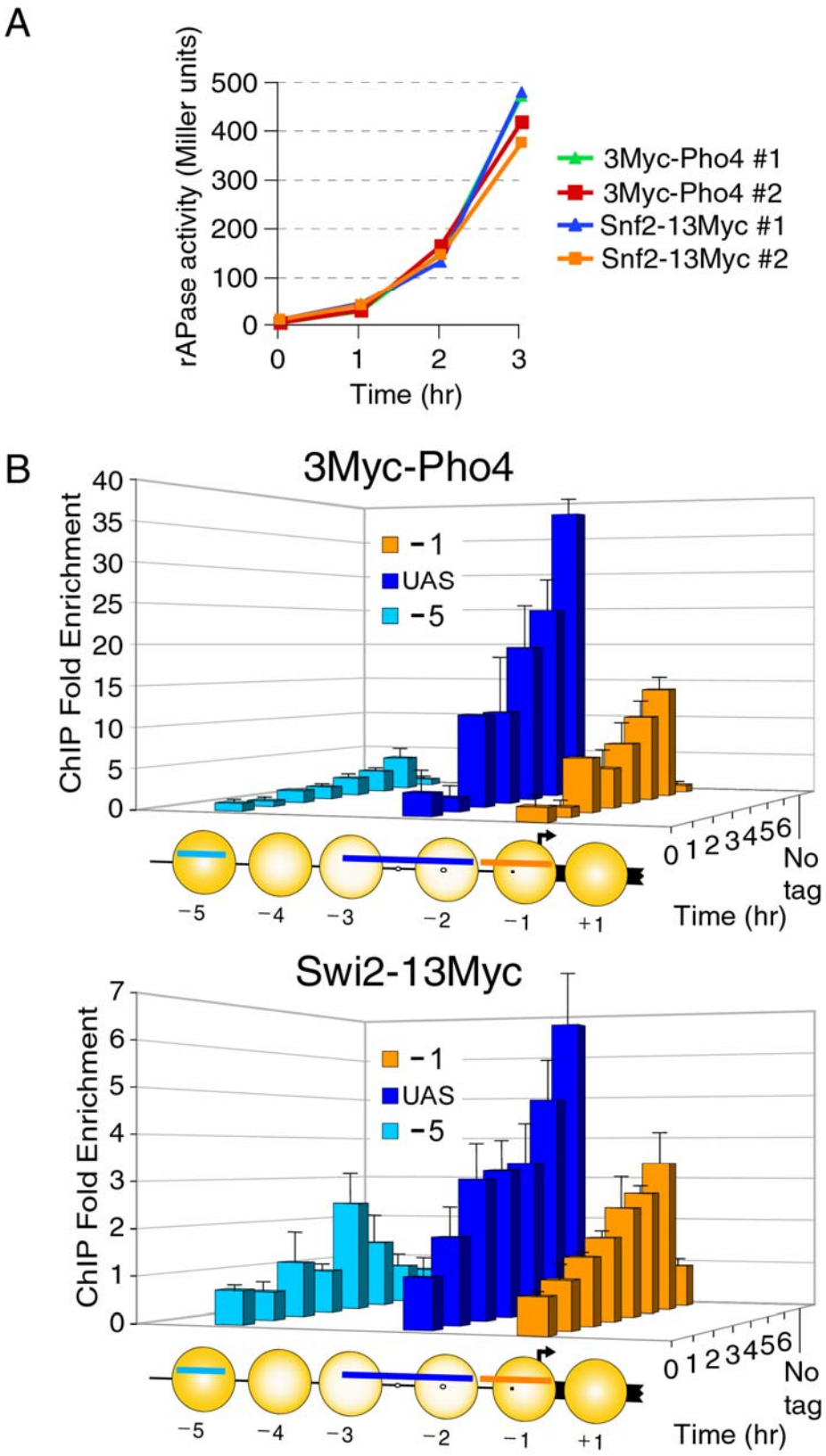
A
rAPase activity (Miller units)
500
400
300
200
100
0
0
1
2
3
Time (hr)
3Myc-Pho4 #1
3Myc-Pho4 #2
Snf2-13Myc #1
Snf2-13Myc #2
B
3Myc-Pho4
ChIP Fold Enrichment
40
35
30
25
20
15
10
5
0
−1
UAS
−5
0 1 2 3 4 5 6
No tag
Time (hr)
−5
−4
−3
−2
−1
+1
Swi2-13Myc
ChIP Fold Enrichment
7
6
5
4
3
2
1
0
−1
UAS
−5
0 1 2 3 4 5 6
No tag
Time (hr)
−5
−4
−3
−2
−1
+1

the Swi2/Snf2 ATPase of the SWI/SNF complex did not affect the initial induction kinetics of *PHO5* (Figure 4-6A). While Pho4 migrates from the cytoplasm to the nucleus within 30-60 min of P_i removal (Komeili and O'Shea, 1999; Barbaric et al., 2001), unexpectedly, Pho4 enrichment at the *PHO5* UASs increases over the entire 6 hr time course (Figure 4-6B, top panel), saturating at 10-12 hr (Dhasarathy et al., 2004). Increased association of Pho4 with the UAS region over time is likely a result of further activator occupancy at UASp1 as well as at UASp2 due to remodeling of nucleosome −2.

SWI/SNF, which is required for a wild-type rate of *PHO5* activation (Neef and Kladde, 2003; Reinke and Hörz, 2003; Steger et al., 2003), also increases its association with the UASs as a function of time (Figure 4-6B, bottom panel). These are the first data demonstrating a significant association of SWI/SNF at the induced *PHO5* promoter. Importantly, enrichment of both 3Myc-Pho4 and Swi2-13Myc is higher at the UAS region than at nucleosomes −1 and −5 and, generally, more SWI/SNF is present at the UAS than at distal regions. The reproducible, transient association of SWI/SNF at nucleosome −5 at 4 hr is consistent with a potential long-range interaction between the UASs and upstream region that we reported previously (Carvin et al., 2003a). Significant enrichment of SWI/SNF but not Pho4 at nucleosome −5 relative to the no tag control excludes the possibility that insufficient chromatin shearing of the upstream promoter region is compromising the resolution of our ChIP analysis. These results demonstrate that increases in Pho4 binding at the *PHO5* promoter over time, likely due to exposure of UASp2 in nucleosome −2, result in higher levels of recruited SWI/SNF. Thus, upon

PHO5 activation, SWI/SNF is recruited to the UAS region. The resulting SWI/SNF localization explains the preferential remodeling of nucleosomes at the *PHO5* UAS, and, moreover, is consistent with the interpretation that the complex plays an active role in propagating the bidirectional disruption of chromatin at *PHO5*.

DISCUSSION

We have provided mechanistic insight into the transition of *PHO5* promoter chromatin during transcriptional activation by performing a novel kinetic examination of the remodeling process in living cells. We find that Pho4 mediates the bidirectional propagation of chromatin remodeling over time that initiates at nucleosomes flanking UASp1 (Figure 4-2). This temporal spreading of nucleosomal disruption is supported by our finding that SWI/SNF is recruited at the *PHO5* UAS region and increases its association over time as more activator binds (Figure 4-6). Thus, our data provide a long-awaited molecular explanation for how and why multiple nucleosomes are targeted for disruption at the *PHO5* promoter following P_i deprivation. Importantly, both SWI/SNF recruitment and the accompanying nucleosomal disruption localize predominantly to the UAS region and fall off markedly by 2 to 3 nucleosomes, even under conditions of full promoter activation (Figures 4-2 and 4-4). This provides a substantial departure from the view that each nucleosome at the *PHO5* promoter is disrupted to a similar extent (Svaren and Hörz, 1995). Detection of these structural differences along the promoter likely derives from our ability to assay chromatin remodeling directly in vivo (Kladde et al., 1996), avoiding procedures like cell

permeabilization or nuclei isolation that disrupt kinetic processes. Moreover, the preferential recruitment and retention of SWI/SNF at sites of Pho4 association is likely the reason for the local minimum of histones detected at UASp2 of *PHO5* upon promoter induction (Boeger et al., 2003; Reinke and Hörz, 2003). The concordance of the distribution of SWI/SNF with the pattern of nucleosome disruption suggests that the complex is a key player in establishing the remodeled domain of *PHO5* chromatin, although additional coactivators are likely to participate in the initial activation process (Barbaric et al., 2001; Barbaric et al., 2003; Neef and Kladde, 2003; Steger et al., 2003; Nourani et al., 2004).

Taken together, our findings are most consistent with a model of chromatin remodeling whereby the level of site-specific activator binding at a promoter dictates nucleosome disruption frequency. Thus, increases in activator binding lead to concomitant increases in both coactivator recruitment and the remodeling of mainly proximal but also distal nucleosomes. High-level accessibility of UAS-proximal nucleosomes (−3 and −2) to either M.HhaI (Figure 4-2A) or R.ClaI [−2 only; (Almer et al., 1986)] indicates that the *PHO5* promoter is remodeled in most cells after prolonged P_i starvation. However, on average, nucleosomes located farther from the UAS region are disrupted in fewer cells. It is likely that Pho4 establishes a gradient of SWI/SNF and accompanying chromatin remodeling across the promoter as it interacts directly with SWI/SNF through its acidic activation domain (Hassan et al., 2002). Additionally, Pho4 and Pho2 target the HAT complexes SAGA (Barbaric et al., 2003) and NuA4 (Nourani et al., 2004), respectively, to the *PHO5* promoter. A similar peak in association of these

complexes at the *PHO5* UAS region could contribute to the observed localization of SWI/SNF, as the remodeler has increased affinity for hyperacetylated nucleosomes (Hassan et al., 2001).

Our results suggest several features of SWI/SNF action at the *PHO5* promoter. First, the increased disruption of UAS-proximal nucleosomes strongly suggests that chromatin remodeling is non-processive. If remodeling were to be highly processive, one would expect all nucleosomes to be perturbed to similar extents, especially at steady-state activation. Indeed, mounting evidence suggests that remodelers like SWI/SNF are not processive, using ATP hydrolysis to translocate along the chromatin fiber in intervals of less than 100 base-pairs (Owen-Hughes, 2003). In this scenario, on average, nucleosomes near the site of coactivator recruitment (the UAS) would be preferentially disrupted because SWI/SNF does not traverse the entire promoter. Non-processive remodelers would limit the need to block the spread of active chromatin between every transcription unit in the genome via boundary elements or insulators. It is also formally possible that a rapid dynamic equilibrium exists in vivo between remodeled and non-remodeled states of the nucleosome, which favors the latter state at increased distances from the UAS (Boeger et al., 2003). In line with this idea, ATP-driven nucleosome remodeling is highly reversible (Logie and Peterson, 1997; Jaskelioff et al., 2000) and transcription requires continuous SWI/SNF function (Biggar and Crabtree, 1999).

Our data agree with most aspects (see below) of a facilitated tracking mechanism for enhancer-stimulated transcription in metazoans as proposed by Blackwood and Kadonaga (1998) and are supported by several recent investigations (Wei and Brennan,

2000; Hatzis and Talianidis, 2002; Mahmoudi et al., 2002; Shang et al., 2002; Kim and Dean, 2004). In this model, coactivator complexes, in association with enhancer-bound activators, incrementally track along the chromatin fiber and 'loop out' intervening chromatin. Thus, upon encountering the cognate basal promoter element, it is proposed that a stable looped structure is formed (Blackwood and Kadonaga, 1998; Hatzis and Talianidis, 2002). However, as induction often requires many hours, it is difficult to envision how activators could stay continuously bound to coactivators and their specific DNA-binding sites.

Thus, we propose the following modified version of the facilitated tracking model. Activator-dependent recruitment of coactivators, including SWI/SNF, initiates mobilization of UAS-proximal nucleosomes by tracking along the promoter (Owen-Hughes, 2003). Non-processive tracking by SWI/SNF, combined with free energy losses as binding contacts are severed, increases dissociation of the remodeler from the chromatin template. Continued tracking is ensured only through the combination of acetylation and reestablishment of DNA-activator-SWI/SNF interactions, which likely work in concert for full retention of coactivators on nucleosomes (Hassan et al., 2001). This view is in line with observations demonstrating that factors and coactivators are in rapid exchange between bound and free states in the nucleus (Shang et al., 2000; Misteli, 2001; Stenoien et al., 2001; Fletcher et al., 2002; Metivier et al., 2003). The inherent instability of factor association may be offset by binding cooperativity and increased factor concentration at organized transcription centers (Cook, 1999). Thus, we favor the idea that a continuous cycle of factor dissociation/reassociation facilitates coactivator

tracking along a promoter. Propagation of chromatin disruption would then provide a molecular basis for the incremental steps proposed in the facilitated tracking model. However, while our results are most consistent with this view of facilitated tracking, we cannot rule out the possibility that transcriptional activation in yeast may be solely driven by concentration gradients of activators and coactivators at their sites of recruitment (Topalidou and Thireos, 2003).

Our proposal for limited facilitated tracking agrees well with each of the model's original tenets (Blackwood and Kadonaga, 1998). In addition, it offers a plausible explanation as to why the remodeling process occurs in a stepwise manner, requires many hours to reach steady-state, and trails off at a distance, as we have observed at the *PHO5* promoter. Our model can also be applied to a broad range of previous observations regarding UAS action in *S. cerevisiae*. First, it is consistent with the pronounced distance dependence of UAS function in *S. cerevisiae* (Ptashne and Gann, 1997). Along these lines, induction by weak activator proteins (e.g., Mcm1) is severely compromised at increased distances (Patterton and Simpson, 1994), possibly because their ability to recruit remodelers and propagate disrupted chromatin is less than that of strong acidic activators (e.g., Pho4 and Gal4). Our results are also consistent with the sequential association of SWI/SNF at different regions along the *HO* promoter (Cosma et al., 1999). Further, our model provides a satisfactory reason as to why a bacterial repressor blocks transcription when its binding site is placed between a core promoter and its UAS (Brent and Ptashne, 1984), possibly by interfering with the propagation of nucleosome disruption. Finally, the limited capability to propagate nucleosome

disruption is also consistent with the general observation in metazoans that nuclease-hypersensitive enhancer and promoter regions are separated by large stretches of unperturbed chromatin.

CHAPTER V

SUMMARY

CONCLUSIONS

The organization of DNA into chromatin is a primary determinant of gene expression. The role of chromatin structure and dynamics in the regulation of nuclear events continues to accumulate and has become central to our understanding of the processes of transcription, replication, cell division, recombination, and DNA repair. These processes occur through the interaction of trans-factors with cis-regulatory elements in DNA. Recognition of DNA cis-regulatory sites requires that they be accessible. Accessible or nucleosome-free regions in chromatin are called nuclease hypersensitive sites and are frequently associated with functional sequences including enhancers and Upstream Activation Sequences (UASs) (i.e., promoter regions), locus control regions, insulators, boundary elements, and replication origins.

Classically, the most common method used to identify nuclease hypersensitive sites is DNase I probing (Gross and Garrard, 1988). Isolated nuclei are subjected to DNase I digestion. Following nuclease digestion, fragmented genomic DNA is purified, digested with a restriction enzyme, separated by gel electrophoresis, transferred to a membrane, and hybridized with a radiolabeled recombinant probe that borders the restriction enzyme site. This technique, called indirect end-labeling (Borchardt et al., 1979; Nedospasov and Georgiev, 1980), is low resolution, with an accuracy ± 50 bp. Additionally, DNA fragments will most likely have nicks (the preferential mechanism of DNase I action is single-strand nicks in double-stranded DNA), which can lead to gel

migration artifacts. Further, DNase I has poor affinity for DNA, is highly sensitive to salt concentration (20 nM NaCl can reduce activity by 30%), shows some site preference towards purine-pyrimidine sequences, and has sensitivity to the structure of the minor groove, giving rise to a distinctive ~10 bp periodicity for rotationally positioned nucleosomes. Due to its almost exclusive preference for the linker region between nucleosomes, another popular nuclease used to study chromatin structure is micrococcal nuclease (MNase) (Simpson, 1999). MNase has a preference for cleaving single-stranded DNA, especially at AT-rich regions flanked by a 5' dC or dG (Drew, 1984; Flick et al., 1986).

The resolution of these techniques can be improved by a method known as primer extension. A specific end-labeled primer is hybridized to the complementary region of genomic DNA of interest. This primer is then utilized by DNA polymerase to synthesize a complementary DNA strand. Regions that are cleaved by DNase I or MNase will result in DNA polymerase extending across the break and off the end of the DNA molecule. The length of the synthesized DNA reflects the number of bases between the end-labeled primer and the cleaved region. Moreover, the preparation of spheroplasts allows for rapid nuclease probing of yeast chromatin as opposed to the time-consuming process of nuclei preparation that may allow for chromatin structural changes to occur and the loss of either DNA-bound proteins (Kent and Mellor, 1995) or short half-life proteins (Murphy et al., 1993). Another disadvantage of nuclei preparation is that the buffers used for nuclease digestion are of low ionic strength, leading to the swelling of chromatin and possible artifacts.

DNA Methyltransferases as Chromatin Probes and the Detection of Protein-DNA Interactions

As in vivo probes of chromatin structure, cytosine-5 DNA methyltransferases (C5 DMTases) offer significant advantages over other more invasive methods (Simpson, 1999), including those discussed above. Perhaps the most exciting advantage is that probing can be done in living cells, allowing one to monitor not only the initial state of factor accessibility but the changes that occur over time as nuclear events ensue in the context of a native chromatin environment. Additionally, protein-DNA interactions can be further elucidated by the fusion of DMTases to the factor of interest (Targeted Gene Methylation, TAGM). In Chapter II, we provide a method for construction of DMTase-expressing strains of *S. cerevisiae*, the screening of such strains for functional DMTases, protocols for the bisulfite treatment of genomic DNA and the subsequent bisulfite sequencing steps, and examples of analysis of both chromatin structure probing and factor binding (TAGM). Further, we present a brief analysis of the *GAL1* promoter identifying activation-dependent changes that occur in chromatin structure as well as factor occupancy at the UAS_G and TATA elements, as seen by the increase in protection at these sites from methylation. Illustrated is yet another significant advantage of DMTases as chromatin probes – their reduced yet detectable access to ~25 bp of DNA at nucleosomal termini. Consequently, regions of protection offered by nucleosomes typically span ~100 bp. We present application of TAGM using the transactivator Pho4 to target methylation by M.CviPI to the *PHO5* promoter (also see Carvin et al., 2003a). Under repressive conditions of high phosphate, de novo translated Pho4 is transiently in

the nucleus prior to phosphorylation by the cyclin-CDK pair Pho80-Pho85 at serine-proline sites 2 and 3 (SP2 and SP3), which target it for export (Komeili and O'Shea, 1999). Consequently, either prior to phosphorylation or export, Pho4 is bound at some low frequency to UASp1 at the *PHO5* promoter. Current techniques used to identify protein-DNA interactions such as chromatin immunoprecipitation (ChIP) are unable to identify the low occupancy of Pho4 at the *PHO5* promoter under high-P_i conditions (Steger et al., 2003). However, emphasizing the sensitivity of the technique, TAGM allows for a clear identification of m^5C targeted upstream of UASp1.

These techniques are amenable to *Saccharomyces cerevisiae* as yeast does not have any endogenous C5 DMTases. Extension of the method for the in vivo study of chromatin structure in *Drosophila melanogaster* and *Caenorhabditis elegans* should be feasible as these genomes contain little or no C5 DMTases, although high levels of expression may lead to developmental defects (Lyko et al., 1999). To this end, transgenic *Drosophila* strains that allow for the overexpression of all known mouse DMTases have recently been developed (Mund et al., 2004). Mammals, however, have endogenous DMTases, the disruption of which results in embryonic lethality (Li et al., 1992).

High-Resolution Chromatin Structure of the *PHO5* Promoter

An archetype for addressing the interplay between chromatin structure and the regulation of transcription is the *PHO5* promoter. However, despite extensive investigation, the promoter structure has never been fully characterized. Thus, we have determined the

translational positions of the *PHO5* promoter nucleosomes −5 to +1 by two complementary techniques, accessibility to MNase and to the DMTase M.CviPI. We demonstrate that nucleosome −5 is positioned between −900 and −742, spanning 158 bp. The increased region of protection >146 bp indicates two translational positions for nucleosome −5 separated by ~one helical turn. Nucleosome −4 is positioned between −711 and −564. During preliminary construction of the *PHO5*^{HhaI} promoter (Chapters III and IV), a HhaI site for nucleosome −4 was introduced at −681, proving to be largely accessible to M.HhaI under repressive conditions of high P_i. In retrospect, this is not too surprising given that −681 positions the HhaI site only 30 bp internal from the upstream edge of nucleosome −4. The combination of site position and low stability of nucleosome −4 explains the high accessibility of −681 to M.HhaI. The final placement of the HhaI site for nucleosome −4 at −638 moved it 43 bp more internal, positioning it at the pseudodyad. The increased accessibility of −681 to M.HhaI relative to −638 further supports the determined translational position of nucleosome −4 presented in Chapter III. Nucleosome −3 is positioned between −546 and −400. Others have reported this nucleosome shifted slightly downstream in both purified, truncated (−1 to −3) *PHO5* minichromosomes (Haswell and O'Shea, 1999) and reconstituted, truncated (−1 to −3) *PHO5* promoter arrays (Terrell et al., 2002). This is surprising given the relatively strong footprint of nucleosome −3 observed in vivo. We speculate that the introduction of the *PHO5* promoter sequence in a divergent position upstream of the *TRP1* promoter on the minichromosome may have affected nucleosome −3, since medium lacking tryptophan was likely used to maintain selection. Regarding the reconstituted *PHO5* promoter array,

we hypothesize that sequences found upstream of nucleosome −3 in these reconstitutions may affect its positioning as sequences from the bacterial plasmid pBR322 have been found to both position nucleosomes (Straka and Hörz, 1991) and serve as UAS sequences in yeast (Sidhu and Bollon, 1990). Additionally, we have found that *PHO5*^{HhaI} promoter chromatin reconstitution using the same uncatalyzed chromatin assembly system based on the histone chaperone Nap1 results in a large fraction of subsaturated arrays (our unpublished data), which additionally may contribute to alternative nucleosome positioning. Nevertheless, our analysis of DNA curvature and conformational stability offers a feasible explanation for the alternative positioning. Furthermore, it is probable that internucleosomal interactions also contribute to overall nucleosome stability. Consistent with this, a more recent in vitro chromatin assembly system based on yeast extracts appears to establish a nucleosomal pattern over the entire *PHO5* promoter (encompassing nucleosomes −1 to −5) that is very similar to the in vivo pattern (Korber and Hörz, 2004).

An extended linker region containing the accessible UAS, UASp1, spans 75 bp. Curiously, it appears as though two hypersensitive sites, −385 and −348, border sequences that are protected by Pho4 and Pho2 (Vogel et al., 1989; Barbaric et al., 1996). It may be that, under repressive conditions of high P_i, Cbf1, a bHLH protein related to Pho4 that also binds E boxes, is bound at UASp1 with Pho2 and contributes to the observed hypersensitive sites bordering the UAS (Kent et al., 2004; Nourani et al., 2004). However, this does not alter our hypothesis that DNA curvature contributes to nucleosome positioning as the positioning of nucleosomes −2 and −3 has been shown to

be independent of the presence of UASp1 (Fascher et al., 1993). Consistent with our model of nucleosome stability, downstream nucleosomes −2 (−325 to −178) and −1 (−142 and +4) typically appear in similar positions in reconstituted nucleosomal arrays or in minichromosomes (assayed by indirect end-labeling). We find that nucleosome +1 is positioned between +21 and +168. Additional indirect end-labeling analysis of the *PHO5* promoter identifies at least two more well-positioned nucleosomes downstream of +1 (Figure 4-1).

Secondary structural analysis of the *PHO5* promoter correlates nucleosome positioning with predicted DNA curvature, proposed by others to stabilize nucleosomes at moderate levels and destabilize nucleosomes at either high or low levels of curvature (Scipioni et al., 2004). One of the main questions asked regarding the *PHO5* promoter is why there is an extended linker region, more than 2.5× the size of the average linker length separating the *PHO5* promoter nucleosomes. We believe the prominent sharp peak in DNA curvature centered between nucleosomes −3 and −2 to be the basis for the enlarged size of the linker. There are two other sharp peaks in curvature in the *PHO5* promoter region; upstream of nucleosome −5 and between nucleosomes −2 and −1. Consistent with a model in which DNA curvature contributes to nucleosome positioning at the *PHO5* promoter, upstream of nucleosome −5 is a known nucleosome-free region, HSR1. The linker region between nucleosomes −2 and −1 is the second largest linker separating the *PHO5* promoter nucleosomes. Interestingly, a local maximum in DNA curvature also appears between nucleosomes −5 and −4 as well as nucleosomes −4 and −3. Further, we have had consistent difficulty manipulating the DNA sequence

encompassing the UASp1 region. Whether by PCR amplification, primer extension, or gel electrophoresis, this sequence consistently poses technical difficulties.

Probing the *PHO5*^{HhaI} promoter in a *pho4*Δ strain with M.HhaI allows us to measure the relative stability of the nucleosomes. Each of the sites for M.HhaI are (i) methylated at the same rate on naked DNA, and (ii) nucleosomes −3 to −5 are located < 5 bp from the pseudodyad of each nucleosome. Thus, the extent of protection from methylation offered to each site by the nucleosome reflects the affinity of histone-DNA interaction (i.e., conformational nucleosome stability). We demonstrate that nucleosome −4 is less stable than either nucleosomes −3 or −5 in both a time- and estrogen-dose-dependent manner. Both these dependencies result in an increased nuclear concentration of M.HhaI. The decreased stability of nucleosome −4 is surprising given that it is positioned between two close nucleosomes, which one would expect to act as boundaries. We infer from these results that the contributions made to nucleosome stability through histone-DNA interaction far surpass the contributions made by internucleosomal interactions. Taken together, our data suggest that in vivo, accessibility of nucleosomal sites to a specific factor is probabilistic, dependent upon both the affinity of histone-DNA interaction and the local concentration of factor. Our findings show that the *PHO5* promoter nucleosomes have diverse stabilities in vivo and suggest that conformational nucleosome stability makes critical contributions to the chromatin organization of the promoter region and consequently nucleosomal repression at *PHO5*.

The conserved pattern of bending observed internal to each of the five promoter nucleosomes has been observed previously in heterochromatic satellite DNA (Fitzgerald

et al., 1994). The pattern presented in Figure 3-8 is striking, with a region of decreased curvature flanked by regions of increasing curvature. Perhaps the simplest explanation for the correlation between DNA curvature and conformational stability may be that DNA with increased curvature requires less energy to wrap around the histone octamer, assuming that the direction of curvature is the same within the nucleosome. There would be a far greater cost in free energy to bend curved DNA in the direction *opposite* its preferred direction – these would be sequences that are unfavorable for incorporation into a nucleosome (Widom, 2001).

Probabilistic Coactivator Recruitment

We have provided mechanistic insight into the transition of *PHO5* promoter chromatin during transcriptional activation by performing a novel kinetic examination of the remodeling process in living cells. We show that, concomitant with the spreading of chromatin disruption at nucleosomes flanking UASp1, a maxima of SWI/SNF association is established, centered at the UAS region. In sum, our results are concordant with a model of chromatin remodeling in which the level of enhancer-bound activator dictates the probability of coactivator recruitment at a given promoter and thus the frequency of nucleosome disruption. In line with observations demonstrating that factors and cofactors are in rapid exchange between bound and free states in the nucleus (Shang et al., 2000; Misteli, 2001; Stenoien et al., 2001; Fletcher et al., 2002; Metivier et al., 2003), a continuous cycle of factor dissociation/reassociation enables coactivators to track across the promoter in a non-processive manner.

In promoter regions, site-specific protein-DNA interaction results in a higher level of factor occupancy or, in the time average, an increased duration of residency time, allowing for an increase in the chance of activator-coactivator interaction (i.e., recruitment). This result defines a critical role for the promoter occupancy of an activator by establishing the extent of coactivator dependency. Increases in Pho4 binding at UASp1 therefore result in the increased recruitment of Gcn5 and SWI/SNF. Recruitment of Gcn5 results in local targeted H3 acetylation, which could contribute to the localization of SWI/SNF observed during *PHO5* activation via bromodomain interactions (Hassan et al., 2002). Promoter activation has previously been associated with localized H3 acetylation both in vitro (with SAGA) (Vignali et al., 2000) and in vivo in higher eukaryotes (Schübeler et al., 2000; Liang et al., 2004). Continued recruitment targets proximal nucleosomes −2 and −3 for disruption by SWI/SNF.

Deletion of *GCN5*, while not affecting the steady-state level of *PHO5* expression, results in a delay in promoter remodeling and transcription at early times of activation (Barbaric et al., 2001). This agrees with *PHO5* being markedly Gcn5-dependent at low levels of promoter occupancy (Dhasarathy et al., 2004). We believe that the attainment of wild-type levels of transcription is therefore achieved through coactivator redundancy, specifically with NuA4, shown recently to be essential for *PHO5* activation (Nourani et al., 2004). An alternative, non-mutually exclusive possibility is that concentration gradients of activators and coactivators drive transcriptional activation. In this scenario, the delay in nucleosome disruption is due to the longer time required for increased Pho4 and coactivator concentrations to sufficiently to overcome the Gcn5 deficiency.

Pho4 Occupancy of UASp2 is Required for *PHO5* Activation

The critical event for *PHO5* activation is the exposure of the high affinity Pho4 binding site, nucleosome-occluded UASp2. This is consistent with a deletion of UASp1 resulting in the lack of detectable nucleosome −2 perturbation or transcriptional activation (Fascher et al., 1993). The exposure of UASp2 would allow for an even greater increase in Pho4 occupancy at the *PHO5* promoter. Interestingly, a third Pho4/Pho2 site (UASp3) of low affinity has been suggested downstream of UASp2, positioned at the edge of nucleosome −2 (Barbaric et al., 1996). We envision that Pho4 and Pho2, binding at UASp1 (centered at −366), facilitate the non-processive tracking of SWI/SNF to UASp2 (centered at −271), and then, by providing additional activator-coactivator interactions downstream at UASp3 (centered at −185), target SWI/SNF to nucleosome −1 to expose the TATA element (centered at −98). The distance between each site is 90 ± 5 bp, corresponding with the ability of chromatin remodelers like SWI/SNF to translocate along the chromatin fiber in intervals of less that 100 bp (Owen-Hughes, 2003). Thus, propagation of chromatin disruption, assisted via the interaction with UAS-bound activators, would provide a molecular basis for the incremental steps proposed in the facilitated tracking model.

FUTURE DIRECTIONS

In this study, we have shown that *PHO5* activation results in the bidirectional propagation of chromatin remodeling from bound activators. Disruption of UAS-proximal nucleosomes occurs preferentially and prior to those more distal. This poses

some interesting questions. Why does nucleosome −3 remodel earlier than nucleosome −2 given that UASp1 is positioned equidistant from both nucleosomes? The conformation of UASp1-bound activators may preferentially target SWI/SNF upstream to nucleosome −3, resulting in the favored remodeling. This idea is being address by the construction of a modified promoter that will allow for the separation of UASp1 and UASp2 through the introduction of a unique HindIII site, centered at −325 (positioned at the upstream edge of nucleosome −2). Digestion with HindIII will allow the separation of upstream and downstream nucleosomes, allowing for independent detection and quantification of SWI/SNF by chromatin immunoprecipitation. Similarly, reversing the orientation of UASp1 may alter the targeting of SWI/SNF as the *Adh* larval enhancer from *Drosophila* was recently shown to have a high degree of orientation preference (Wei and Brennan, 2000). This was unexpected given the paradigm that enhancers are position and orientation independent.

In contrast to a targeting mechanism, as nucleosome −2 is less accessible than −3, suggesting increased histone-DNA affinity (Chapter III), SWI/SNF may encounter both nucleosomes simultaneously but require more time to remodel nucleosome −2. This would then be manifested in a temporal difference in remodeling, indicating the increased time required for nucleosome −2 disruption. In support of this idea, Straka and Hörz assessed the role of nucleosomes in gene activation by replacing nucleosome −2 of the *PHO5* promoter with a fragment of African green monkey α-satellite DNA (Straka and Hörz, 1991). The resulting array had a positioned nucleosome over the satellite DNA fragment and completely eliminated promoter inducibility. This result suggests

that nucleosome conformational stability is responsible for the observed temporal difference in the remodeling of nucleosomes −2 and −3.

Perhaps the most intriguing question evoked from these results involves the mechanism of propagation. Do coactivators track in a non-processive manner across a chromatin fiber or is transcriptional activation driven exclusively by concentration (Chapter IV)? These two models are not mutually exclusive! In an attempt to further study the propagatory mechanism of *PHO5* transactivation, Pho4 and Pho2 binding at UASp1 has been abolished through 18 point mutations, referred to as UASp1-mut [UASp1-mutant, (Barbaric et al., 1998)]. In addition to the wild-type *PHO5* promoter position of UASp2 within nucleosome −2, a second high-affinity UASp2 site is being introduced upstream of nucleosome −5 in HSR1. By repositioning the site of activator binding, we will target nucleosome −5 for remodeling. The increase in Pho4 occupancy at UASp2 upstream of nucleosome −5 should result in the propagation of chromatin remodeling from upstream to downstream nucleosomes. Additionally, we have left the wild-type UASp2 element intact. Propagation of chromatin remodeling from nucleosome −5 need only to propagate to nucleosome −2. Critical exposure of nucleosome-occluded UASp2 should allow for Pho4 binding and recruitment of SWI/SNF, thus enabling the targeted remodeling of nucleosome −1 and exposure of the TATA-element. Moreover, nuclear levels of Pho4 and hence UASp2 occupancy can be modulated by the concentration of P_i in the medium.

Chromatin is divided into two types, euchromatin (decondensed, transcriptionally active) and heterochromatin (condensed, transcriptionally inactive). The spreading of

heterochromatin, composed of Sir2, Sir3, and Sir4 in yeast, interact with nucleosomes, condensing chromatin as it propagates along the chromosome (Moazed, 2001). Novel sequence elements called insulators have been identified, mostly in *Drosophila* but also recently in vertebrates, which have been shown to be associated with boundaries and/or boundary elements. Yeast boundary elements, functionally similar to metazoan boundary/insulator elements, block enhancer-promoter communication (if placed between the enhancer and promoter) and protect euchromatin from advancing heterochromatin (West et al., 2002).

Recently in *S. cerevisiae*, a genome-wide screen was performed to identify proteins that block the spread of silent chromatin when inserted between a silencer and a promoter (Oki et al., 2004). In *MAT*α strains deleted for the *HMR* locus, a plasmid-borne copy of *HMR* lacking the *HMR-I* silencer was used to screen for silencing of the *MAT***a***1* reporter gene, mediated solely by the *HMR-E* silencer. Four Gal4 binding sites were inserted between *HMR-E* and *MAT***a***1*. A second plasmid contained an *ADH1* promoter driving expression of the Gal4 DNA-binding domain fused in frame to each yeast ORF. In the absence of barrier activity, silencing from *HMR-E* encompassed *MAT***a***1* allowing the *MAT*α strain to mate with a *MAT***a** tester and form diploid colonies on selective plates. Proteins isolated that had silencing blocking activity included factors previously shown to be involved in chromatin dynamics, including subunits of SWI/SNF, mediator, TFIID, SAGA, NuA3, and NuA4. They also showed that both histone acetylation and chromatin remodeling occurred at barrier regions. A significant peak in H3 acetylation has also been observed at the chicken β-globin HS4 insulator (Mutskov et al., 2002). It

has further been demonstrated that nucleosome exclusion is a mechanism for establishment of silent chromatin domains (Bi et al., 2004). The presence of the gypsy insulator in *Drosophila* increases the accessibility of promoter-proximal, but not promoter-distal, regions of the *yellow* gene to nucleases (Chen and Corces, 2001). This is consistent with the limited propagation we observed at *PHO5* during transcriptional activation and supports a hypothesis of insulators serving to remove nucleosomes from chromatin. Thus, while it has been suggested that transcription blocks the spread of silent chromatin (Renauld et al., 1993), we predict it to be the targeted remodeling of nucleosomes resulting in the subsequent removal of histones from DNA (Boeger et al., 2003; Reinke and Hörz, 2003; Adkins et al., 2004; Boeger et al., 2004; Nourani et al., 2004).

A proposed mechanism for the establishment of broad acetylation patterns observed in eukaryotes is spreading via acetylated lysine-bromodomain interactions (Forsberg and Bresnick, 2001). Along these lines, if chromatin remodelers require a chromatin substrate in order to propagate efficiently from enhancer-bound activators to basal promoter elements, then the enlarged linker containing UASp1-mut may prevent the spread of nucleosome disruption from upstream to downstream nucleosomes. Likewise, the introduction of nucleosome excluding structures should serve to impede chromatin-tracking complexes. In the event that nucleosome disruption is able propagate from nucleosome −5 to −1 and activate transcription, we will able to compare and contrast levels of Pho4 binding and coactivator dependencies with those of the wild type *PHO5* promoter.

Metazoan enhancers are able to activate gene expression from distances as far as several thousand base-pairs upstream or downstream of a gene (Khoury and Gruss, 1983). In contrast, yeast UAS elements have been shown to work only when located upstream of a gene (Struhl, 1984) at distances of less than ~1 kbp (Guarente and Hoar, 1984; Barberis et al., 1995). It has been suggested that the inability of transcriptional activators to function at a distance in yeast may due to a limitation of euchromatin to loop, as an enhancer positioned 1-2 kbp downstream of a gene has been shown to be activated if the reporter is linked to a telomere but not if it is positioned internal to a chromosome (de Bruin et al., 2001). However, this does not explain the lack of activation when the binding site for a bacterial repressor is placed between a core promoter and its UAS element (Brent and Ptashne, 1984). We expect the positioning UASp2 upstream of nucleosome −5 to address the proposed models of UAS function and provide additional data to further elucidate the molecular mechanism(s) by which yeast UAS elements are both location- and distance-dependent.

REFERENCES

Aalfs, J. D., and Kingston, R. E. (2000). What does 'chromatin remodeling' mean? Trends Biochem. Sci. *25*, 548-555.

Adams, C. C., and Workman, J. L. (1995). Binding of disparate transcriptional activators to nucleosomal DNA is inherently cooperative. Mol. Cell. Biol. *15*, 1405-1421.

Adkins, M. W., Howar, S. R., and Tyler, J. K. (2004). Chromatin disassembly mediated by the histone chaperone Asf1 is essential for transcriptional activation of the yeast *PHO5* and *PHO8* genes. Mol. Cell *14*, 657-666.

Agalioti, T., Lomvardas, S., Parekh, B., Yie, J., Maniatis, T., and Thanos, D. (2000). Ordered recruitment of chromatin modifying and general transcription factors to the IFN-β promoter. Cell *103*, 667-678.

Ahn, S. C., Baek, B. S., Oh, T., Song, C. S., and Chatterjee, B. (2000). Rapid mini-scale plasmid isolation for DNA sequencing and restriction mapping. BioTechniques *29*, 466-468.

Almer, A., and Hörz, W. (1986). Nuclease hypersensitive regions with adjacent positioned nucleosomes mark the gene boundaries of the *PHO5*/*PHO3* locus in yeast. EMBO J. *5*, 2681-2687.

Almer, A., Rudolph, H., Hinner, A., and Hörz, W. (1986). Removal of positioned nucleosomes from the yeast *PHO5* promoter upon *PHO5* induction releases additional upstream activating DNA elements. EMBO J. *5*, 2689-2696.

Anderson, J. D., Thåström, A., and Widom, J. (2002). Spontaneous access of proteins to buried nucleosomal DNA target sites occurs via a mechanism that is distinct from nucleosome translocation. Mol. Cell. Biol. *22*, 7147-7157.

Anderson, J. D., and Widom, J. (2000). Sequence and position-dependence of the equilibrium accessibility of nucleosomal DNA target sites. J. Mol. Biol. *296*, 979-987.

Anderson, J. D., and Widom, J. (2001). Poly(dA-dT) promoter elements increase the equilibrium accessibility of nucleosomal DNA target sites. Mol. Cell. Biol. *21*, 3830-3839.

Angermayr, M., Oechsner, U., Gregor, K., Schroth, G. P., and Bandlow, W. (2002). Transcription initiation in vivo without classical transactivators: DNA kinks flanking the core promoter of the housekeeping yeast adenylate kinase gene, *AKY2*, position nucleosomes and constitutively activate transcription. Nucleic Acids Res. *30*, 4199-4207.

Ausio, J., Levin, D. B., De Amorim, G. V., Bakker, S., and Macleod, P. M. (2003). Syndromes of disordered chromatin remodeling. Clin. Genet. *64*, 83-95.

Balasubramanian, B., and Morse, R. H. (1999). Binding of Gal4p and bicoid to nucleosomal sites in yeast in the absence of replication. Mol. Cell. Biol. *19*, 2977-2985.

Barbaric, S., Fascher, K. D., and Hörz, W. (1992). Activation of the weakly regulated *PHO8* promoter in *S. cerevisiae*: chromatin transition and binding sites for the positive regulatory protein PHO4. Nucleic Acids Res. *20*, 1031-1038.

Barbaric, S., Münsterkötter, M., Goding, C., and Hörz, W. (1998). Cooperative Pho2-Pho4 interactions at the *PHO5* promoter are critical for binding of Pho4 to UASp1 and for efficient transactivation by Pho4 at UASp2. Mol. Cell. Biol. *18*, 2629-2639.

Barbaric, S., Münsterkötter, M., Svaren, J., and Hörz, W. (1996). The homeodomain protein Pho2 and the basic-helix-loop-helix protein Pho4 bind DNA cooperatively at the yeast *PHO5* promoter. Nucleic Acids Res. *24*, 4479-4486.

Barbaric, S., Reinke, H., and Hörz, W. (2003). Multiple mechanistically distinct functions of SAGA at the *PHO5* promoter. Mol. Cell. Biol. *23*, 3468-3476.

Barbaric, S., Walker, J., Schmid, A., Svejstrup, J. Q., and Hörz, W. (2001). Increasing the rate of chromatin remodeling and gene activation – a novel role for the histone acetyltransferase Gcn5. EMBO J. *20*, 4944-4951.

Barberis, A., Pearlberg, J., Simkovich, N., Farrell, S., Reinagel, P., Bamdad, C., Sigal, G., and Ptashne, M. (1995). Contact with a component of the polymerase II holoenzyme suffices for gene activation. Cell *81*, 359-368.

Bash, R., and Lohr, D. (2001). Yeast chromatin structure and regulation of GAL gene expression. Prog. Nucleic Acid Res. Mol. Biol. *65*, 197-259.

Bergman, L. W., and Kramer, R. A. (1983). Modulation of chromatin structure associated with derepression of the acid phosphatase gene of *Saccharomyces cerevisiae*. J. Biol. Chem. *258*, 7223-7227.

Bhoite, L. T., Yu, Y., and Stillman, D. J. (2001). The Swi5 activator recruits the Mediator complex to the *HO* promoter without RNA polymerase II. Genes Dev. *15*, 2457-2469.

Bi, X., Yu, Q., Sandmeier, J. J., and Zou, Y. (2004). Formation of boundaries of transcriptionally silent chromatin by nucleosome-excluding structures. Mol. Cell. Biol. *24*, 2118-2131.

Biggar, S. R., and Crabtree, G. R. (1999). Continuous and widespread roles for the Swi-Snf complex in transcription. EMBO J. *18*, 2254-2264.

Blackwood, E. M., and Kadonaga, J. T. (1998). Going the distance: a current view of enhancer action. Science *281*, 61-63.

Boeger, H., Griesenbeck, J., Strattan, J. S., and Kornberg, R. D. (2003). Nucleosomes unfold completely at a transcriptionally active promoter. Mol. Cell *11*, 1587-1598.

Boeger, H., Griesenbeck, J., Strattan, J. S., and Kornberg, R. D. (2004). Removal of promoter nucleosomes by disassembly rather than sliding in vivo. Mol. Cell *14*, 667-673.

Boerkoel, C. F., Takashima, H., John, J., Yan, J., Stankiewicz, P., Rosenbarker, L., Andre, J. L., Bogdanovic, R., Burguet, A., Cockfield, S., et al. (2002). Mutant chromatin remodeling protein SMARCAL1 causes Schimke immuno-osseous dysplasia. Nat. Genet. *30*, 215-220.

Borchardt, R. T., Eiden, L. E., Wu, B., and Rutledge, C. O. (1979). Sinefungin, a potent inhibitor or S-adenosylmethionine: protein O-methyltransferase. Biochem. Biophys. Res. Commun. *89*, 919-924.

Brazas, R. M., and Stillman, D. J. (1993a). Identification and purification of a protein that binds DNA cooperatively with the yeast SW15 protein. Mol. Cell. Biol. *13*, 5524-5537.

Brazas, R. M., and Stillman, D. J. (1993b). The Swi5 zinc-finger and Grf10 homeodomain proteins bind DNA cooperatively at the yeast *HO* promoter. Proc. Natl. Acad. Sci. USA *90*, 11237-11241.

Brent, R., and Ptashne, M. (1984). A bacterial repressor protein or a yeast transcriptional terminator can block upstream activation of a yeast gene. Nature *312*, 612-615.

Brent, R., and Ptashne, M. (1985). A eukaryotic transcriptional activator bearing the DNA specificity of a prokaryotic repressor. Cell *43*, 729-736.

Breslauer, K. J., Frank, R., Blocker, H., and Markey, L. A. (1986). Predicting DNA duplex stability from the base sequence. Proc. Natl. Acad. Sci. USA *83*, 3746-3750.

Brower-Toland, B. D., Smith, C. L., Yeh, R. C., Lis, J. T., Peterson, C. L., and Wang, M. D. (2002). Mechanical disruption of individual nucleosomes reveals a reversible multistage release of DNA. Proc. Natl. Acad. Sci. USA *99*, 1960-1965.

Brownell, J. E., Zhou, J. X., Ranalli, T., Kobayashi, R., Edmondson, D. G., Roth, S. Y., and Allis, C. D. (1996). Tetrahymena histone acetyltransferase A: a homolog to yeast Gcn5p linking histone acetylation to gene activation. Cell *84*, 843-851.

Bryant, G. O., and Ptashne, M. (2003). Independent recruitment in vivo by Gal4 of two complexes required for transcription. Mol. Cell *11*, 1301-1309.

Carvin, C. D., Dhasarathy, A., Friesenhahn, L. B., Jessen, W. J., and Kladde, M. P. (2003a). Targeted cytosine methylation for in vivo detection of protein-DNA interactions. Proc. Natl. Acad. Sci. USA *100*, 7743-7748.

Carvin, C. D., Parr, R. D., and Kladde, M. P. (2003b). Site-selective in vivo targeting of cytosine-5 DNA methylation by zinc-finger proteins. Nucleic Acids Res. *31*, 6493-6501.

Chen, S., and Corces, V. G. (2001). The gypsy insulator of Drosophila affects chromatin structure in a directional manner. Genetics *159*, 1649-1658.

Clapier, C. R., Langst, G., Corona, D. F., Becker, P. B., and Nightingale, K. P. (2001). Critical role for the histone H4 N terminus in nucleosome remodeling by ISWI. Mol. Cell. Biol. *21*, 875-883.

Clark, S. J., Harrison, J., Paul, C. L., and Frommer, M. (1994). High sensitivity mapping of methylated cytosines. Nucleic Acids Res. *22*, 2990-2997.

Cook, P. R. (1999). The organization of replication and transcription. Science *284*, 1790-1795.

Cosma, M. P., Tanaka, T., and Nasmyth, K. (1999). Ordered recruitment of transcription and chromatin remodeling factors to a cell cycle- and developmentally regulated promoter. Cell *97*, 299-311.

Czarnota, G. J., and Ottensmeyer, F. P. (1996). Structural states of the nucleosome. J. Biol. Chem. *271*, 3677-3683.

Davey, C. A., Sargent, D. F., Luger, K., Maeder, A. W., and Richmond, T. J. (2002). Solvent mediated interactions in the structure of the nucleosome core particle at 1.9 Å resolution. J. Mol. Biol. *319*, 1097-1113.

de Bruin, D., Zaman, Z., Liberatore, R. A., and Ptashne, M. (2001). Telomere looping permits gene activation by a downstream UAS in yeast. Nature *409*, 109-113.

Dhasarathy, A., Carvin, C. D., Jessen, W. J., and Kladde, M. P. (2004). Modifying chromatin remodeling enzyme requirements by regulating levels of promoter-bound transactivator. Submitted.

Dickerson, R. E. (1998). DNA bending: the prevalence of kinkiness and the virtues of normality. Nucleic Acids Res. *26*, 1906-1926.

Dorner, L. F., and Schildkraut, I. (1994). Direct selection of binding proficient/catalytic deficient variants of BamHI endonuclease. Nucleic Acids Res. *22*, 1068-1074.

Drew, H. R. (1984). Structural specificities of five commonly used DNA nucleases. J. Mol. Biol. *176*, 535-557.

Drew, H. R., and Travers, A. A. (1985). DNA bending and its relation to nucleosome positioning. J. Mol. Biol. *186*, 773-790.

Dudley, A. M., Rougeulle, C., and Winston, F. (1999). The Spt components of SAGA facilitate TBP binding to a promoter at a post-activator-binding step in vivo. Genes Dev. *13*, 2940-2945.

Eberharter, A., Sterner, D. E., Schieltz, D., Hassan, A., Yates, J. R., III, Berger, S. L., and Workman, J. L. (1999). The ADA complex is a distinct histone acetyltransferase complex in *Saccharomyces cerevisiae*. Mol. Cell. Biol. *19*, 6621-6631.

el Hassan, M. A., and Calladine, C. R. (1996). Propeller-twisting of base-pairs and the conformational mobility of dinucleotide steps in DNA. J. Mol. Biol. *259*, 95-103.

Farrell, S., Simkovich, N., Wu, Y., Barberis, A., and Ptashne, M. (1996). Gene activation by recruitment of the RNA polymerase II holoenzyme. Genes Dev. *10*, 2359-2367.

Fascher, K. D., Schmitz, J., and Hörz, W. (1990). Role of trans-activating proteins in the generation of active chromatin at the *PHO5* promoter in *S. cerevisiae*. EMBO J. *9*, 2523-2528.

Fascher, K. D., Schmitz, J., and Hörz, W. (1993). Structural and functional requirements for the chromatin transition at the *PHO5* promoter in *Saccharomyces cerevisiae* upon *PHO5* activation. J. Mol. Biol. *231*, 658-667.

Fazzio, T. G., and Tsukiyama, T. (2003). Chromatin remodeling in vivo: evidence for a nucleosome sliding mechanism. Mol. Cell *12*, 1333-1340.

Fedor, M. J., Lue, N. F., and Kornberg, R. D. (1988). Statistical positioning of nucleosomes by specific protein-binding to an upstream activating sequence in yeast. J. Mol. Biol. *204*, 109-127.

Fischle, W., Wang, Y., Jacobs, S. A., Kim, Y., Allis, C. D., and Khorasanizadeh, S. (2003). Molecular basis for the discrimination of repressive methyl-lysine marks in histone H3 by Polycomb and HP1 chromodomains. Genes Dev. *17*, 1870-1881.

Fitzgerald, D. J., Dryden, G. L., Bronson, E. C., Williams, J. S., and Anderson, J. N. (1994). Conserved patterns of bending in satellite and nucleosome positioning DNA. J. Biol. Chem. *269*, 21303-21314.

Flaus, A., and Richmond, T. J. (1998). Positioning and stability of nucleosomes on MMTV 3' LTR sequences. J. Mol. Biol. *275*, 427-441.

Fletcher, T. M., Xiao, N., Mautino, G., Baumann, C. T., Wolford, R., Warren, B. S., and Hager, G. L. (2002). ATP-dependent mobilization of the glucocorticoid receptor during chromatin remodeling. Mol. Cell. Biol. *22*, 3255-3263.

Flick, J. T., Eissenberg, J. C., and Elgin, S. C. (1986). Micrococcal nuclease as a DNA structural probe: its recognition sequences, their genomic distribution and correlation with DNA structure determinants. J. Mol. Biol. *190*, 619-633.

Forsberg, E. C., and Bresnick, E. H. (2001). Histone acetylation beyond promoters: long-range acetylation patterns in the chromatin world. BioEssays *23*, 820-830.

Frommer, M., MacDonald, L. E., Millar, D. S., Collis, C. M., Watt, F., Grigg, G. W., Molloy, P. L., and Paul, C. L. (1992). A genomic sequencing protocol that yields a positive display of 5-methylcytosine residues in individual DNA strands. Proc. Natl. Acad. Sci. USA *89*, 1827-1831.

Fry, C. J., and Peterson, C. L. (2001). Chromatin remodeling enzymes: who's on first? Curr. Biol. *11*, R185-R197.

Gasser, S. M., Paro, R., Stewart, F., and Aasland, R. (1998). Introduction: the genetics of epigenetics. Cell. Mol. Life Sci. *54*, 1-5.

Gaudreau, L., Keaveney, M., Nevado, J., Zaman, Z., Bryant, G. O., Struhl, K., and Ptashne, M. (1999). Transcriptional activation by artificial recruitment in yeast is influenced by promoter architecture and downstream sequences. Proc. Natl. Acad. Sci. USA *96*, 2668-2673.

Gaudreau, L., Schmid, A., Blaschke, D., Ptashne, M., and Hörz, W. (1997). RNA polymerase II holoenzyme recruitment is sufficient to remodel chromatin at the yeast *PHO5* promoter. Cell *89*, 55-62.

Gavin, I. M., Kladde, M. P., and Simpson, R. T. (2000). Tup1p represses Mcm1p transcriptional activation and chromatin remodeling of an **a**-cell-specific gene. EMBO J. *19*, 5875-5883.

Gavin, I. M., and Simpson, R. T. (1997). Interplay of yeast global transcriptional regulators Ssn6p-Tup1 and Swi-Snf and their effect on chromatin structure. EMBO J. *16*, 6263-6271.

Grant, P. A., Duggan, L., Cote, J., Roberts, S. M., Brownell, J. E., Candau, R., Ohba, R., OwenHughes, T., Allis, C. D., Winston, F., et al. (1997). Yeast Gcn5 functions in two multisubunit complexes to acetylate nucleosomal histones: characterization of an Ada complex and the SAGA (Spt/Ada) complex. Genes Dev. *11*, 1640-1650.

Gregory, P. D., Schmid, A., Zavari, M., Lui, L., Berger, S. L., and Hörz, W. (1998). Absence of Gcn5 HAT activity defines a novel state in the opening of chromatin at the *PHO5* promoter in yeast. Mol. Cell *1*, 495-505.

Gregory, P. D., Schmid, A., Zavari, M., Münsterkötter, M., and Hörz, W. (1999). Chromatin remodelling at the *PHO8* promoter requires SWI-SNF and SAGA at a step subsequent to activator binding. EMBO J. *18*, 6407-6414.

Griffin-Burns, L., and Peterson, C. L. (1997). The yeast SWI-SNF complex facilitates binding of a transcriptional activator to nucleosomal sites in vivo. Mol. Cell. Biol. *17*, 4811-4819.

Gross, D. S., and Garrard, W. T. (1988). Nuclease hypersensitive sites in chromatin. Annu. Rev. Biochem. *57*, 159-197.

Guarente, L., and Hoar, E. (1984). Upstream activation sites of the *CYC1* gene of *Saccharomyces cerevisiae* are active when inverted but not when placed downstream of the "TATA box". Proc. Natl. Acad. Sci. USA *81*, 7860-7864.

Han, M., and Grunstein, M. (1988). Nucleosome loss activates yeast downstream promoters in vivo. Cell *55*, 1137-1145.

Han, M., Kim, U. J., Kayne, P., and Grunstein, M. (1988). Depletion of histone H4 and nucleosomes activates the *PHO5* gene in *Saccharomyces cerevisiae*. EMBO J. *7*, 2221-2228.

Hansen, J. C. (2002). Conformational dynamics of the chromatin fiber in solution: determinants, mechanisms, and functions. Annu. Rev. Biophys. Biomol. Struct. *31*, 361-392.

Harp, J. M., Hanson, B. L., Timm, D. E., and Bunick, G. J. (2000). Asymmetries in the nucleosome core particle at 2.5 Å resolution. Acta Crystallogr. D *56*, 1513-1534.

Hassan, A. H., Neely, K. E., and Workman, J. L. (2001). Histone acetyltransferase complexes stabilize SWI/SNF binding to promoter nucleosomes. Cell *104*, 817-827.

Hassan, A. H., Prochasson, P., Neely, K. E., Galasinski, S. C., Chandy, M., Carrozza, M. J., and Workman, J. L. (2002). Function and selectivity of bromodomains in anchoring chromatin-modifying complexes to promoter nucleosomes. Cell *111*, 369-379.

Haswell, E. S., and O'Shea, E. K. (1999). An in vitro system recapitulates chromatin remodeling at the *PHO5* promoter. Mol. Cell. Biol. *19*, 2817-2827.

Hatzis, P., and Talianidis, I. (2002). Dynamics of enhancer-promoter communication during differentiation-induced gene activation. Mol. Cell *10*, 1467-1477.

Haynes, S. R., Dollard, C., Winston, F., Beck, S., Trowsdale, J., and Dawid, I. B. (1992). The bromodomain: a conserved sequence found in human, Drosophila and yeast proteins. Nucleic Acids Res. *20*, 2603.

Hecht, A., Laroche, T., Strahlbolsinger, S., Gasser, S. M., and Grunstein, M. (1995). Histone H3 and H4 N-termini interact with SIR3 and SIR4 proteins: a molecular model for the formation of heterochromatin in yeast. Cell *80*, 583-592.

Holstege, F. C. P., Jennings, E. G., Wyrick, J. J., Lee, T. I., Hengartner, C. J., Green, M. R., Golub, T., Lander, E. S., and Young, R. A. (1998). Dissecting the regulatory circuitry of a eukaryotic genome. Cell *95*, 717-728.

Howe, L., Brown, C. E., Lechner, T., and Workman, J. L. (1999). Histone acetyltransferase complexes and their link to transcription. Crit. Rev. Eukaryot. Gene Expr. *9*, 231-243.

Iyer, V., and Struhl, K. (1995). Poly(dA:dT), a ubiquitous promoter element that stimulates transcription via its intrinsic DNA structure. EMBO J. *14*, 2570-2579.

Jaskelioff, M., Gavin, I. M., Peterson, C. L., and Logie, C. (2000). SWI-SNF-mediated nucleosome remodeling: role of histone octamer mobility in the persistence of the remodeled state. Mol. Cell. Biol. *20*, 3058-3068.

Jeppesen, P., and Turner, B. M. (1993). The inactive X chromosome in female mammals is distinguished by a lack of histone H4 acetylation, a cytogenetic marker for gene expression. Cell *74*, 281-289.

Jessen, W. J., Dhasarathy, A., Carvin, C. D., and Kladde, M. P. (2004a). Bidirectionally propagated chromatin remodeling during transcriptional activation in vivo. Submitted.

Jessen, W. J., Dhasarathy, A., Hoose, S. A., Carvin, C. D., Risinger, A. L., and Kladde, M. P. (2004b). Mapping chromatin structure in vivo using DNA methyltransferases. Methods *33*, 68-80.

Jin, Y., Wang, Y., Walker, D. L., Dong, H., Conley, C., Johansen, J., and Johansen, K. M. (1999). JIL-1: a novel chromosomal tandem kinase implicated in transcriptional regulation in Drosophila. Mol. Cell *4*, 129-135.

Jones, K. A., and Kadonaga, J. T. (2000). Exploring the transcription-chromatin interface. Genes Dev. *14*, 1992-1996.

Kadonaga, J. T. (1998). Eukaryotic transcription: an interlaced network of transcription factors and chromatin-modifying machines. Cell *92*, 307-313.

Keaveney, M., and Struhl, K. (1998). Activator-mediated recruitment of the RNA polymerase II machinery is the predominant mechanism for transcriptional activation in yeast. Mol. Cell *1*, 917-924.

Kent, N. A., Bird, L. E., and Mellor, J. (1993). Chromatin analysis in yeast using NP-40 permeabilised sphaeroplasts. Nucleic Acids Res. *21*, 4653-4654.

Kent, N. A., Eibert, S. M., and Mellor, J. (2004). Cbf1p is required for chromatin remodeling at promoter-proximal CACGTG motifs in yeast. J. Biol. Chem. *279*, 27116-27123.

Kent, N. A., and Mellor, J. (1995). Chromatin structure snap-shots: rapid nuclease digestion of chromatin in yeast. Nucleic Acids Res. *23*, 3786-3787.

Khoury, G., and Gruss, P. (1983). Enhancer elements. Cell *33*, 313-314.

Kim, A., and Dean, A. (2004). Developmental stage differences in chromatin subdomains of the β-globin locus. Proc. Natl. Acad. Sci. USA *101*, 7028-7033.

Kladde, M. P., and Simpson, R. T. (1994). Positioned nucleosomes inhibit Dam methylation in vivo. Proc. Natl. Acad. Sci. USA *91*, 1361-1365.

Kladde, M. P., Xu, M., and Simpson, R. T. (1996). Direct study of DNA-protein interactions in repressed and active chromatin in living cells. EMBO J. *15*, 6290-6300.

Klein, C., and Struhl, K. (1994). Increased recruitment of TATA-binding protein to the promoter by transcriptional activation domains in vivo. Science *266*, 280-282.

Komeili, A., and O'Shea, E. K. (1999). Roles of phosphorylation sites in regulating activity of the transcription factor Pho4. Science *284*, 977-980.

Korber, P., and Hörz, W. (2004). In vitro assembly of the characteristic chromatin organization at the yeast *PHO5* promoter by a replication independent extract system. J. Biol. Chem., *279*, 35113-35120.

Krebs, J. E., Fry, C. J., Samuels, M. L., and Peterson, C. L. (2000). Global role for chromatin remodeling enzymes in mitotic gene expression. Cell *102*, 587-598.

Krebs, J. E., Kuo, M. H., Allis, C. D., and Peterson, C. L. (1999). Cell cycle-regulated histone acetylation required for expression of the yeast *HO* gene. Genes Dev. *13*, 1412-1421.

Kuo, M., Zhou, J., Jambeck, P., Churchill, M. E. A., and Allis, C. D. (1998). Histone acetyltransferase activity of yeast Gcn5p is required for the activation of target genes in vivo. Genes Dev. *12*, 627-639.

Lee, K. P., Baxter, H. J., Guillemette, J. G., Lawford, H. G., and Lewis, P. N. (1982). Structural studies on yeast nucleosomes. Can. J. Biochem. *60*, 379-388.

Lemon, B., and Tjian, R. (2000). Orchestrated response: a symphony of transcription factors for gene control. Genes Dev. *14*, 2551-2569.

Li, E., Bestor, T. H., and Jaenisch, R. (1992). Targeted mutation of the DNA methyltransferase gene results in embryonic lethality. Cell *69*, 915-926.

Li, Q. L., Zhang, M. H., Duan, Z. J., and Stamatoyannopoulos, G. (1999). Structural analysis and mapping of DNase I hypersensitivity of HS5 of the β-globin locus control region. Genomics *61*, 183-193.

Liang, G., Lin, J. C., Wei, V., Yoo, C., Cheng, J. C., Nguyen, C. T., Weisenberger, D. J., Egger, G., Takai, D., Gonzales, F. A., and Jones, P. A. (2004). Distinct localization of histone H3 acetylation and H3-K4 methylation to the transcription start sites in the human genome. Proc. Natl. Acad. Sci. USA *101*, 7357-7362.

Logie, C., and Peterson, C. L. (1997). Catalytic activity of the yeast SWI/SNF complex on reconstituted nucleosome arrays. EMBO J. *16*, 6772-6782.

Lomvardas, S., and Thanos, D. (2002). Modifying gene expression programs by altering core promoter chromatin architecture. Cell *110*, 261-271.

Luger, K., Mader, A. W., Richmond, R. K., Sargent, D. F., and Richmond, T. J. (1997). Crystal structure of the nucleosome core particle at 2.8 Å resolution. Nature *389*, 251-260.

Luger, K., and Richmond, T. J. (1998). DNA binding within the nucleosome core. Curr. Opin. Struct. Biol. *8*, 33-40.

Lusser, A., and Kadonaga, J. T. (2003). Chromatin remodeling by ATP-dependent molecular machines. BioEssays *25*, 1192-1200.

Lyko, F., Ramsahoye, B. H., Kashevsky, H., Tudor, M., Mastrangelo, M. A., Orr-Weaver, T. L., and Jaenisch, R. (1999). Mammalian (cytosine-5) methyltransferases cause genomic DNA methylation and lethality in Drosophila. Nat. Genet. *23*, 363-366.

Mahmoudi, T., Katsani, K. R., and Verrijzer, C. P. (2002). GAGA can mediate enhancer function in trans by linking two separate DNA molecules. EMBO J. *21*, 1775-1781.

Martinez-Campa, C., Politis, P., Moreau, J. L., Kent, N., Goodall, J., Mellor, J., and Goding, C. R. (2004). Precise nucleosome positioning and the TATA box dictate requirements for the histone H4 tail and the bromodomain factor Bdf1. Mol. Cell *15*, 69-81.

McAndrew, P. C., Svaren, J., Martin, S. R., Hörz, W., and Goding, C. R. (1998). Requirements for chromatin modulation and transcription activation by the Pho4 acidic activation domain. Mol. Cell Biol. *18*, 5818-5827.

McGhee, J. D., and Felsenfeld, G. (1980). Nucleosome structure. Annu. Rev. Biochem. *49*, 1115-1156.

McNamara, A. R., Hurd, P. J., Smith, A. E., and Ford, K. G. (2002). Characterisation of site-biased DNA methyltransferases: specificity, affinity and subsite relationships. Nucleic Acids Res. *30*, 3818-3830.

Metivier, R., Penot, G., Hubner, M. R., Reid, G., Brand, H., Kos, M., and Gannon, F. (2003). Estrogen receptor-α directs ordered, cyclical, and combinatorial recruitment of cofactors on a natural target promoter. Cell *115*, 751-763.

Misteli, T. (2001). Protein dynamics: implications for nuclear architecture and gene expression. Science *291*, 843-847.

Moazed, D. (2001). Common themes in mechanisms of gene silencing. Mol. Cell *8*, 489-498.

Morse, R. H., Roth, S. Y., and Simpson, R. T. (1992). A transcriptionally active transfer RNA gene interferes with nucleosome positioning in vivo. Mol. Cell. Biol. *12*, 4015-4025.

Mund, C., Musch, T., Strodicke, M., Assmann, B., Li, E., and Lyko, F. (2004). Comparative analysis of DNA methylation patterns in transgenic Drosophila overexpressing mouse DNA methyltransferases. Biochem. J. *378*, 763-768.

Munteanu, M. G., Vlahoviček, K., Parthasarathy, S., Simon, I., and Pongor, S. (1998). Rod models of DNA: sequence-dependent anisotropic elastic modelling of local bending phenomena. Trends Biochem. Sci. *23*, 341-347.

Murphy, M. R., Shimizu, M., Roth, S. Y., Dranginis, A. M., and Simpson, R. T. (1993). DNA-protein interactions at the *S. cerevisiae* α2 operator in vivo. Nucleic Acids Res. *21*, 3295-3300.

Mutskov, V. J., Farrell, C. M., Wade, P. A., Wolffe, A. P., and Felsenfeld, G. (2002). The barrier function of an insulator couples high histone acetylation levels with specific protection of promoter DNA from methylation. Genes Dev. *16*, 1540-1554.

Narlikar, G. J., Fan, H. Y., and Kingston, R. E. (2002). Cooperation between complexes that regulate chromatin structure and transcription. Cell *108*, 475-487.

Nedospasov, S. A., and Georgiev, G. P. (1980). Non-random cleavage of SV40 DNA in the compact minichromosome and free in solution by micrococcal nuclease. Biochem. Biophys. Res. Commun. *92*, 532-539.

Neef, D. W., and Kladde, M. P. (2003). Polyphosphate loss promotes SNF/SWI- and Gcn5-dependent mitotic induction of *PHO5*. Mol. Cell. Biol. *23*, 3788-3797.

Nourani, A., Utley, R. T., Allard, S., and Cote, J. (2004). Recruitment of the NuA4 complex poises the *PHO5* promoter for chromatin remodeling and activation. EMBO J.

Oki, M., Valenzuela, L., Chiba, T., Ito, T., and Kamakaka, R. T. (2004). Barrier proteins remodel and modify chromatin to restrict silenced domains. Mol. Cell. Biol. *24*, 1956-1967.

O'Neill, E. M., Kaffman, A., Jolly, E. R., and O'Shea, E. K. (1996). Regulation of PHO4 nuclear localization by the PHO80-PHO85 cyclin-CDK complex. Science *271*, 209-212.

Otero, G., Fellows, J., Li, Y., de Bizemont, T., Dirac, A. M., Gustafsson, C. M., Erdjument-Bromage, H., Tempst, P., and Svejstrup, J. Q. (1999). Elongator, a multisubunit component of a novel RNA polymerase II holoenzyme for transcriptional elongation. Mol. Cell *3*, 109-118.

Owen, D. J., Ornaghi, P., Yang, J. C., Lowe, N., Evans, P. R., Ballario, P., Neuhaus, D., Filetici, P., and Travers, A. A. (2000). The structural basis for the recognition of acetylated histone H4 by the bromodomain of histone acetyltransferase Gcn5p. EMBO J. *19*, 6141-6149.

Owen-Hughes, T. (2003). Colworth memorial lecture. Pathways for remodelling chromatin. Biochem. Soc. Trans. *31*, 893-905.

Owen-Hughes, T., and Workman, J. L. (1994). Experimental analysis of chromatin function in transcription control. Crit. Rev. Eukaryot. Gene Expr. *4*, 403-441.

Packer, M. J., Dauncey, M. P., and Hunter, C. A. (2000). Sequence-dependent DNA structure: dinucleotide conformational maps. J. Mol. Biol. *295*, 71-83.

Patterton, H. G., and Simpson, R. T. (1994). Nucleosomal location of the *STE6* TATA-box and Matα2p mediated repression. Mol. Cell. Biol. *14*, 4002-4010.

Pilon, J., Terrell, A., and Laybourn, P. J. (1997). Yeast chromatin reconstitution system using purified yeast core histones and yeast nucleosome assembly protein-1. Protein Expr. Purif. *10*, 132-140.

Polach, K. J., and Widom, J. (1995). Mechanism of protein access to specific DNA sequences in chromatin: a dynamic equilibrium model for gene regulation. J. Mol. Biol. *254*, 130-149.

Pray-Grant, M. G., Schieltz, D., McMahon, S. J., Wood, J. M., Kennedy, E. L., Cook, R. G., Workman, J. L., Yates, J. R., 3rd, and Grant, P. A. (2002). The novel SLIK histone acetyltransferase complex functions in the yeast retrograde response pathway. Mol. Cell. Biol. *22*, 8774-8786.

Pringle, J. R., and Hartwell, L. H. (1981). The *Saccharomyces cerevisiae* cell cycle. In The Molecular Biology of the Yeast Saccharomyces: Life Cycle and Inheritance, J. N. Strathern, E. W. Jones, and J. R. Broach, ed. (Cold Spring Harbor, NY: Cold Spring Harbor Laboratory Press), pp. 97-142.

Protacio, R. U., Polach, K. J., and Widom, J. (1997). Coupled-enzymatic assays for the rate and mechanism of DNA site exposure in a nucleosome. J. Mol. Biol. *274*, 708-721.
Ptashne, M., and Gann, A. (1997). Transcriptional activation by recruitment. Nature *386*, 569-577.

Ravindra, A., Weiss, K., and Simpson, R. T. (1999). High-resolution structural analysis of chromatin at specific loci: *Saccharomyces cerevisiae* silent mating-type locus HMR**a**. Mol. Cell. Biol. *19*, 7944-7950.

Reid, J. L., Iyer, V. R., Brown, P. O., and Struhl, K. (2000). Coordinate regulation of yeast ribosomal protein genes is associated with targeted recruitment of Esa1 histone acetylase. Mol. Cell *6*, 1297-1307.

Reinke, H., and Hörz, W. (2003). Histones are first hyperacetylated and then lose contact with the activated *PHO5* promoter. Mol. Cell *11*, 1599-1607.

Renauld, H., Aparicio, O. M., Zierath, P. D., Billington, B. L., Chhablani, S. K., and Gottschling, D. E. (1993). Silent domains are assembled continuously from the telomere and are defined by promoter distance and strength, and by *SIR3* dosage. Genes Dev. *7*, 1133-1145.

Renbaum, P., Abrahamove, D., Fainsod, A., Wilson, G., Rottem, S., and Razin, A. (1990). Cloning, characterization, and expression in *Escherichia coli* of the gene coding for the CpG DNA from *Spiroplasma sp* strain MQ-1 (M.SssI). Nucleic Acids Res. *18*, 1145-1152.

Richmond, T. J., and Davey, C. A. (2003). The structure of DNA in the nucleosome core. Nature *423*, 145-150.

Roux-Rouquie, M., Chauvet, M. L., Munnich, A., and Frezal, J. (1999). Human genes involved in chromatin remodeling in transcription initiation, and associated diseases: An overview using the GENATLAS database. Mol. Genet. Metab. *67*, 261-277.

Ryan, M. P., Jones, R., and Morse, R. H. (1998). SWI-SNF complex participation in transcriptional activation at a step subsequent to activator binding. Mol. Cell. Biol. *18*, 1774-1782.

Ryan, M. P., Stafford, G. A., Yu, L., and Morse, R. H. (2000). Artificially recruited TATA-binding protein fails to remodel chromatin and does not activate three promoters that require chromatin remodeling. Mol. Cell. Biol. *20*, 5847-5857.

Sambrook, J., Fritsch, E. F., and Maniatis, T. (1989). Molecular Cloning: A laboratory manual, 2nd ed (Cold Spring Harbor, NY: Cold Spring Harbor Laboratory Press).

Samudio, I., Vyhlidal, C., Wang, F., Stoner, M., Chen, I., Kladde, M., Barhoumi, R., Burghardt, R., and Safe, S. (2001). Transcriptional activation of deoxyribonucleic acid polymerase α gene expression in MCF-7 cells by 17β-estradiol. Endocrinology *142*, 1000-1008.

Schübeler, D., Francastel, C., Cimbora, D. M., Reik, A., Martin, D. I., and Groudine, M. (2000). Nuclear localization and histone acetylation: a pathway for chromatin opening and transcriptional activation of the human β-globin locus. Genes Dev. *14*, 940-950.

Scipioni, A., Pisano, S., Anselmi, C., Savino, M., and De Santis, P. (2004). Dual role of sequence-dependent DNA curvature in nucleosome stability: the critical test of highly bent *Crithidia fasciculata* DNA tract. Biophys. Chem. *107*, 7-17.

Shang, Y., Hu, X., DiRenzo, J., Lazar, M. A., and Brown, M. (2000). Cofactor dynamics and sufficiency in estrogen receptor-regulated transcription. Cell *103*, 843-852.

Shang, Y., Myers, M., and Brown, M. (2002). Formation of the androgen receptor transcription complex. Mol. Cell *9*, 601-610.

Sheen, J.-Y., and Seed, B. (1988). Electrolyte gradient gels for DNA sequencing. BioTechniques *6*, 942-944.

Shimizu, M., Roth, S. Y., Szent-Gyorgyi, C., and Simpson, R. T. (1991). Nucleosomes are positioned with base-pair precision adjacent to the α2 operator in *Saccharomyces cerevisiae*. EMBO J. *10*, 3033-3041.

Sidhu, R. S., and Bollon, A. P. (1990). Bacterial plasmid pBR322 sequences serve as upstream activating sequences in *Saccharomyces cerevisiae*. Yeast *6*, 221-229.

Simpson, R. T., Thoma, F., and Brubaker, J. M. (1985). Chromatin reconstituted from tandemly repeated cloned DNA fragments and core histones: a model system for study of higher order structure. Cell *42*, 799-808.

Simpson, R. T. (1990). Nucleosome positioning can affect the function of a cis-acting DNA element in vivo. Nature *343*, 387-389.

Simpson, R. T. (1999). In vivo methods to analyze chromatin structure. Curr. Opin. Genet. Dev. *9*, 225-229.

Sivolob, A. V., and Khrapunov, S. N. (1995). Translational positioning of nucleosomes on DNA: the role of sequence-dependent isotropic DNA bending stiffness. J. Mol. Biol. *247*, 918-931.

Smith, C. L., Horowitz-Scherer, R., Flanagan, J. F., Woodcock, C. L., and Peterson, C. L. (2003). Structural analysis of the yeast SWI/SNF chromatin remodeling complex. Nat. Struct. Biol. *10*, 141-145.

Smith, E. R., Eisen, A., Gu, W., Sattah, M., Pannuti, A., Zhou, J., Cook, R. G., Lucchesi, J. C., and Allis, C. D. (1998). ESA1 is a histone acetyltransferase that is essential for growth in yeast. Proc. Natl. Acad. Sci. USA *95*, 3561-3565.

Soutoglou, E., and Talianidis, I. (2002). Coordination of PIC assembly and chromatin remodeling during differentiation-induced gene activation. Science *295*, 1901-1904.

Steger, D. J., Haswell, E. S., Miller, A. L., Wente, S. R., and O'Shea, E. K. (2003). Regulation of chromatin remodeling by inositol polyphosphates. Science *299*, 114-116.

Steger, D. J., and Workman, J. L. (1999). Transcriptional analysis of purified histone acetyltransferase complexes. Methods *19*, 410-416.

Stenoien, D. L., Nye, A. C., Mancini, M. G., Patel, K., Dutertre, M., O'Malley, B. W., Smith, C. L., Belmont, A. S., and Mancini, M. A. (2001). Ligand-mediated assembly and real-time cellular dynamics of estrogen receptor α-coactivator complexes in living cells. Mol. Cell. Biol. *21*, 4404-4412.

Strahl, B. D., and Allis, C. D. (2000). The language of covalent histone modifications. Nature *403*, 41-45.

Straka, C., and Hörz, W. (1991). A functional role for nucleosomes in the repression of a yeast promoter. EMBO J. *10*, 361-368.

Struhl, K. (1984). Genetic properties and chromatin structure of the yeast *gal* regulatory element: an enhancer-like sequence. Proc. Natl. Acad. Sci. USA *81*, 7865-7869.

Struhl, K. (1996). Chromatin structure and RNA polymerase II connection: implications for transcription. Cell *84*, 179-182.

Sudarsanam, P., Cao, Y., Wu, L., Laurent, B. C., and Winston, F. (1999). The nucleosome remodeling complex, Snf/Swi, is required for the maintenance of transcription in vivo and is partially redundant with the histone acetyltransferase, Gcn5. EMBO J. *18*, 3101-3106.

Sudarsanam, P., Iyer, V. R., Brown, P. O., and Winston, F. (2000). Whole-genome expression analysis of snf/swi mutants of *Saccharomyces cerevisiae*. Proc. Natl. Acad. Sci. USA *97*, 3364-3369.

Svaren, J., and Hörz, W. (1995). Interplay between nucleosomes and transcription factors at the yeast *PHO5* promoter. Semin. Cell Biol. *6*, 177-183.

Syntichaki, P., Topalidou, I., and Thireos, G. (2000). The Gcn5 bromodomain co-ordinates nucleosome remodelling. Nature *404*, 414-417.

Terrell, A. R., Wongwisansri, S., Pilon, J. L., and Laybourn, P. J. (2002). Reconstitution of nucleosome positioning, remodeling, histone acetylation, and transcriptional activation on the *PHO5* promoter. J. Biol. Chem. *277*, 31038-31047.

Thåström, A., Bingham, L. M., and Widom, J. (2004). Nucleosomal locations of dominant DNA sequence motifs for histone-DNA interactions and nucleosome positioning. J. Mol. Biol. *338*, 695-709.

Thåström, A., Lowary, P. T., Widlund, H. R., Cao, H., Kubista, M., and Widom, J. (1999). Sequence motifs and free energies of selected natural and non-natural nucleosome positioning DNA sequences. J. Mol. Biol. *288*, 213-229.

Tjian, R., and Maniatis, T. (1994). Transcriptional activation: a complex puzzle with few easy pieces. Cell *77*, 5-8.

Topalidou, I., and Thireos, G. (2003). Gcn4 occupancy of open reading frame regions results in the recruitment of chromatin-modifying complexes but not the mediator complex. EMBO J. *4*, 872-876.

Tsukiyama, T. (2002). The in vivo functions of ATP-dependent chromatin-remodelling factors. Nat. Rev. Mol. Cell. Biol. *3*, 422-429.

van Steensel, B., and Henikoff, S. (2000). Identification of in vivo DNA targets of chromatin proteins using tethered dam methyltransferase. Nat. Biotechnol. *18*, 424-428.

Venter, U., Svaren, J., Schmitz, J., Schmid, A., and Hörz, W. (1994). A nucleosome precludes binding of the transcription factor Pho4 in vivo to a critical target site in the *PHO5* promoter. EMBO J. *13*, 4848-4855.

Vettese-Dadey, M., Grant, P. A., Hebbes, T. R., Cranerobinson, C., Allis, C. D., and Workman, J. L. (1996). Acetylation of histone H4 plays a primary role in enhancing transcription factor binding to nucleosomal DNA in vitro. EMBO J. *15*, 2508-2518.

Vignali, M., Hassan, A. H., Neely, K. E., and Workman, J. L. (2000). ATP-dependent chromatin-remodeling complexes. Mol. Cell. Biol. *20*, 1899-1910.

Vlahoviček, K., Kaján, L., and Pongor, S. (2003). DNA analysis servers: plot.it, bend.it, model.it and IS. Nucleic Acids Res. *31*, 3686-3687.

Vogel, K., Hörz, W., and Hinnen, A. (1989). The two positively acting regulatory proteins PHO2 and PHO4 physically interact with *PHO5* upstream activation regions. Mol. Cell. Biol. *9*, 2050-2057.

Voth, W. P., Richards, J. D., Shaw, J. M., and Stillman, D. J. (2001). Yeast vectors for integration at the *HO* locus. Nucleic Acids Res. *29*, E59-59.

Vyhlidal, C., Samudio, I., Kladde, M. P., and Safe, S. (2000). Transcriptional activation of transforming growth factor α by estradiol: requirement for both a GC-rich site and an estrogen response element half-site. J. Mol. Endocrinol. *24*, 329-338.

Wang, J. C., and Giaever, G. N. (1988). Action at a distance along a DNA. Science *240*, 300-304.

Wang, L., Liu, L., and Berger, S. L. (1998). Critical residues for histone acetylation by *GCN5*, functioning in ADA and SAGA complexes, are also required for transcriptional function in vivo. Genes Dev. *12*, 640-653.

Warnecke, P. M., Stirzaker, C., Song, J., Grunau, C., Melki, J. R., and Clark, S. J. (2002). Identification and resolution of artifacts in bisulfite sequencing. Methods *27*, 101-107.

Wei, W., and Brennan, M. D. (2000). Polarity of transcriptional enhancement revealed by an insulator element. Proc. Natl. Acad. Sci. USA *97*, 14518-14523.

Weischet, W. O., Tatchell, K., van Holde, K. E., and Klump, H. (1978). Thermal denaturation of nucleosomal core particles. Nucleic Acids Res. *5*, 139-160.

Weiss, K., and Simpson, R. T. (1998). High-resolution structural analysis of chromatin at specific loci: *Saccharomyces cerevisiae* silent mating type locus *HMLα*. Mol. Cell. Biol. *18*, 5392-5403.

West, A. G., Gaszner, M., and Felsenfeld, G. (2002). Insulators: many functions, many mechanisms. Genes Dev. *16*, 271-288.

Widom, J. (2001). Role of DNA sequence in nucleosome stability and dynamics. Q. Rev. Biophys. *34*, 269-324.

Winston, F., and Allis, C. D. (1999). The bromodomain: a chromatin-targeting module? Nat. Struct. Biol. *6*, 601-604.

Wolffe, A. P., Urnov, F. D., and Guschin, D. (2000). Co-repressor complexes and remodelling chromatin for repression. Biochem. Soc. Trans. *28*, 379-386.

Wu, C. (1997). Chromatin remodeling and the control of gene expression. J. Biol. Chem. *272*, 28171-28174.

Xiao, H., Friesen, J. D., and Lis, J. T. (1995). Recruiting TATA-binding protein to a promoter: transcriptional activation without an upstream activator. Mol. Cell. Biol. *15*, 5757-5761.

Xu, G. L., and Bestor, T. H. (1997). Cytosine methylation targetted to pre-determined sequences. Nat. Genet. *17*, 376-378.

Xu, M., Kladde, M. P., Van Etten, J. L., and Simpson, R. T. (1998a). Cloning, characterization and expression of the gene coding for cytosine-5-DNA methyltransferase recognizing GpC sites. Nucleic Acids Res. *26*, 3961-3966.

Xu, M., Simpson, R. T., and Kladde, M. P. (1998b). Gal4p-mediated chromatin remodeling depends on binding site position in nucleosomes but does not require DNA replication. Mol. Cell. Biol. *18*, 1201-1212.

Yager, T. D., McMurray, C. T., and van Holde, K. E. (1989). Salt-induced release of DNA from nucleosome core particles. Biochemistry *28*, 2271-2281.

Yudkovsky, N., Logie, C., Hahn, S., and Peterson, C. L. (1999). Recruitment of the SWI/SNF chromatin remodeling complex by transcriptional activators. Genes Dev. *13*, 2369-2374.

VITA

NAME: Walter Joseph Jessen

ADDRESS: 938 E. Greenwood Ave.
Crown Point, IN 46307

EDUCATION: Ph.D., Biochemistry (2004)
Texas A&M University
College Station, TX 77843

B.S., Physics (1998)
Purdue University Calumet
Hammond, IN 46323

PUBLICATIONS:

Carvin C. D., Dhasarathy A., Friesenhahn L. B., Jessen W. J., and Kladde M. P. (2003). Targeted cytosine methylation for in vivo detection of protein-DNA interactions. Proc. Natl. Acad. Sci. USA *100*, 7743-7748.

Jessen W. J., Dhasarathy A., Hoose S. A., Carvin C. D., Risinger A. L., and Kladde M. P. (2004). Mapping chromatin structure in vivo using DNA methyltransferases. Methods *33*, 68-80.

Jessen W. J., Dhasarathy A., Carvin C. D., and Kladde M. P. (2004). Bidirectionally propagated chromatin remodeling during transcriptional activation in vivo. Submitted.

Dhasarathy A., Carvin C. D., Jessen W. J., and Kladde M. P. (2004). Modifying chromatin remodeling enzyme requirements by regulating levels of promoter-bound transactivator. Submitted.

Jessen W. J., Hoose S. A., Gavin I. M., Pilon J. L., Layborne P. J. and Kladde M. P. Nucleosome conformational stability and the accessibility of nucleosomal sites at the *PHO5* promoter in vivo. Submitted.